TITLE: VECTOR ACOUSTIC MISS DISTANCE INDICATION

AUTHOR: RGW Thomson; Pr Eng, C Eng,
MBL (S Africa), BSc (Elec Eng) (Pretoria),
MIEE, MIEEE, MSAIEE

This thesis is submitted to the University of Cape Town in complete fulfillment of the requirements for the Master's Degree in Electrical Engineering.

This thesis has not been published elsewhere or submitted to any other university or organization for degree or other purposes.

SUPERVISOR: Prof SG McLaren

Date of Submission: 21 August 1985

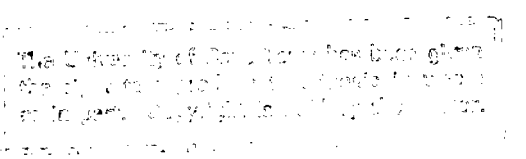

Dedication: To my wife Nancy

CONTENTS PAGE

(i) ACKNOWLEDGEMENTS (i).5

(ii) SURVEY OF THE WORK COVERED BY THIS THESIS (i).7

1 INTRODUCTION 1
1.1 A summary of the Requirements for Miss Distance Indication (MDI) Equipment 1
1.2 General Requirements of Miss Distance Indications Systems 5
1.3 Classification of Miss Distance Indication Systems 7

2 THE LITERATURE SURVEY 11
2.1 Introduction to Survey 11
2.2 Photographic MDI 12
2.3 Cooperative Doppler MDI 16
2.4 Cooperative Radio Active MDI 18
2.5 Acoustic Miss Distance Indication 20
2.6 Conclusions of Literature Survey 24

3 THE PRINCIPLES AND POTENTIAL OF ACOUSTIC MISS DISTANCE INDICATION 25
3.1 Characteristics of Shock Waves suggested by Literature Search. 25
3.2 Practical Investigation of Suggested Characteristics 28
3.3 Conclusions Regarding predicted and Measured Results 31
3.4 Practical Implementation of Acoustic MDI Systems of Literature Survey 31
3.5 Conclusion regarding Acoustic Miss Distance Indication 36

4	THESIS ADVANCED BY THE AUTHOR		37
	4.1	General statement	37
	4.2	Practical implication of Experimental Experience	37
	4.3	The choice of N-wave period as Independent Variable	38
	4.4	Verification of Thesis and Development of Theory	40
5	THEORETICAL WORK		41
	5.1	The Model of the Shell in Flights	41
	5.2	Deduction of Period of N-wave from the Model	45
	5.3	Conversion of Firing Table Information into Polynomial Form	47
	5.4	Simplified Empirical Model of N-wave - Period Distance Relationship	51
	5.5	Locating the Trajectory of a Shell	55
	5.6	Specification and Design of Hardware to measure the Required Times	62
	5.7	Experimental Procedure	71
6	CONCLUSIONS		81
7	REFERENCES		82

APPENDICES

I	SCHLIEREN PHOTOGRAPHS OF 20 MM ROUNDS FOR VARIOUS MACH NUMBERS.	A.2
II	DIMENSIONS OF 20 MM ROUND USED IN ALL THE EXPERIMENTS	A.9
III	PHOTOGRAPHS OF RECORDED N-WAVES	A.11
IV	SPECIFICATION OF REFERENCE - AXES OF THE TARGET SYSTEM	A.15
V	MATHEMATICAL ANALYSIS: ESTIMATING THE COORDINATES OF TWO POSSIBLE POINTS	A.19
VI	EXAMPLES OF CALCULATIONS	A.25
VII	MATHEMATICAL ANALYSIS (ALTERNATIVE METHOD)	A.29
VIII	DISCUSSION OF RESULTS	A.34
IX	EXPERIMENTAL READINGS	A.54

SYMBOLS, ABBREVIATIONS AND UNITS USED IN THIS THESIS

Symbols

Mo	Mach No; dimensionless
v(t)	instantaneous velocity of round (m s^{-1})
S(t)	instantaneous displacement of round (m)
o	period of N-wave (s or μs)
C	local speed of sound (m s^{-1})
θ_1	half angle of leading or bow shock cone of projectile (degrees)
θ_2	half angle of trailing shock cone of projectile (degrees)
r_i	estimates of distance from a known point, P_i, to the source of a disturbing phenomenon
P_i	location of known points
t_i	time at which simulation of the i-th sensor takes place (s or μs)
t_o	instant when the shell leaves the muzzle of the gun
τ_i	period of the i-th N-wave

Abbreviations

MDI	Miss Distance Indication
AMDI	Acoustic Miss Distance Indication
RPM	Rounds per minute

(i) ACKNOWLEDGEMENTS

The work described in this thesis was performed at the National Institute for Aeronautics and Systems Technology of the South African Council for Scientific and Industrial Research. The author gratefully acknowledges the use made of many of the Council's facilities and for the permission of the Council to use this work as the basis for an MSc thesis submitted to the University of Cape Town.

The author would, in particular, like to thank the individuals mentioned below for their assistance to perform the work needed to complete this thesis.

Dr DH Martin for his help in generating the theory for the MMD method and for his assistance in analyzing the results.

Mr H Kappetijn, Head of the Electronic Instrumentation Division of NIAST for the substantial contribution made to the work by ensuring that overall high standards of hardware design and construction were maintained throughout. Mr Kappetijn assisted at many field trials and contributed to the early computer analysis of the results.

Mr JPS Bennett, then of NIAST for the developments of prototype hardware and early field work.

Mr AR Dragt of NIAST for his able and experienced assistance in the field trials often under very trying conditions.

Mr AS Neophytou of NIAST for his assistance with aspects of the field trials.

Mrs LS Kritzinger of NIAST for typing and correcting the several drafts of this document.

(ii) SURVEY OF THE WORK COVERED BY THIS THESIS

(ii).1 GENERAL

"In 1981 the author decided to investigate means of accurately measuring the passage of anti-aircraft shells past a towed airborne target. This decision was based on the observation that available literature showed a need for low cost miss distance indication equipment. A feasibility study showed that the task would be multi-disciplinary entailing aerodynamics telemetry, weapons performance studies and investigation of the techniques of measurement of shell location currently in use.

The decision was made by the author to concentrate on a study of the technique measurements of shell location and the analysis of such measurements in view of the fact that, at least in isolation, knowledge of the other factors mentioned was fairly complete although unevenly spread in South Africa.

Initial work concerned a study of the General Requirements for such target systems and the classification of these. A literature survey was conducted by the author which indicated that systems already in service made use of several measurement techniques, including photographic, radar and acoustic phenomena. Of these, acoustic means appeared to offer a cheap and simple solution to the measurement problem.

The author then explored the principles and potential of Acoustic Miss Distance indication and arrived at the conclusion that such a system, based on measurements of the period of the shockwave accompanying a supersonic shell, would be feasible.

This conclusion led to the Thesis presented in this document, that firstly measurement of the shock-wave period could enable deduction of the distance between the sensor and the flight path of a supersonic shell and secondly, that several such measurements would enable the miss vector to be calculated.

Theoretical work regarding the nature of the shockwaves accompanying supersonic shells was undertaken by the author and a useful empirical model was developed.

A problem central to the whole thesis was that of calculating the vector from the measurements. The solution of this problem is described in detail in chapter 5 and in Appendix V. It is the author's contention that this method has general application in several other classes of location problem where estimates are subject to errors in fields such as Sonar, Lighting Location, Geological Sounding and acoustics target location.

In order to reduce the complexity of the experimental procedure the author decided to restrict initial tests to targets mounted on fixed posts above the ground located at known distance from the gun. When predictable results, consistent with the theory developed and explainable in terms of the models used, were obtained, at pre-set miss distances, the experiments could be broadened in scope to include unknown ranges and miss-distances as well as moving targets.

This thesis describes the results obtained in the ground-based tests and applies the theory in analysing the results. Test data for 380 shells are presented and the miss vector is calculated in each case.

The calibre selected for the experiments was 20 mm. The basis of this choice was beyond the control of the author. Safety considerations required that these rounds could be fired only under very carefully controlled circumstances which added considerably to the difficulty, opportunity and cost of performing experiments.

The work covered by the thesis includes details of the laboratory-model measurement system, the field trial results and a discussion of the results with a view to demonstrating the feasibility of proposed vector acoustic miss distance indication system.

(ii).2 OVERALL REQUIREMENTS FOR THE FEASIBILITY STUDY

(a) The intended target will be airborne and towed at 200-300 knots some 1000-4000 m behind the towing aircraft.

(b) No connection other than the towing wire is allowed between target and towing aircraft, e.g. no connection to the power, communication or navigation system of the aircraft is allowed.

(c) No direct connection to the gun or fire control system is allowed.

(d) No modifications to the rounds are possible.

(e) The exact location of the towing aircraft at any time is unknown.

The overall requirements for the system are further explored in Chapter 1.

(ii).3 WORK PERFORMED BY THE AUTHOR DURING THE WRITING OF THIS THESIS

Based on the literature surveyed (Chapter 2), the author recommended a study of acoustic means and in particular the period of shockwaves generated by supersonic shells. This work is described in Chapter 3 of this thesis.

The author then undertook the following theoretical work (described in Chapter 5):

(a) development of a model of a shell in flight (formation of shock waves, relationship of period of shock wave to miss distance and development of a simplified empirical model for general use)

(b) development of theory for locating shells (method of four triangles). This work replaces the commonly used "string computer".

(c) The work above led to the development by the author of the thesis outlined in Chapter 4.

(d) The author designed and specified the apparatus used in the early experiments. In 1984 the apparatus was completely re-designed and built, to higher standards of reliability, by the the Instrumentation Section of the Technical Support laboratory of NIAST.

(e) The author specified and conducted the field trials needed to generate practical, measured data against which to evaluate the theory.

(ii).4 GENERAL CONCLUSIONS

The feasibility of the method must depend on the quality of the results it provides. Quality in this context is defined in terms of the usefulness of such results to any actual or potential user. To date the author has not encountered any formal definition of a user requirement which states requirements on accuracy in terms of

- scalar miss distance
- angular error
- error distance
- error vector

In the opinion of the author it is extremely significant that the SPAAG WILDCAT trials (Ref 4) held as recently as 1982/83 made use of a zone only, Acoustic Miss Distance Indicator. As discussed in Chapter 3 of this thesis, the zone system has an inherent possibility of error equal to twice the zone radius on any reading.

This limitation suggests that the system described in this thesis which resolves distance, on a continuous scale, to within 10% at a range of 500 m and angular error to within 20° or less, for about 70% of readings, provides a significant potential improvement over existing apparatus.

The following general systems design recommendations are made by the author:

(a) The measured period τ of the shockwave provides a sensitivity of about 10μs per meter which is well within the resolution of low-cost instrumentation. This is an adequate basis for a MDI system.

(b) The method of four-triangles will resolve the vector angle to within 20° in general. Given better data concerning the distance-period relationship, smaller angular errors will be obtained. The alternative analysis, the MMD method, gives results to within ±10° in most cases.

(c) The empirical relationship of paragraph 5.4 shows a systematic error of +10% at 500 meters and +37% at 1000 meters. These errors were clear from a batch of 85 shots fired on 18th June 1985 and correction entails simple fieldwork and deduction of better correction factors as shown in Chapter 5.

(d) Failure of certain microphones to read, owing to masking or system mal-function implies that redundancy is desirable. A redundancy of sensors of between 4 out of 5 to 4 out of 6 is recommended by the author.

(e) A large measuring base is vital. Increasing the average distance between microphones from 300 mm to 1000 mm reduced errors owing to masking from 12,2% to 9,4%. Because of the irreducible noise in the readings, derived distances are subject to error. The results acceptable for further analysis rose from 22,1% to 88,1% by increasing the measuring base from the average 300 mm to 1000 mm.

(f) The overall conclusion is that the method is feasible and worth developing further. The accuracies obtained are believed by the author to be sufficient to increase the state of training of guns' crews and to provide useful information especially of scalar miss distance to technical weapons maintenance units.

(ii).5 FUTURE WORK

A Moving Targets

To date work has concerned stationary targets. No theory has been developed for targets whose speed is in the range 20-60% of that of the shells.

B Sequence of Stimulation of Sensors

As discussed in Chapter 3, the N-wave is a noisy phenomenon with the greatest source of noise in the trailing wave. Some theoretical work has been done to develop a means of analysis which makes use of only the nose wave which is quieter and generally better defined. As can readily be seen in Chapter IX, the sequences are robust and few violations are observed. Theoretical work shows that the sequence of stimulation of sensors is robust and enables a miss sector to be identified with very little processing. The sequence method forms the basis for further work at another department of CSIR.

C Noise in Vicinity of towed Targets

The author has found no published data concerning the acoustic noise present at microphones on the surface of structures moving at 200-300 kts behind jet aircraft. The author has started a programme of measurements to obtain useful design figures.

D Hardware Design

The major issues concerning hardware design are

- Redundancy
- Data Transmission
- Burst Firings

Because Flight Test Instrumentation frequencies and practice prescribe data rates, any increase in redundancy of sensors (and hence data) will impose load on the data link. A practical solution will be to use a large memory in the target to buffer the data, until it can be sent to the monitor.

Bursts of rounds might reach 1000 RPM i.e. one round every 60 ms. This rate is not high in terms of data transmission rates or processing speeds. Work is needed to establish how best to discriminate between successive muzzle blasts.

A potential problem exists where two barrels are used asynchronously (the usual practice). The principal problem being that synchronization between muzzle blasts and shells arriving at the target could be lost.

Remark: Most of the problems described above would be reduced considerably by a coordinated System Engineering Study given a clear set of user requirements.

1.1 A SUMMARY OF THE REQUIREMENTS FOR MISS DISTANCE INDICATION EQUIPMENT

Miss Distance Indication is an essential aspect of the Scientific Evaluation of Ballistic Weapons Performance. In simple systems a paper or fabric target might be used and the number and position of holes in the target used to calculate a score which in turn could be used to evaluate the weapon and its operator. This means has been in use, with modifications of a minor sort since before the first World War. Stationary targets erected on the ground have been in use by Armies since at least Roman Times. The emphasis in this thesis will be on airborne targets for the calibration and evaluation of computer-controlled anti-aircraft guns and operators.

Development since the second World War which have led to more stringent requirements on Miss Distance Indication include :

(i) the need to fire at high speed aircraft and missiles

(ii) the use of fire control computers and tracking radar to aim the gun

Because of the complexity of modern gunnery, scientific evaluation is necessary if weaknesses of human or other sorts are to be identified in systems which can cost up to US $4 000 000 each.

The type of problem the fire control system is required to solve can be illustrated by a very simple example.

Example

An aircraft flying at approximately Mach 1,0 moves at about 346 ms^{-1} depending on altitude and temperature. A 20mm shell will cover 1km in about 1 second. At a range of 1km, the gun must be aimed approximately 20° ahead of the target for the first shell in a burst to reach it; this angle is referred to as the "lead angle".

Typically a 1 to 2 second burst is fired, which at 1200 rounds per minute includes 20 - 40 shells.

During the duration of the burst of fire, the aircraft will have continued to move so that each shell is fired from a different azimuth setting of the gun which has to track the target by rotating at about 20^{o} per second or more. This situation is shown schematically in Figure 1.

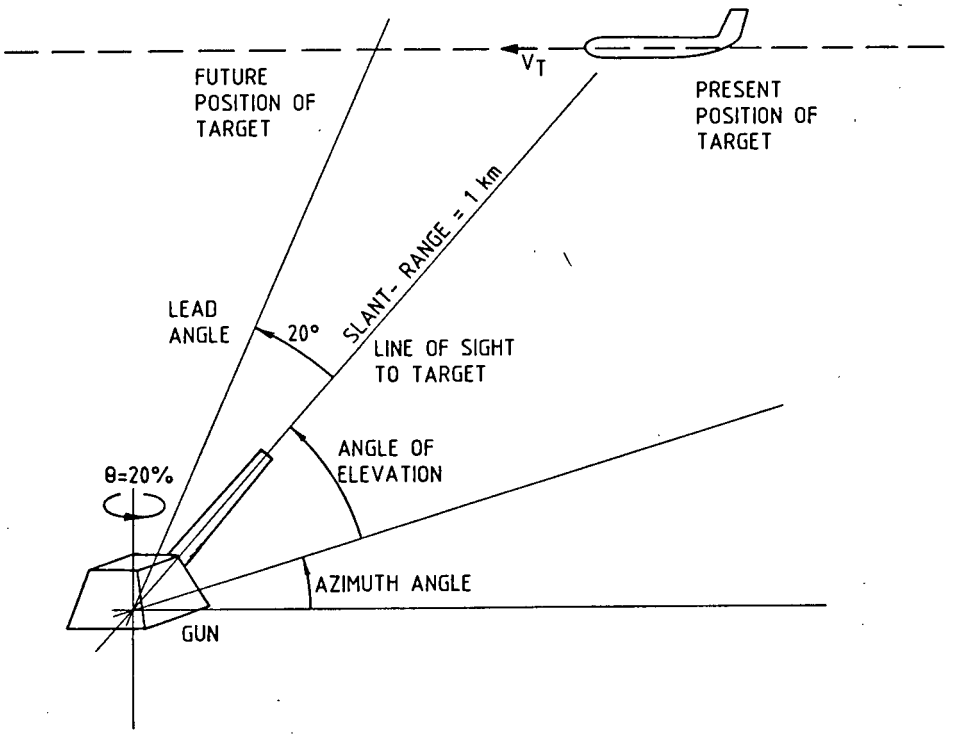

FIGURE 1: Ground to Air Engagement

In practical cases the target moves in three dimensions and has to be tracked in range, elevation and azimuth by the Radar, Computer, Operator, Gun-system. At close range the gun must be slewed more rapidly resulting in greater tracking error. At longer ranges the slewing-rate is slower and accuracy of radar ranging and knowledge of the dynamic behaviour of the shells becomes critical.

It is prohibitively expensive to fly full-size targets at real attack speeds and ranges to test anti-aircraft gunnery systems.

What is usually done is to fly a small scale model at reduced range and speed. This results in the following effects :

(i) The reduced size results in reduced Radar Cross Section. This can be countered by including a suitable reflector to ensure accurate radar tracking.

(ii) The reduced range results in higher slewing rates for the gun and radar positioners. This is a useful effect because it can be used to reproduce the effect of higher aircraft speed.

(iii) The reduced range results in less vertical displacement of shell owing to gravity. This tendency improves accuracy unnaturally.

(iv) Any deviation of the shells from the centre of gravity of the target constitutes a miss. In the case of a large (actual) target, shells can strike at fairly large distances from the centre of gravity and still inflict lethal damage. In the case of a small, scale model, a deviation from the centre of gravity of a similar distance might represent a total miss.

The Miss Distance Indication problem can be summed up as being 'the provision of a cheap target which can be made to move (by towing or other means) in a way which closely imitates the oppdrent manoeuvres of a real target and which provides information on the passage of shells which may miss it altogether.

The cost and performance of the target form the subject of an on going argument amongst anti-aircraft gunnery evaluation officials. If a target is to be effective, it is almost certainly going to be expensive. Expense in this sense implies relative expense in the context of a training or evaluation mission.

This cost of the mission includes:

- Preparation and maintenance of target and towing aircraft by ground crew.
- Cost of ammunition which can reach US $1000 per second of firing time.
- Cost of preparation and maintenance of guns.
- Wear on barrels which may have useful life times of 600 to 2000 rounds.
- Overall mission logistics such as fuel, food, accommodation and transport of weapons and crew to a suitable range.

The cost-performance argument will not be explored further in this thesis. The author has performed approximate calculations which show that airborne Miss Distance Indication Equipment costing US $25000 per target would be considered very cheap by most developed, modern defence forces. A similar amount would be required for an analysis system.

The airborne system is subject to damage caused by direct hits and rough landings. Typically a target may be used for about six missions.

To reduce the probability of damage caused by direct hits, a deliberate error can be introduced into the fire-control system. To evaluate the results obtained from firing trials in this case requires that Miss-distances are indicated with sufficient accuracy to establish system performance by calculation.

These introductory paragraphs are intended to show that Miss Distance Indication is essential when analyzing the performance of costly, complex anti-aircraft gunnery systems in evaluation engagements of scale targets at scale speed and range. A system cost of US $50 000 to 100 000 is believed by the author to be acceptable to most military authorities.

1.2 GENERAL REQUIREMENTS OF MISS DISTANCE INDICATION (MDI) SYSTEMS

The measured performance characteristics of guns which are required for design and calibration are also generally required for tactical games and operations research and can also have application in training of gun crews. The differences in requirements for training and scientific or technical purposes will be discussed in more detail in subsequent paragraphs.

Measured quantities include:

(i) identification of each shot by sequence number

(ii) identification of miss distance by length and angle from reference axes on the target

(iii) quick conversion from target co-ordinates to bore-sight co-ordinates

(iv) a measure of dispersion such as an indication of the position of the salvo-centre relative to the target together with range and deviation or varience

(v) output from a graphics plotter within five minutes if the MDI device is to be used as a training aid.

Note: The objectives of calibration and training missions overlap only broadly in that they are both intended to

- improve the first round hit probability
- reduce dispersion (ie achieve tight grouping).

(vi) time of flight of the round from the muzzle to the target

(vii) instantaneous velocity of the round at the target.

Note: When the range to the target is known, velocity and time of flight measurements for large numbers of shell become of great interest to the manufacturer who has to provide this information to the designer of the fire-control algorithm.

In the system designed by the author, (iii) above was not addressed other than in passing, (vii) above, instantaneous velocity, was measurable only under controlled conditions; (v) above, graphic output, was feasible but not addressed. All the other characteristics were incorporated.

1.3 CLASSIFICATION OF MISS DISTANCE INDICATION SYSTEMS

1.3.1 APPLICATION

The natural classification of MDI systems is by application for example :

- airborne targets
- sea surface targets
- ground surface targets.

1.3.2 MOVING AND FIXED TARGETS

A further subdivision is possible ie moving and fixed targets. However, when target velocity is much slower than that of the projectile, this distinction is not important. It is also the contention of the author that any MDI system that will perform satisfactorily on a moving target will do so on a fixed target.

1.3.3 TRAINING AND CALIBRATION MISSIONS

The distinction between training and calibration missions and targets has already been mentioned. This may most easily be shown by means of a table. (See Table 1).

TABLE 1: Differing Requirements for Processing Time, Accuracy and Cost for Different Missions

FEATURE OF MDI SYSTEM	MISSION	
	TRAINING	CALIBRATION
ACCURACY	LOW	HIGH
PROCESSING TIME	FAST	SLOW
MISSION COST	LOW	HIGH

Table 1 states general assertions. The indicated features are relative to each other and open to interpretation based on the relative marginal improvement in the property involved. Thus the indicated miss distance in training missions should not be less accurate than will advance the state of training of the crew, but may be less accurate than that required for system calibration.

The processing time should, for psychological reasons, such as re-inforcement of instruction be shorter for training than for calibration because of great differences in education and behaviour between gunners and technicians.

Similarly cost is very relative and often depends on external political and economic circumstances rather than on operational research. In general, many more training missions than calibration missions are undertaken for the reason that mechanistic experience can be measured and transferred by instruments to whole batteries of guns. Human experience is not as easily transferred.

It is suggested by the author that significant work could be undertaken in an operations research organisation to determine the means of measuring the cost effectiveness of MDI systems in training anti-aircraft gunners.

1.3.4 SINGLE OR BURST FIRING.

A second important subdivision of MDI systems can be made according to whether modifications to the projectile are possible. From the literature survey conducted by the author, it appears that possible modification can be grouped with other properties as shown below in Table 2, with the rate of fire being a dominant consideration.

TABLE 2: Properties of Rounds

RATE OF FIRE	PROPERTIES OF ROUND
Single Shot	• Generally costly • Heavy (many kg in mass) • Modifications possible • Costly modifications allowable
Burst (approx. 1000 rounds per minute)	• Generally cheap • Light (0,5kg) • No modifications possible

Single shot rounds include large shells and missiles. These often include devices such as proximity fuses which emit Radio Frequency impulses which can be detected by a target and used to determine Miss Distance by Doppler means. Such systems are termed 'Co-operative Miss Distance Indication Systems'. The environmental requirements on any device mounted in a shell are harsh and include

- accelerations up to 100 000g
- rapid heating during passage along the barrel
- very high angular accelerations and velocities resulting in destructive centrifugal forces.

Including such devices in shells which are used at the rate of 1000 per minute is possible but prohibitively expensive.

1.3.5 PRINCIPLE OF OPERATION

Miss Distance Indicators can also be classified according to the broad principle of operation. Exploration of these means was the object of the literature survey. In addition, a means was sought which offered adequate performance in terms of the General Requirements of paragraph 1.2. It was also required that a means be found which was perceived as being fairly simple to implement.

Means reviewed included:

(i) Photographic MDI
(ii) Co-operation Doppler MDI
(iii) Co-operative Radio Active MDI
(iv) Acoustic MDI

2 THE LITERATURE SURVEY

2.1 INTRODUCTION TO THE SURVEY

In this summary of the survey only the briefest description of each system is given. For further details the references shown should be consulted. The survey is structured to show the following for each system listed:

(i) Manufacturer
(ii) System Name and/or type No
(iii) Description of method
(iv) Published or claimed accuracy
(v) Processing time
(vi) Comments
(vii) Reference number in chapter 7 of this thesis (Ref)

Note: Where information is not stated, in the material reviewed the item is left blank in the tables.

Twelve references (Reference 1 - 12) were found to contain very useful information. Other references were found which included topics such as:

- Seismic MDI for surface impacts on land
- Splash detection MDI for use at sea
- Shock Plane MDI which provides automatic indication of impact with sensitized sheets.

These references have been excluded from this thesis which is concerned with MDI for airborne targets.

The summary of the survey presents a short description of the techniques found in the literature, a table of manufactured systems identified and remarks about the technique in general. In each case a major goal has been brevity with a view to expanding in much more detail upon acoustic MDI in a separate part of this thesis.

2.2 PHOTOGRAPHIC MDI

These methods entail modifications to the target in that a camera or cameras together with synchronizing and triggering equipment have to be installed. Alternatively a fixed tracking camera can be used at ground level and the target and projectile filmed either together on one film or separately on two or more films which are synchronized wrt a time base. Both methods imply the use of a large projectile or one which carries a flare or tracer.

Systems for which some data are available are shown in Table 3 below.

Mfg	NAME	DESCRIPTION	ACCURACY	PROCESS TIME	COMMENTS	REF NO
-	FEI	• 4 High speed cameras mounted on target • Cameras are time correlated			• Vector results	2
-	WSMR I	• Two objects per frame	slow		• Very complex analysis • Sensitive to timing errors	1
-	RADOT KMR	• Recording Automatic Digital Optic tracker • 8 RADOTS used	± 14m		• Objects must be visible	1
-	WSMR	• Single object per film frame		slow	• Timing to ± 0,3 m/sec	1
Contraves	SKYTRACK	• Cine Theodelite	-	-	• Suitable for Rockets and shells	15
Royal Aircraft Establish-ment	-	• Single Camera (GW1 Mk 1A, GW2 Mk 2) • 120° angle of view		- -	• Very complex Analysis • Trajectory of round must be straight line • No synch. needed	16

TABLE 3: Photographic MDF

2.2.1 CAMERAS CARRIED BY THE TARGET

Figure 2 below, shows an airborne target carrying two wing-tip mounted cameras. A radio synchronization system is also shown. This is used to impose a timing code at the edge of each film. Generally this would indicate the elapsed time as determined by a time code generator from a master clock (such as a crystal oscillator) and transmitted to the target by a radio up-link. Over any practical distance the propagation-time of this link is generally of no importance, being in any event almost exactly the same for each camera. The Q of the transmitter tank circuit, that of the Receiver front-end and that of the Receiver Intermediate- frequency amplifier filters can cause time delays of up to one milli-second. This delay should be measured for each Transmitter - Receiver pair used.

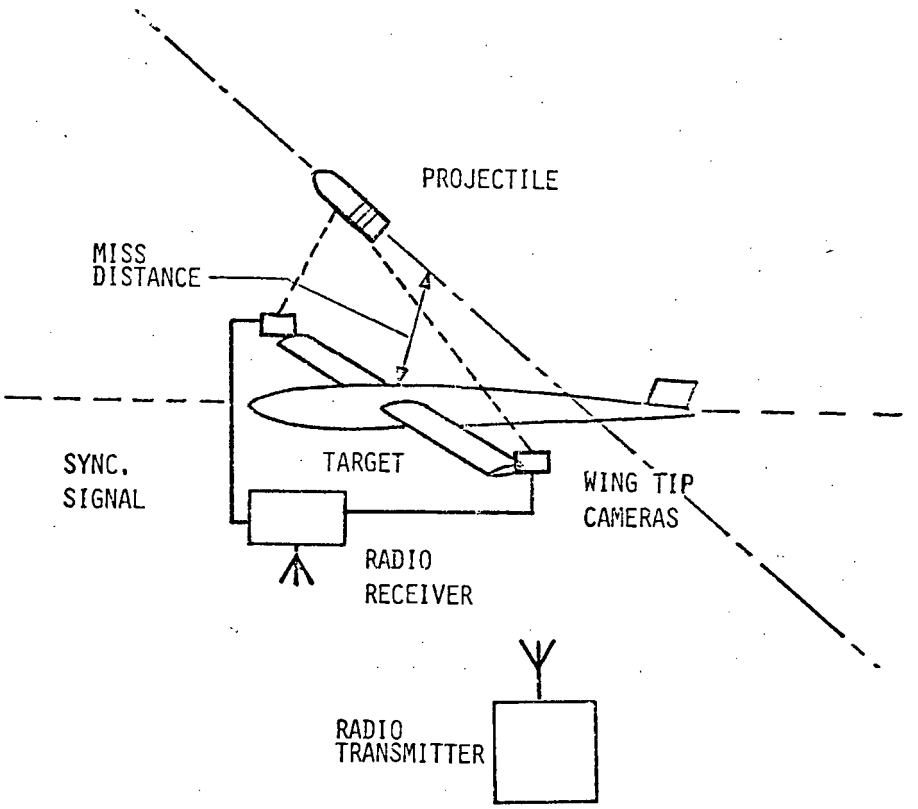

FIGURE 2: Target Mounted Cameras Synchronized from a Base Station

This system has the advantage that all events in the mission can be related to one master clock and time code generator.

The cameras can be synchronized from a clock carried by the target. In this case, mission time need be synchronized only at the moment of take-off of the target.

Provided that the cameras and film can survive the environmental requirements such as :

- vibration
- acceleration
- rough landings
- moisture, soaking, spray
- extremes of temperature

the means may be applied for air, land or sea-borne targets.

It is also an essential requirement that the projectile enters the field of view of the cameras which are of fixed orientation on the target structure.

2.2.2 GROUND BASED CAMERAS

If the range is short and the visibility good one or more synchronized cameras might be mounted on the ground as shown in Figure 3 below.

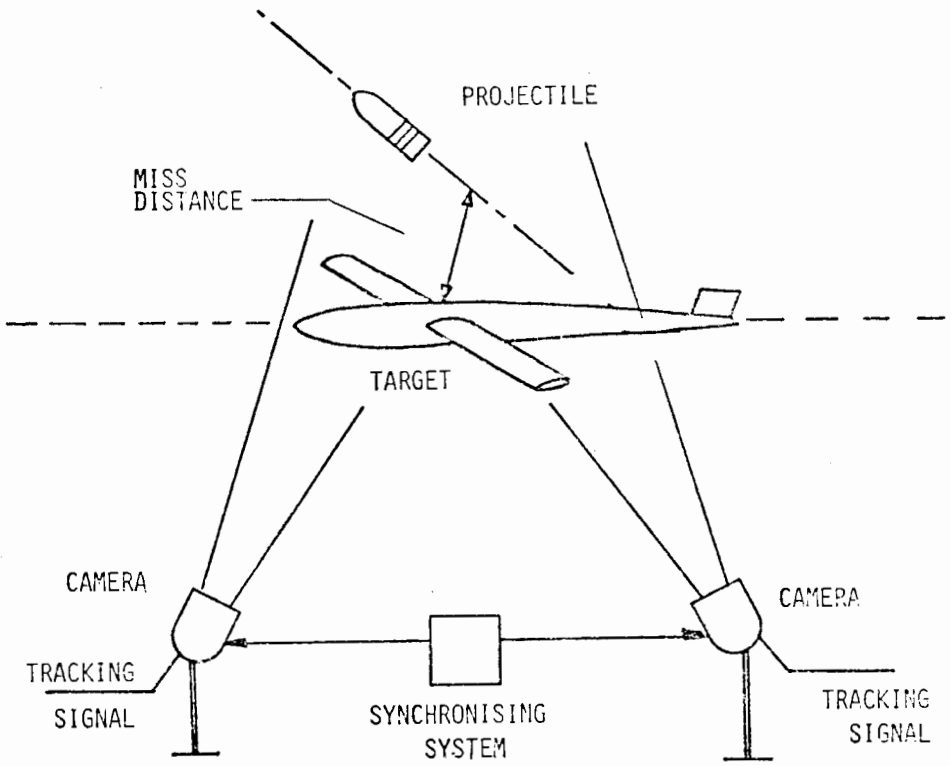

FIGURE 3: Tracking Camera MDI

The tracking signals shown are included for generality and can be derived from tracking radars, television or optical systems operated by human observers.

A synchronizing signal is shown which might either phase-lock the shutters of the cameras or simply impose time codes on the films.

2.2.3 TELEVISION MDI

There appears to be no reason why television cameras could not be used where photographic cameras are used for MDI. Advantages which might be obtained include :

- processing for image enhancement
- use of TV image-locking, tracking etc
- easy play-back, frame by frame
- easy super-positioning of X-Y cursors for digital data acquisition and analysis

2.2.4 COMMENTS ON PHOTOGRAPHIC MDI

(i) Where film is used, processing times are long

(ii) Cameras are very expensive and subject to damage when target-mounted

(iii) Analysis is off-line, slow and very complex

(iv) Television could be a strong contender

(v) Innovation in this field will be costly.

2.3 CO-OPERATIVE DOPPLER MDI

The basic principle of operation is described in Ref 1. The target includes a receiver which receives a signal emitted by a transmitter which is carried in the round. (As stated earlier, this method is accordingly expensive). The received signal is mixed with a signal from a local oscillator, also mounted in the target and the difference frequency is transmitted via a down link to the ground station. The difference frequency is proportional to the relative velocities of the target and round; by integration, relative displacement can be calculated as discussed in detail in Ref 1.

The data obtained from the search are summed up in Table 4 below.

TABLE 4: Co-operative Doppler MDI

Mfg	NAME	DESCRIPTION	ACCURACY	PROCESS TIME	COMMENTS	REF NO
-	DRQ4	• Cooperative Doppler, S BAND	± 1,2m 60m range	10 mins	• Range depends on TX power • No vector information	1
BABCOCK USA	800B	• Pulse Doppler	not stated 16m range	Not real time	• No vector info	2,3
BABCOCK USA	DIGIDOPS DSQ-24	• Non cooperative radar • L-Band	± 0,8m 60m range			1
BABCOCK USA	BBCS		93% (not defined)		• Very large target required approx 5m fin size	1
-	AN-DSQ-37	• L-Band Doppler	high accuracy		• Only used for large rounds Dia approx 75 mm • Mainly naval use	2
	AN-DSQ-40	• L-band Doppler	5m range			2
	AN-DSQ--41A	• L-band Doppler	10-16m		• Instant readout	2
	BQS	• S-band Doppler			• Quadrant scores	2
Sanders Associates USA	RASCORE -S	• Pulsed Doppler ampl	6m	Real time	• No vector, single zone • 7,62mm - 40mm rounds	3
Sanders Associates USA	RASCORE AP	• Pulsed Doppler ampl	4m	Real time	• No vector info	3
	RASCORE M	• Pulsed Doppler correlation			• No zone, no vector information	

2.3.1 COMMENT ON CO-OPERATIVE DOPPLER MDI

(i) Fitting oscillators into shells is expensive. Any device fitted into a shell must withstand acceleration of up to 100 000g (Ref 16). The shells would also have to contain a battery which could withstand these conditions and also have a reasonable shelf life.

(ii) Modern signal processing makes the method very feasible - especially for larger calibres.

(iii) To obtain vector information, the target should include three or more antennas and receivers which mix the received frequency with a common mixer frequency to obtain beat notes from which velocity and displacement can be obtained.

(iv) The method appears to be well evolved and to be suitable for rounds which are already fitted with oscillators such as proximity fused shells which are available from about 40mm upwards.

2.4 CO-OPERATIVE RADIO ACTIVE MDI

This is a cheap and simple way of causing a shell to radiate.

A highly radio-active slug is inserted into the nose of the round. Some compensation must be required to maintain dynamic behaviour (longitudinal moment of inertia, centre of gravity, overall mass) given the high density of most radio active materials.

A simple detector such as a geiger counter or scintillation counter is placed in the target and linked to a ground station by telemetry over radio.

The detected count is inversely proportional to the square of the miss distance. Good reliability is claimed by the article in Ref 1. Table 5 below, summarises the finding of the search.

TABLE 5: Co-operative Radio Active MDI

MFG	NAME	DESCRIPTION	ACCURACY	PROCESS TIME	COMMENTS	REF NO
- (USA)	-	Radio-active slug in projectile. Geiger-counter in target. Count depends on proximity.	± 10% up to 16m Range not less than 1,1 m	Should be fast near real time	Calibration easy Extreme handling problems with toxic slugs. No vector info available. Used on BQM34A target	1
- - FRANCE	DEP-1 DEP-2	As above				
- UK	RAMDI UK	As above				

2.4.1 COMMENTS ON CO-OPERATIVE RADIO-ACTIVE MDI

(i) In Ref 1, the article states the major problem regarding this method, viz, the extreme hazzard to personnel handling the rounds. Every round fired would have to be recovered or be seen to land in deep sea water for environmental safety to be preserved.

To be detectable at reasonable distances, say up to 15m, the slug will have to be highly radio-active. This also entails danger to the ammunition-shop staff who have to fit the slugs. If demands were very large, the process could be automated and a world wide code of practice brought into being. There is no evidence of this taking place.

(ii) To obtain vector information, at least four sensors would have to be used. The resolution in average count per unit time obtainable during the approach and departure of a round moving at about 1000 ms^{-1} would have to be established. The maximum count at each sensor would have to be detected for the closest point of approach to be computed. Depending on the sampling rate, quite large quantizing errors could result.

(iii) The density of most highly radio-active materials implies that the dynamic characteristics of the rounds would have to be verified if realistic trajectories are to be followed.

(iv) Security arrangements for the storage of large masses of radio-active material contained in thousands of rounds will probably prove to be very cumbersome.

(v) The method is attractive but logistically infeasible.

2.5 ACOUSTIC MISS DISTANCE INDICATION

2.5.1 GENERAL PROPERTIES

Acoustic MDI, in all the references found, (Ref 5,3,6,7,8,9,10,11,12) depends on the fact that a shell moving at supersonic speed generates a conical shock wave at both nose and base. Knowledge of the nature of these shockwaves enables miss distance to be measured by observing the outputs of pressure sensors stimulated by the passing shock wave.

Snow (Ref 13) and Du Mond (Ref 14) show that the pressure jump (amplitude) of the shock wave is inversely proportional to the distance from the path of flight from which it is measured. The period between the nose and base waves is shown to be proportional to the distance between the sensor and the path of the supersonic round.

Table 6 overleaf shows summaries of the properties of eleven acoustic MDI systems. It is of passing interest to note that of these, only three are produced in the USA.

Of the eleven systems shown, nine use the amplitude relationship and two the period-distance relationship. All of the systems reviewed depend on the round being supersonic which is not a restriction in the case of direct fire weapons which are generally only specified for this velocity range.

An encouraging characteristic rather quickly emerged, namely, that one claim for vector resolution (Ref 6) three for four-sector (or quadrant) resolution (Ref 3, 7, 11) two for zone and sector (Ref 3, 7) and one ambiguous claim for directional readout (Ref 12) were made. These claims encouraged the author to believe that, using modern signal processing devices and micro-computers, full vector acoustic Miss Distance Indication would be possible to develop.

TABLE 6: Acoustic MDI

MFG	NAME	DESCRIPTION	ACCURACY	PROCESS TIME	COMMENTS	REF NO
SFENA FRANCE	MAE-15	• Acoustic MDI using single microphone offering 2 zones approx 0-2,0m and 2-3m radius. • Uses amplitude.	± 0,2m on each zone	Near real	• System often used with Secapem 90 target. • Rounds must be supersonic. • No vector result • Calibrated per round calibre	5
OLLE-BULOW AB SWEDEN	BT-23	• Acoustic MDI uses 3 zones 0-4m, 4-8m & 8-16m. • Uses amplitude distance relation.	-	Near real	• Supersonic rounds only. • No vector information. • 3 zones. • Set up for each calibre used.	3
Aeronic AB SWEDEN	AS-100	• Acoustic MDI. • Uses Ampl/distance relation.	10% to 20% up to 20m		• Supersonic rounds only • 12 zone, 4 sector output S	3
Swedair AB SWEDEN	MDC-80 ATA/CTA	• Acoustic MDI. • Uses 5 sensors. • Uses period of shockwave.	10% or ±0,5m at 30m	Real and off line	• Supersonic rounds only. • Set for any round 6mm to approx 30mm. • Full vector display. V • Target or gunners axis display.	6
Royal Aircraft Establishment	Sector Acoustic MDI (SAMDI)	• Acoustic MDI. • Uses 4 sensors. • Detects amplitude of shockwave.	5%	Off line	• Supersonic rounds only. • Used with Rushton target. • 2 zone, 4 sector output. S	7
Thiokol Chemical USA	TIMASS	• Acoustic	±5% 0-3,3m	-		8
Melpar USA	Gunshot Detector		- 0-30m	-		8
SEP FRANCE	CCA3	• Acoustic. • Uses 4 sensors. • Uses amplitude of shockwave.		Near real	• Supersonic rounds only. • 12,5 - 100mm rounds (by presetting). • Displays 3 zones of scoring.	9
Sellman	Projectile Miss Dist Device	• Uses amplitude property of shockwave. • Uses changing spectrum of shockwave as function of distance • Uses 4 sensors.	Not stated	Fast real time	• Supersonic rounds only.	10
SFENA	System for acoustic detection	• Uses amplitude property of shockwave. • Uses 4 sensors. • Sensors placed in resonant cavities.	Not stated	Fast	• Supersonic rounds only. • Proposes 4 quadrant resolution. Q	11
Office National d'Etudes et de Recherches Aeronautiques	Acoustic Firing Indicator	• Uses period of shockwave to measure distance. • Uses 4 sensors.	Not stated	Real time	• Uses broadband microphones as sensors (20Hz to 10DHz) • Supersonice rounds only. S • Some directional readout possible	12

In addition the systems had the very important common factor that no modifications of standard ball or tracer ammunition were required.

Note: High Explosive (HE) rounds should not be used with these devices; the explosion will saturate and probably destroy the sensors which are generally high-bandwidth microphones.

The fact that some of the systems were commercially advertised (Ref 5, 6, 9, 11) and in recent use (Ref 4) was one that differentiated acoustic MDI systems from the often vague descriptions of others.

Without wishing to claim a generality on limited material, it is of interest to note that by the end of 1984, the author had discovered no acoustic MDI equipment advertised by American companies.

2.5.2 SIGNIFICANT PROPERTIES OF ACOUSTIC MDI

From the points of view of local development, acoustic miss distance indication offers certain opportunities. These are listed below in no particular order of importance :

(i) passive, unmodified rounds may be used

(ii) because the frequencies involved are in or near the audio band, signal processing should be simple and cheap

(iii) vector or at least multiple sector and zone resolution of miss distance appears to be possible

(iv) even at high rates of fire (say 4000 rounds per minute) electronic processing speeds are such as to allow round counting and buffering of measured, digitized information for very nearly real time processing and display

2.6 CONCLUSIONS OF LITERATURE SURVEY

(i) The impression was gained, although it cannot be proved from the references quoted, that information regarding the use and nature of MDI systems is only released when it is nearly obsolete.

(ii) A strong requirement exists for a vector MDI system which entails no modification of artillery rounds.

(iii) Environmental and operator-level considerations indicate that the MDI system should be robust and reliable and fairly simple to use or maintain.

(iv) The cost of sensors should be low when taken into account with overall mission costs.

(v) Further investigation of acoustic Miss Distance Indication was likely to be fruitful in achieving the aims of (i) to (iv) above and those of paragraph 1.2, (i) to (vii).

3 THE PRINCIPLES AND POTENTIAL OF ACOUSTIC MISS DISTANCE INDICATION

3.1 CHARACTERISTICS OF SHOCKWAVES SUGGESTED BY THE LITERATURE SEARCH

Two articles are repeatedly quoted by authors writing about shockwave or acoustic MDI, viz, those by Du Mond et al Ref 14 and Snow Ref 13. It is useful to refer to Figure 4 below to visualize the shock cones which form at the nose and base of a supersonic projectile.

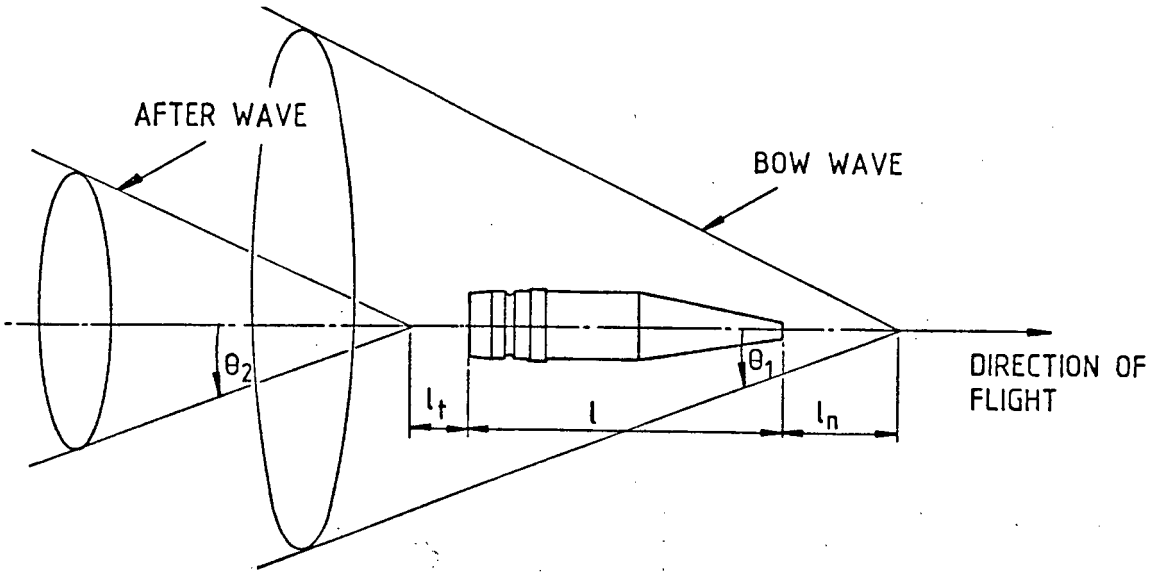

FIGURE 4 : Shock Cones of Round in Flight

The theoretical properties and relationships predicted by the references cited above are listed below :

(i) Shape of Shockwaves

The shockwaves at the nose and base of a projectile are closely approximated by right circular cones (see Figure 3)

(ii) Bow Wave Angle

The half angle of the cone at the nose is

$$\theta = \arcsin \frac{1}{M}$$ (See Refs 7, 13 and 14 and Appendix I)

M = Mach Number of projectile

$$= \frac{v}{c}$$

v = velocity of projectile (ms^{-1})

c = local speed of sound (ms^{-1})

(iii) Wavelength of Shockwave

The wavelength, L, of the shockwave could be approximately defined as:

$$L \doteq \frac{1{,}82\ M^{1/4}\ d\ y^{1/4}}{\ell^{1/4}}$$

where L = wavelength
M = Mach Number
d = diameter of round
ℓ = length of round
y = distance from the round at which L is measured

(Clearly a consistent set of units must be used in this measurement).

Note: Snow Ref 13 uses the term "wavelength", the product of velocity and N-wave period. The term "wavelength" is probably not strictly accurate in this application. The Author therefore prefers the terms "duration" or "period" of N-wave.

(iv) Amplitude of Shockwave

The positive pressure jump at the nose shock cone has an amplitude of

$$p = \frac{0{,}53\ P_o\ (M_o^2 - 1)^{1/8}}{\ell^{1/4}\ g^{3/4}}\ d$$

where p = pressure jump at nose cone

d = diameter of round

ℓ = length of round

P_o = ambient pressure

M_o = Mach Number

y = distance from the round at which p is measured.

(v) Waveform of Shockwave

The amplitude variation of the shockwave with time has an approximately N-shaped graph as shown below in Figure 5.

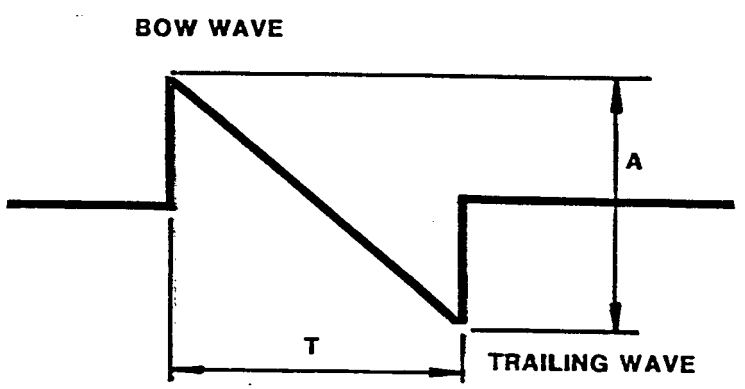

FIGURE 5: Theoretical Amplitude-Time Relationship

Note: This characteristic waveform is commonly called an N-wave in almost all of the literature surveyed.

3.2 PRACTICAL INVESTIGATION OF SUGGESTED CHARACTERISTICS

(i) Shape of Shockwaves

This was verified in the high speed wind tunnel at National Institute for Aeronautics and System Technology of the CSIR. One result a Schlieren photograph of a 20mm round at mach 2,2 is shown in Figure 6 below.

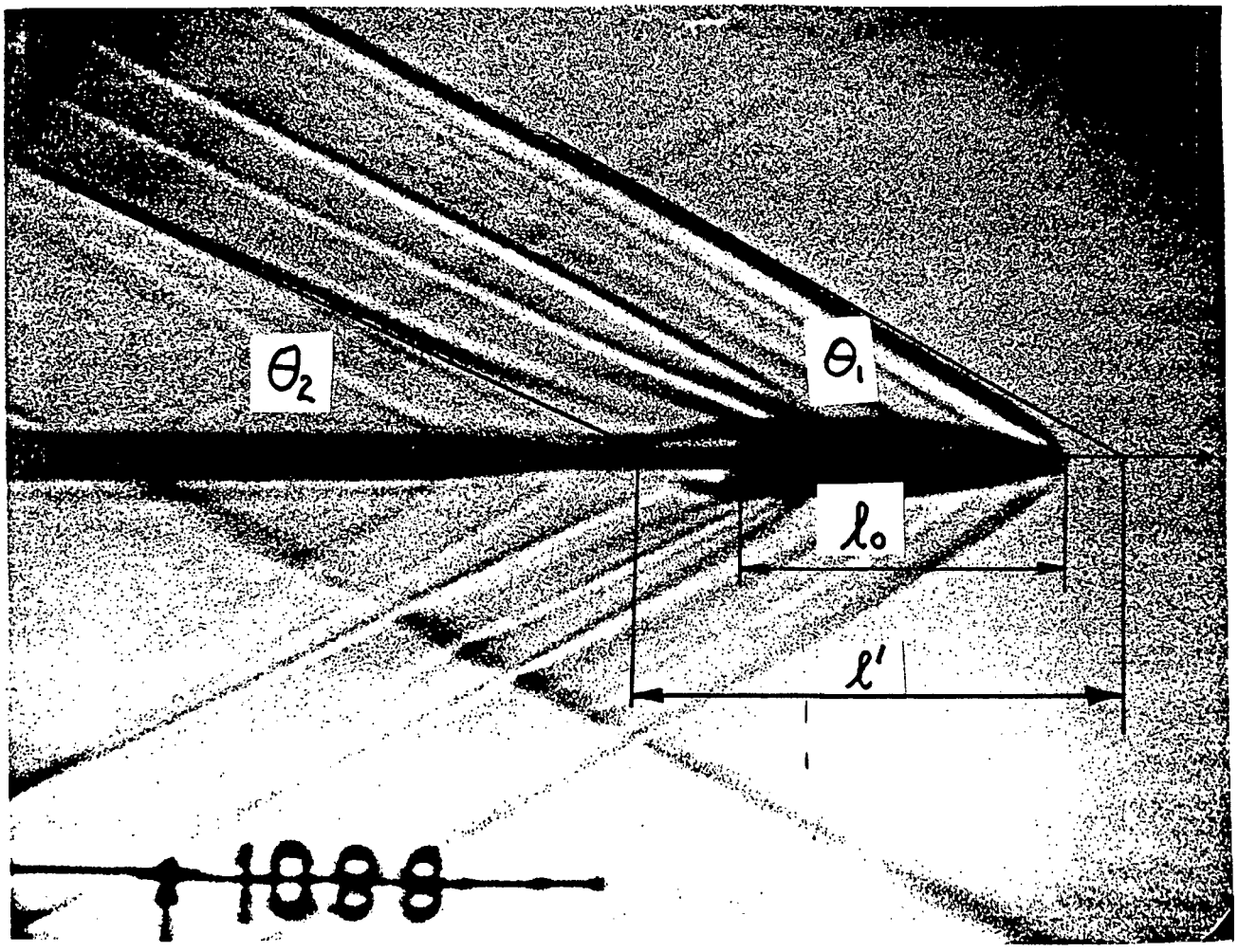

FIGURE 6: Schlieren Photograph of 20mm Round at Mach 2,2

A disadvantage of measuring in a practical wind tunnel is that only near-field effects can be observed. For miss distance work effects at 500 diameters are of more significance.

Photographs of rounds at several velocities are shown in Appendix I.

A drawing of the round is shown in Appendix II.

(ii) Bow Wave Angle

This was verified by the Schlieren Photographs and the effect is widely acknowledged to be as described.

(iii) Wavelength of Shockwave

The calculations by Snow Ref 13 were found by the author to give answers of approximately the correct value for 20mm rounds at Miss Distances in the range 5-15m. However, the predicted results were too low (eg 349 micro sec vs 480 micro sec) and the increase in wavelength with increasing miss distance was found to be too rapid.

This discrepancy led to an investigation by the author with the objective of finding an empirical relationship which would relate measured wavelength to miss distance.

(iv) Amplitude of Shockwave

Because of the experimental difficulty entailed, this property was not explored.

For the same reason it was decided to restrict the experimental work to time measurements. This decision is discussed elsewhere in this thesis. (Paragraph 4.3).

(v) Waveform of Shockwave

These were measured by placing a Bruël and Kjaer microphone Ref 18 on a stand a given distance from a target. The waveform of the shockwave caused by a passing shell was recorded on a storage oscilloscope.

An example of one of these photographs is shown in Figure 7 below.

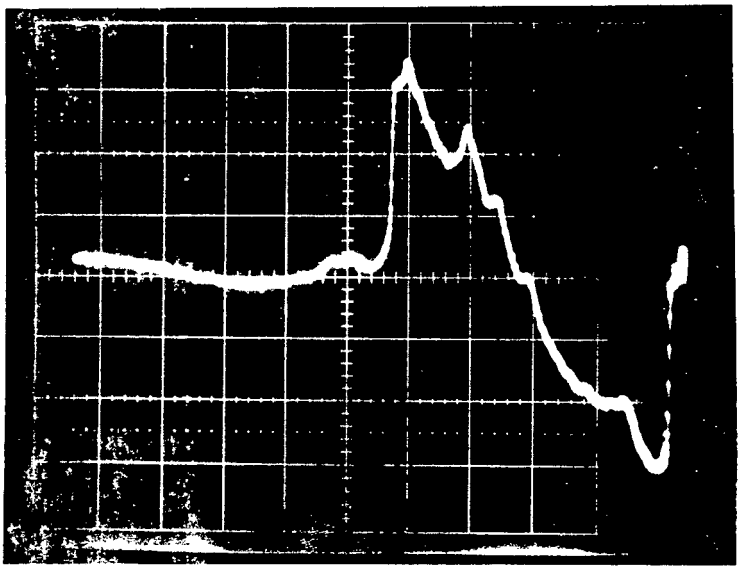

Scale
H: 125 µs/cm
V: 50 mV/cm

FIGURE 7: N-Wave for 20mm Round at 10m Miss Distance

Further Examples of N-Waves at several Miss Distances are shown in Appendix III.

Effects which are noteworthy, and not described by Snow are the following :

(i) Distortion

The N-wave is often heavily distorted. This is ascribed to any of several factors:

- Precession of round in flight
- Nutation of round in flight
- Vibration of structure supporting the microphone
- Pressure of hot expanding gas due to use of tracer.

(ii) Zone of rapid change of Amplitude

Even when distorted, there are two amplitude excursions which are invariably present:

- a rapid positive rise when dv/dt exceeds 0,1v per microsecond
- a second rapid rise when dv/dt is similarly large
- these rapid changes are not always near the zero axis as implied in the literature but can be found at up to 50 or 60mV away from the zero axis.

3.3 CONCLUSION REGARDING PREDICTED AND MEASURED RESULTS

The N-wave is fairly easy to study and the period, defined as the time interval separating the first rapid positive excursion from the second is readily measurable.

Because the amplitude of the shockwave is so great (approx 110 dB) the signal to Noise Ratio (SNR) is high and signal processing is simplified.

The increase of the N-wave period with increasing miss distance appeared to be predictable and the author proposed that this relationship could form the basis of a Miss Distance Indicator.

3.4 PRACTICAL IMPLEMENTATION OF ACOUSTIC MISS DISTANCE INDICATORS OF LITERATURE SURVEY

3.4.1 ZONE MDI; PRINCIPLE OF OPERATION

The systems described as using the amplitude-distance relationship (SFENA, Olle-Bülow) operate in a straight forward amplitude-comparing manner. Referring to Figure 8 below, a microphone, M, (mounted on a drone or towed target) is stimulated by the N-wave of a passing shell.

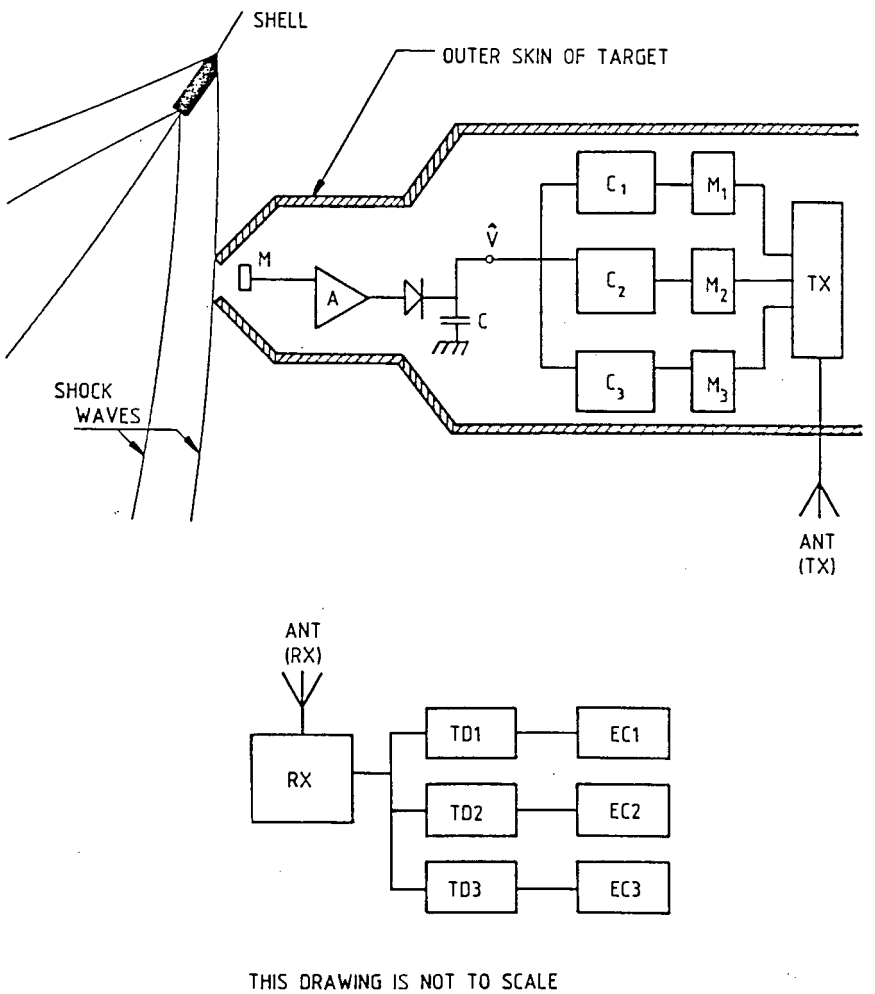

FIGURE 8: Simplified Block Diagram of a Zone MDI System

The signal is amplified by the non saturating amplifier A to a level of 1-2 V_{RMS}. This is detected and stored on a capacitor, C. The stored voltage is applied to the high impedance, buffered inputs of the comparatators C_1, C_2 and C_3.

The reference values of the comparators are set so that C_3 is least sensitive, C_2 less and C_1 most sensitive.

The outputs of C_1, C_2 and C_3 control modulators M_1, M_2 and M_3 which respectively cause the target transmitter to radiate preset bursts at frequencies f_1, f_2 or f_3.

These frequencies are received by the base-station receiver R_x and the combined output applied to the three tone decoders TD1, TD2 and TD3 which respond to the respective frequencies f_1, f_2 or f_3.

The event counters EC1, EC2 and EC3 count the outputs of the tone decoders.

Using the amplitude-distance relationship, the response of the system may be resolved into zones as shown in Figure 9.

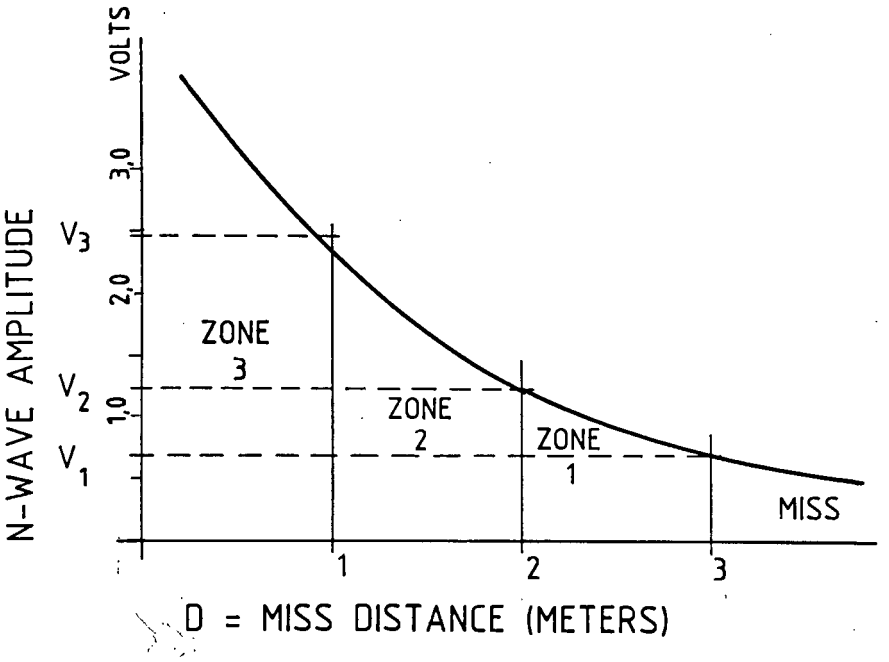

FIGURE 9 : Graph of Response of Amplitude MDI System

The response of the comparators is as follows :

for $\hat{V} > V_1$; $C_1 = 1$

$\hat{V} > V_2$; $C_2 = 1$

$\hat{V} > V_3$; $C_3 = 1$

Using conventional positive logic notation,

for $C_3 \cdot C_2 \cdot C_1$; $D_1 > D$ (Very close)

$\bar{C}_3 \cdot C_2 \cdot C_1$; $D_2 > D > D_1$ (Close)

$\bar{C}_3 \cdot \bar{C}_2 \cdot C_1$; $D_3 > D > D_2$ (Far)

$\bar{C}_3 \cdot \bar{C}_2 \cdot \bar{C}_1$; $D > D_3$ (Miss)

These logical relationships can be established and displayed within a few seconds after each firing (single or burst).

The definition (Miss to Very Close) of Miss Distance are shown in Figure 10.

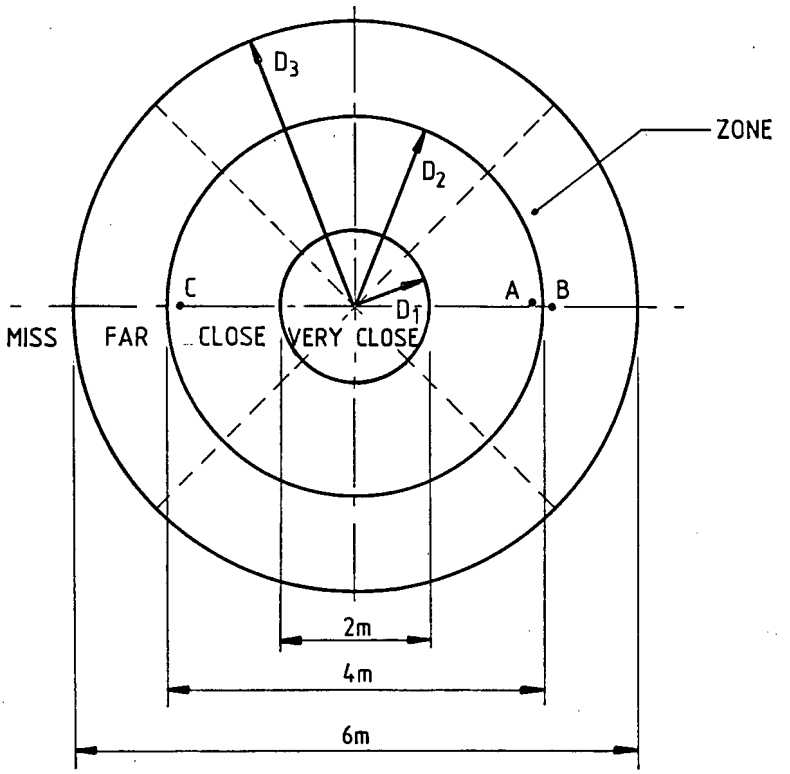

FIGURE 10: Scoring Zones for Amplitude MDI

3.4.2 ZONE MDI; LIMITATIONS

The limitations on zone MDI performance are the following which are readily predictable for a system which quantises into four states, all possible outcomes regarding the location of a recently fired shell.

(i) Directionality

It is impossible to mount a microphone on a target so that it is equally sensitive in all directions. If mounted in the nose of the target, its response may well be quasi-cardiod as shown in Figure 11.

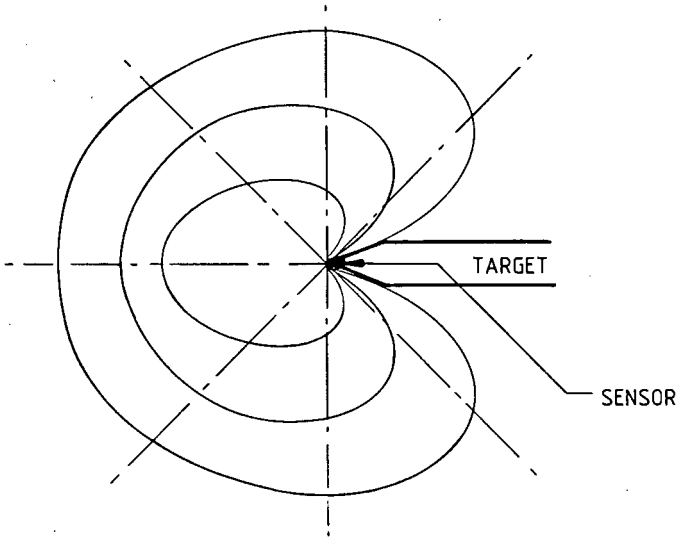

FIGURE 11: Deviation from Ideal Microphone Response

Fins, the fuselage, etc all contribute to masking of the microphone.

(ii) No Grouping Information

Referring to Figure 10, sample shots are shown at A, B and C. A and B although very close will score in different zones. A and C although far apart will score in the same zone.

(iii) Unequal Directionality

The effect of this is to cause even greater errors in scoring result.

Note: The results for the amplitude-distance relation are largely what would be achieved using a period distance relationship ie 4 zones. A slight signal processing advantage and the feasibility of hard limiting the measured signal would lead to less distortion of the (ideal) spherical response of the microphone.

The fact that period increases with distance (compared with amplitude which decreases) leads to a simple reversal of the zone-detecting logic. Further instead of using an amplitude comparator use would be made of an interval comparator. The essential point is that zone MDI systems do not make use of all the available information.

3.4.3 IMPROVEMENTS TO THE BASIC MDI SYSTEM

One improvement is to use several microphones arranged on the target in such a way to supply the comparators with voltages almost independent of orientation. In this case a voting system selects the highest output of any microphone and, assuming that their separation is small with respect to the miss distance, uses this input as a best estimate.

This technique solves the problem of 3.4.3(i) above but not that of 3.4.2(ii).

Some companies place several microphones in symmetrical arrays and compare outputs using analogue computers mounted on the target Ref 9,7,12. In this way an attempt is made to divide the response into sectors, depending on which pairs of microphones are stimulated.

Only Swedair Ref 6 makes a claim for full vector ie

- resolution of miss distance on a continuous scale
- resolution of <u>position</u> of passage of shell relative to a target-borne system of reference axes.

3.5 CONCLUSIONS REGARDING ACOUSTIC MISS DISTANCE INDICATION

In view of the predictable behaviour of the miss distance N-wave period relationship, the author decided that a full vector acoustic miss distance indicator (VAMDI) could be constructed.

All subsequent work in this thesis relates the efforts, problems encountered and progress made towards this goal.

4 THESIS ADVANCED BY THE AUTHOR

4.1 GENERAL STATEMENT

(i) The distance between the flight path of a supersonic shell and a sensor can be deduced, on a continuous scale, from measurement of the period of the shockwave which accompanies the shell (see Chapter 5.4).

(ii) Several such measurements can be used to calculate at least one point on the flight-path of the shell and thereby the miss-vector relative to a system of axes on which the measuring point are located (se Chapter 5.5).

4.2 PRACTICAL IMPLICATIONS OF EXPERIMENTAL EXPERIENCE

(i) To deduce the distance from a sensor to the trajectory of a shell (the Miss Distance) entails knowledge of the following :

(a) the velocity of the shell at the instant of observation
(b) the relationship between miss distance and period of the N-wave

(ii) To deduce the co-ordinates of one point on the trajectory of the shell requires that measurement of period and deduction of miss distance be made from at least four points.

Knowledge of the location of one point on the trajectory clearly enables the miss vector to be calculated.

4.3 THE CHOICE OF N-WAVE PERIOD AS INDEPENDENT VARIABLE

The relationship between Miss Distance and period and amplitude of the N-wave have been discussed in Chapter 3 paragraph 3.1 (iii) and (iv) respectively. The author was obliged to choose a basis for further work on theoretical and limited experimental practical grounds.

The use of the distance period relationship was decided in the light of the following factors :

(i) Availability of Standards

Time standards are very easy to implement up to an accuracy of 1 in 10^7 or10^8 and to a stability if 1 in 10^7 or 10^8 per day, using quartz crystals. For the expected range of frequencies, ie 100 to 5000Hz, a 1MHz clock rate was deemed sufficient.

No really portable absolute acoustic standard was known.

(ii) Distortion of N-wave

The photographs in Appendix III show that in practice the N-wave is often distorted owing to:

(a) resonance of the structure supporting the sensor (microphone)
(b) reflection or masking leading to vector addition of two waves or parts of two waves at the microphones
(c) overshoots which give false impressions of N-wave amplitude.
(d) bandwidth and group delay.

(iii) High Signal to Noise Ratio (SNR)

The high SNR (at least 80dB) favours either amplitude or period measurements equally. The presence of overshoots however, favoured time measurements.

(iv) Zones of rapid change of amplitude with respect to time.

It was found by measuring several N-waves, that there were always two features present even in heavily distorted N-waves :

(a) a portion of the voltage waveform V(t) where $\frac{dV}{dt}$ was very high and positive

(b) a later portion where $\frac{dV}{dt}$ was again high and positive.

These regions were believed to be the rapid transitions derived by Snow in Ref 13.

(v) Identification of N-waves and Measurements of their Period

Identification of N-waves required the observation of three quantities:

(a) that the amplitude of the signal was greater than some reference level
(b) that the amplitude remained above the preset level for longer than a certain time
(c) that the two rapid transitions were present

Measurement of the period was then accomplished by measuring the period between the two transitions mentioned in (iv) a and b above.

4.4 VERIFICATION OF THESIS AND DEVELOPMENT OF THEORY

The author embarked in 1981 on work in the following areas :

(i) Theoretical models of shells in flight

(ii) Deduction of period of N-waves from the model

(iii) Conversion of firing-table information into polynomials describing velocity and displacement as functions of time.

(iv) Proposal of a simple empirical relationship between N-wave period and Miss Distance

(v) Proposal of a means of locating a point on the trajectory of the shell (The method of four triangles)

(vi) The design and specification of hardware to measure the quantities mentioned above.

(vii) The specification of the use of the hardware in a series of experiments to verify the theory developed.

5 THEORETICAL WORK

5.1 THE MODEL OF THE SHELL IN FLIGHT

Note: All the work that follows concerns properties of the 20mm shell illustrated in Appendix II. Except for empirical relationships derived, the theory should be valid in general and could equally well be applied to other rounds.

The presence of a conical shockwave at both the nose and base of a supersonic shell is well documented and described in Ref 13 and 14.

From the firing tables for the 20mm round in question, the average velocity and displacement are stated for specific times of flight.

In paragraph 3.1 (i) and (ii) the generally accepted relationship for the half angle of the nose shock cone was stated ie

$$\theta = \text{arc sin } \frac{1}{M}$$

where

$$M = \text{Mach Number}$$

$$= \frac{\text{instantaneous velocity}}{\text{local speed of sound}}$$

$$= \frac{v(t)}{c}$$

c, the local speed of sound in determined from the relationship:

$$c = \sqrt{\gamma R T_a}$$

where

γ = Specific Heat Ratio for Air
= 1,4
R = Universal Gas Constant
= 287,04 J/°K
T_a = Absolute local temperature (Kelvin)
= °C + 273

Note: (i) The experiments conducted by the author took place at groundlevel in the Transvaal. The average velocity of sound was found to be 346 meters per second.
(ii) This velocity was used throughout further calculations.

Knowledge of velocity, displacement and time of flight enabled the author to draw Figure 12 shown below.

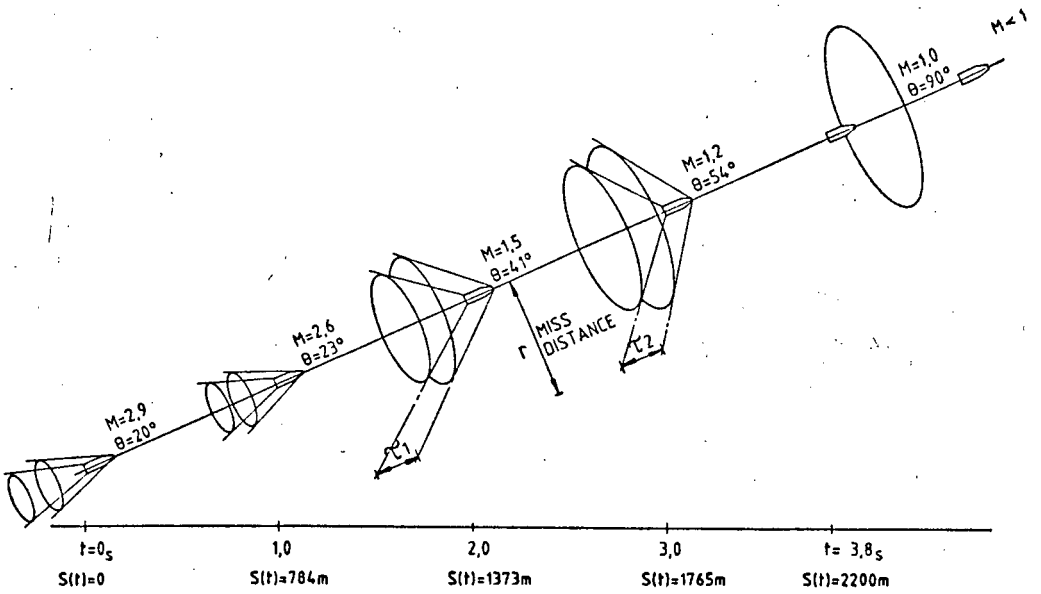

FIGURE 12: Illustration of Shock Cones Expanding during time of Flight

Figure 12 also shows the cone at the base of the shell which from the Schlieren Photographs of Appendix I is known to be of a slightly smaller half angle.

At muzzle velocity of mach 2.9, $\theta = 20°$. After a flight of 3,8 sec the velocity has dropped to mach 1,0, and $\theta = 90°$. Below this velocity, the shockwave detaches and vanishes. The mechanism at the transonic region is complex and is not further pursued in this thesis.

If the half angle of the shock cone at the base of the shell is θ_2 and if θ_2 is always less than θ_1, then the cones diverge. If the relationship between θ_1 and θ_2 could be deduced and knowledge of v(t), (from the firing table for the round) is reliable, then the time difference between the two shock cones should be predictable.

Consider the cones shown in Figure 13 below.

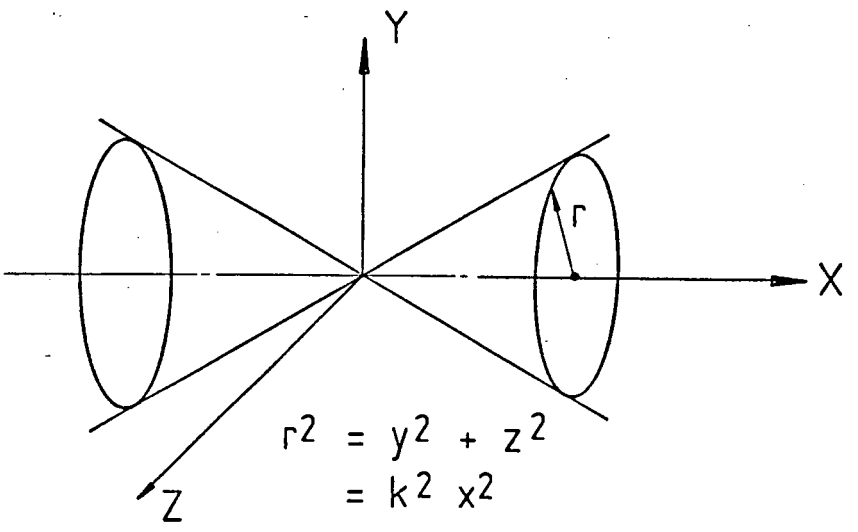

FIGURE 13: A Pair of Cones on the X-Axis

The equation

$$r^2 = y^2 + z^2 = k^2 x^2 \qquad (5.1)$$

fully describes these cones. For convenience it is assumed that the shell is flying along the x-axis.

Let the apex of the left hand cone and the nose of the shell coincide. The position of this point is described by S(t), the displacement of the round. θ_1 is derived from the velocity v(t) as already discussed.

Let the muzzle of the gun be located at the origin.

The nose of the shell is at x = S(t) at any time t.

The radius of the cone at the distance x from the origin is given by :

$$\frac{r}{S(t) - x} = k = \tan \theta \qquad (5.2)$$

as shown in Figure 14.

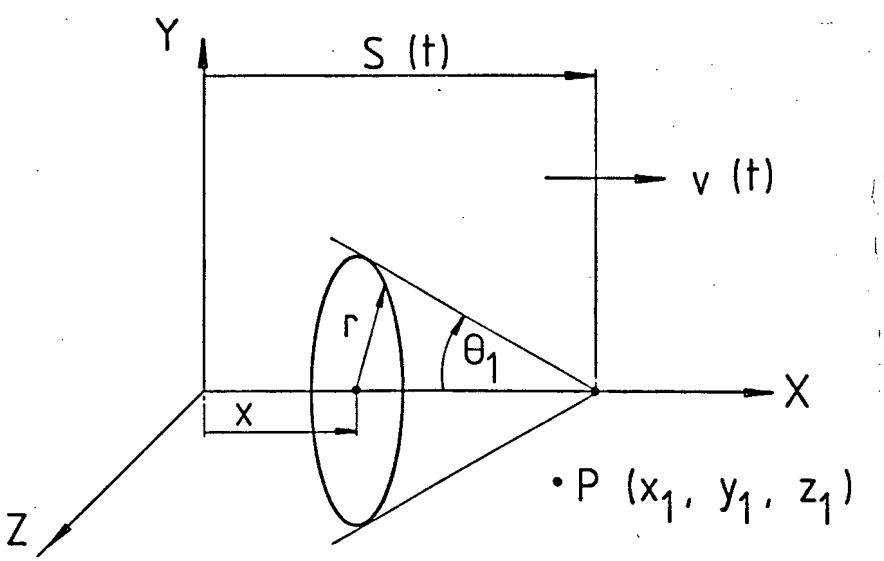

FIGURE 14: Single Moving Cone

Now, $\sin \theta_1 = \frac{c}{v(t)}$

hence $\tan \theta, = \frac{c}{\sqrt{v(t)^2 - c^2}}$ (5.3)

Thus from equations 5.1, 5.2 and 5.3,

$$\frac{c^2}{v(t)^2 - c^2} (S(t) - x)^2 = y^2 + z^2$$

or

$$\frac{c^2}{v(t)^2 - c^2} (S(t) - x)^2 - y^2 - z^2 = 0 \quad (5.4)$$

Thus, if v(t) and S(t) were known, equation (5.4) could be solved for t, for any point, P_1, (x_1, y_1, z_1).

The time by when the shock cone would reach a given point (the location of a sensor) can thus be predicted.

Equation (5.4) is called, by the author, the Equation of Approach.

If knowledge of θ_2 relative to time or to θ_1 exists, and the length of the round is known, then the period between the nose and base shock cones, the period of the N-wave can be predicted.

5.2 DEDUCTION OF PERIOD OF N-WAVE FROM THE MODEL

It was found as discussed in paragraph 5.3 below that the displacement of the round could be described by a 6th order polynomial of the flight time.

The velocity of the round was given by a 5th order polynomial.

Solution of equation (5.4) was not found to be analytically feasible and a Newton's method was used. This is feasible because equation (5.1) has no discontinuities anywhere. The starting value of t was chosen so that the solution for the left hand cone of figure 13 was the one found.

By subtracting the length of the round (92mm) from S(t), the apex of the base cone could be located.

Repetition of the solution procedure yielded a second time to intersect a given point. The difference between the two values should equal the N-wave period.

From the Schlieren Photographs it was clear that the nose- and base-cones had apices separated by somewhat more than the length of the round.

Very good experimental agreement between predicted and actual values for the time difference between the two cones was obtained for a range of 500m, **but only when the actual length of the round was increased by a factor of 3,8 to 349mm.**

The predicted and experimental results are shown below in Table 7.

TABLE 7 : Actual and predicted time differences between shock cones arriving at a point (x,y,z).

MISS DISTANCE $\sqrt{y^2 + z^2}$ METRES	MEASURED TIME DIFFERENCE MICROSECONDS	PREDICTED TIME DIFFERENCE MICROSECONDS
5,0	483,2	479,9
7,07	495,7	499,7
10,0	529,5	527,8
11,18	545,9	539,1
15,0	580,1	575,6
16,0	592,1	583,3

It was decided by the author to investigate the length-multiplication factor experimentally, in a simpler model to find a more direct way of predicting the period of the N-wave, τ, and more importantly, to find out if knowledge of τ would enable calculation of the miss distance.

5.3 CONVERSION OF FIRING-TABLE INFORMATION INTO POLYNOMIAL FORM

The firing tables prepared by the manufacturer are compiled from thousands of firings. The summarised form which is supplied to users of the ammunition include 18 pages of data for velocity v(t) and displacement s(t) along the slant-range with the elevation angle (alpha) in mils as parameter. Each page contains 45 lines of values for v(t) and s(t). (Note 1 mill = $2\pi/6\ 400$).

Because of the many occasions on which, particularly, v(t) would be required for calculations the author decided that a formula which described it would be more useful than the tables. This decision would be especially justified if v(t) could be established without having to measure the angle of elevation at the instant of firing.

The manufacturers supply a graph, reproduced in part in Figure 15 for times of flight to three seconds, for angles of elevation from 0 to 1 500 mils. Within this range slant range appears to be independent of angle of elevation.

Under the direction of the author, examination of the firing tables was undertaken by two engineers in training.

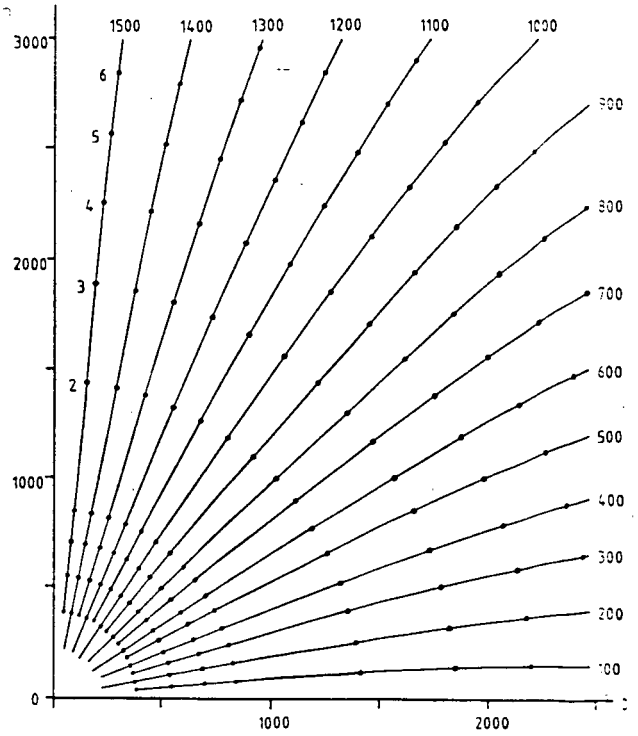

FIGURE 15 : Slant range for several elevation angles.

Values for the angles of elevation 0, 800 and 1 500 mils for velocity and displacement are shown in Table 8 below. The values are for a flight time of two seconds.

TABLE 8 : Speed and displacement for three values of angle of elevation.

ANGLE OF ELEVATION mils	DISPLACEMENT m	SPEED ms^{-1}
0	1 443,02	498,9
800	1 436,89	506,9
1 500	1 445,23	510,0

The polynomials were derived using a curve-fitting algorithm. Rapid convergence between the values for the polynomial and those from the tables was found as the order of the polynomial was increased. After 6th order for displacement and 5th order for velocity, no noticeable improvement was found.

Graphs of the displacement s(t) in metres and of the velocity v(t) of the 20 mm round are shown in Figures 16 and 17 respectively.

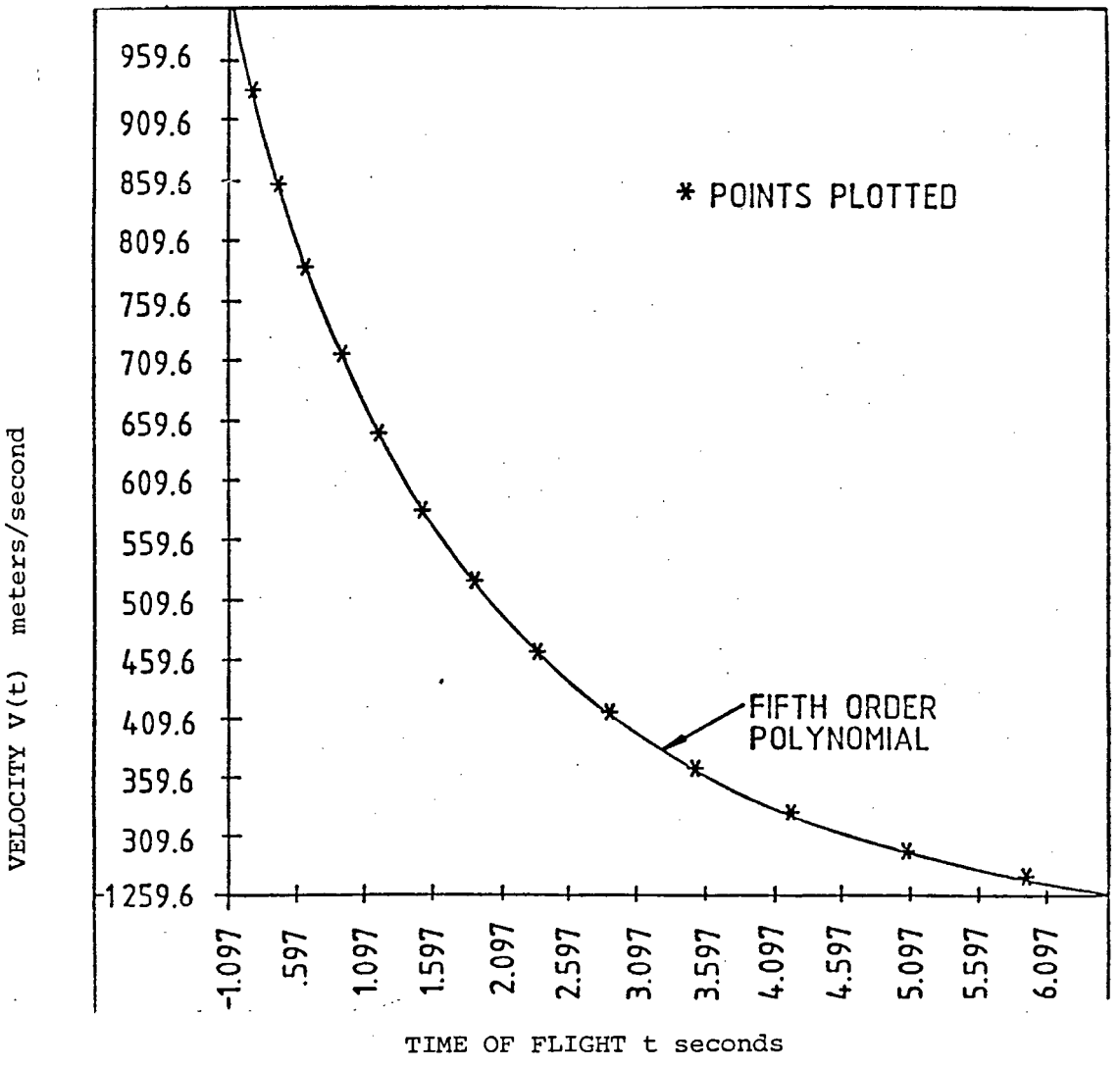

FIGURE 16: Velocity of round vs time.

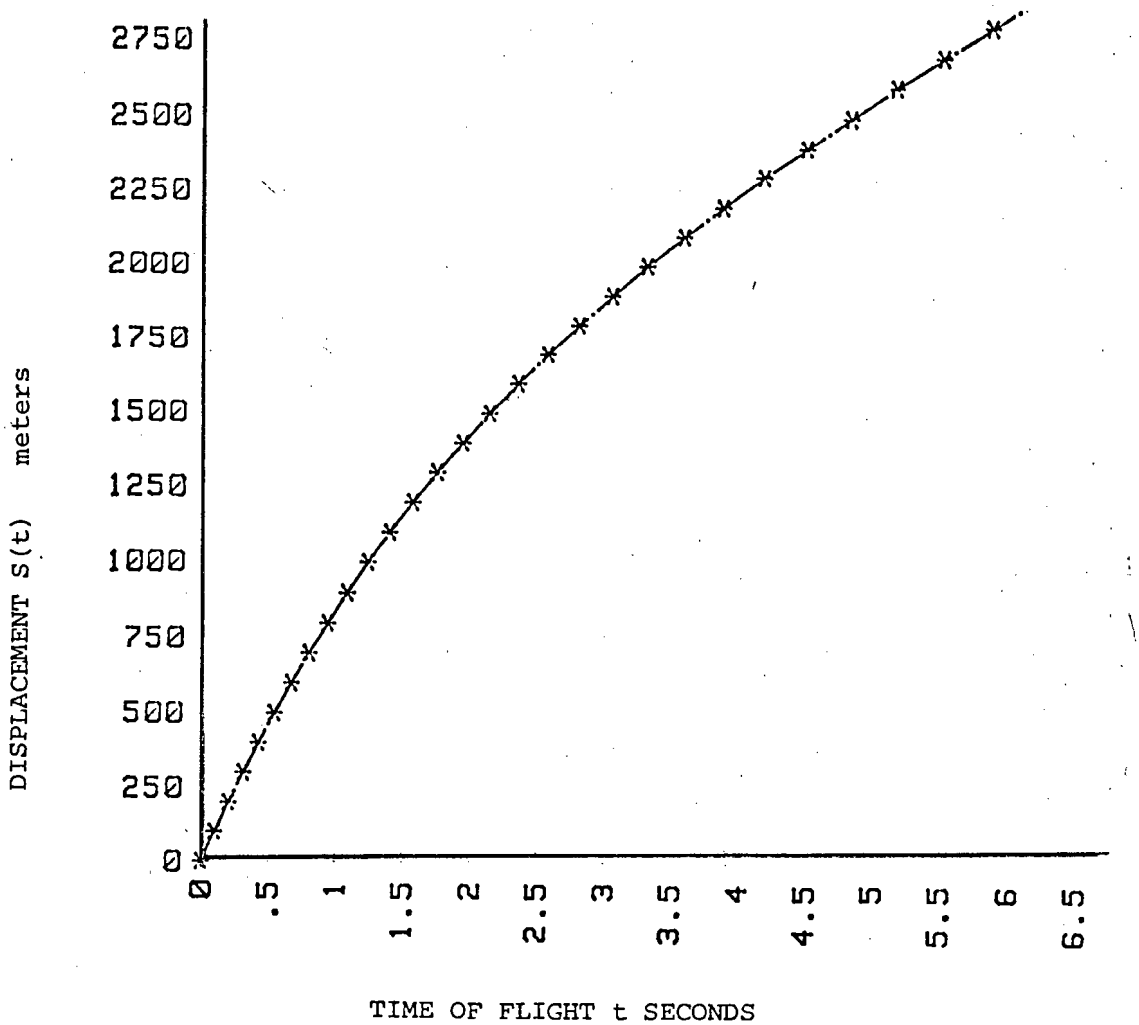

FIGURE 17: Displacement of round vs time.

The polynomial for displacement was found to be

$$s(t) = -0{,}044\ t^6 + 1{,}0181\ t^5 - 9{,}932\ t^4 + 57{,}9026\ t^3 - 248{,}534\ t^2 + 1051{,}484\ t + 0{,}13047 \qquad (5.3.1)$$

The polynomial for velocity was found to be

$$v(t) = -0{,}231\ t^5 + 4{,}6034\ t^4 - 37{,}359\ t^3 + 169{,}191\ t^2 - 494{,}316\ t + 1051{,}383 \qquad (5.3.2)$$

(It is worth noting that at t = 1 both v(t) and the differential of s(t) give values of 693 ms^{-1} which agrees with the value in the firing tables).

There are two advantages gained in the use of a polynomial

(i) Less memory space is used up in any computer used to calculate values of v(t) or s(t).

(ii) No interpolation is required when values of time, the independent variable in most of the calculations in this thesis do not correspond to those in the tables.

A possible disadvantage is that considerable effort is required to deduce the polynomials in the first place. There is also the slight loss of generality in that the polynomial using average values for the constants does cause a very slight error in calculations of v(t) and s(t). The error on v(t) is found to cause errors of less than 2° in the calculation of shock-cone angle.

5.4 SIMPLIFIED EMPIRICAL MODEL OF N-WAVE - DISTANCE RELATIONSHIP

Consider a shell flying at supersonic speed as shown in Figure 18. The shell and the nose and base shock cones are shown in cross section.

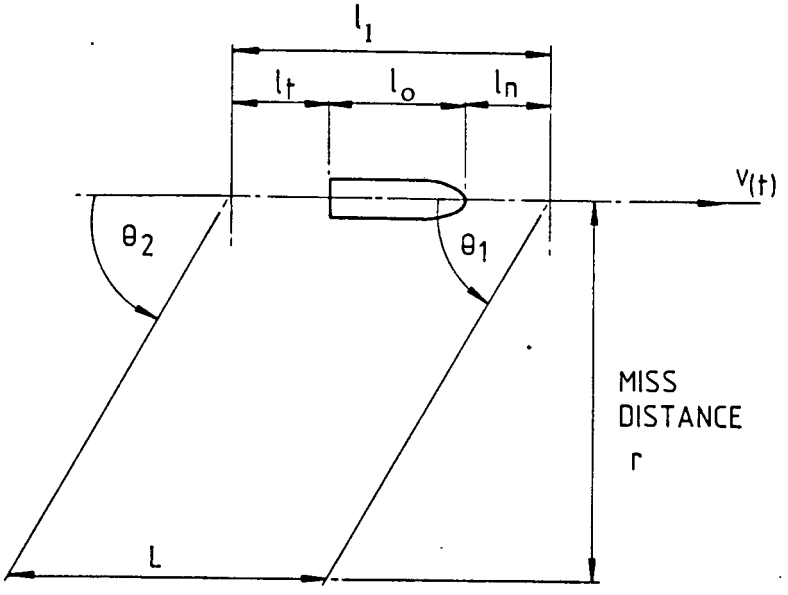

FIGURE 18: Supersonic shell in flight.

From the Schlieren photographs it is clear that the apex of the nose shock-cone is located some distance ahead of the shell. It is also clear that the apex of the base shock cone, a combination of several other cones, is located some distance behind the shell.

Let the true length of the shell = ℓ_o.

Let the distance between the apices of nose and base shock cones be ℓ_1.

Define $\ell_1 = m\,\ell_o$.

where m is some dimensionless constant.

Let the half angle of the nose shock cone be θ_1. Let the half angle of the base shock cone be θ_2.

At some distance r from the line of flight of the shell, the separation of the cones is L metres.

It can be shown that

$$L = \ell_1 + r\,(\cot\theta_2 - \cot\theta_1)$$

Define $\tan\theta_2 = \frac{1}{k}\,(\tan\theta_1)$

Then $$L = \ell_1 + r(k-1)\cdot\cot\theta_1$$

Since $\sin\theta_1 = \frac{1}{M_o}$ (From Refs 7, 13 and 14. See footnote to this page)

$$L = \ell_1 + r(k-1)\sqrt{M_o^2 - 1}$$

Note: This relationship was experimentally verified by the author by means of the Schlieren Photographs shown in Appendix I.

The shell is moving at v(t) metres per second so the time to cover the distance L is L/v(t).

Define $\tau = \frac{L}{v(t)}$

$= $ period of shock wave.

Thus

$$\tau = \frac{\ell_1 + r(k-1)\sqrt{M_o^2 - 1}}{v(t)}$$

$$= \frac{m\ell_o + r(k-1)\sqrt{M_o^2 - 1}}{v(t)} \qquad (5.7)$$

Equation (5.7) was used to find average values for m and k-1 over a range of preset miss distances at ranges of 500 and 1 000 metres.

The intention of this calculation was to find out whether k-1 and m varied with the velocity.

The results are shown in Table 9.

TABLE 9 : Values of m and k-1 for ranges of 500 and 1 000 m.

RANGE (m)	VELOCITY (ms^{-1})	ℓ_1 (m)	k-1	m
500	841,8	0,3202	$4,8416 \times 10^{-3}$	3,5274
1 000	664,59	0,2855	$3,5764 \times 10^{-3}$	3,1032

The implied variation of m and k-1 are:

$$m = 1.68785 + 2.1296 \times 10^{-3} v(t) \tag{5.8}$$

$$k-1 = 7.13951 \times v(t)_{\times 10^{-6}} - 1.1684 \times 10^{-3} \tag{5.9}$$

These relationships were used in all subsequent calculations.

To determine the miss distance from a given value of N-wave period, τ, equation (5.7) is rewritten as

$$r = \frac{\tau\, v(t) - m\ell_o}{(k-1)\sqrt{M_o^2 - 1}} \tag{5.10}$$

The expression for m and k-1 of equations (5.8) and (5.9) are substituted into equation (5.10) to yield

$$r = \frac{\tau\, v(t) - \ell_o\left(1.68785 + 2.1296 \times 10^{-3} v(t)\right)}{\left(7.139 \times 10^{-6} v(t) - 1.1684 \times 10^{-3}\right)\sqrt{M_o^2 - 1}} \tag{5.11}$$

for the 20 mm round used this expression becomes

$$r = \frac{\tau\, v(t) - 0.15528 - 1.95923 \times 10^{-4} v(t)}{\left(7.139 \times 10^{-6} v(t) - 1.1684 \times 10^{-3}\right)\sqrt{M_o^2 - 1}} \tag{5.12}$$

Equation (5.12) was used in all subsequent calculations to derive the miss distance from measured values of N-wave period.

The results obtained provided estimates of miss distance that were within 5-10% of the preset aimed miss distances.

The expression of equation (5.12) has considerable advantages of simplicity of calculation over that of equation (5.4), viz

(i) Only v(t) and τ need to be known (v(t) is known in all cases from the manufacturer's published firing tables).

(ii) The calculation can be performed by means of a very simple algorithm.

This empirical model of the shock waves of a supersonic shell takes no account of the thermodynamic or physical origin of the waves. It is based on one measured quantity τ and one derived quantity v(t) which is obtained from the time of flight and the polynomial for velocity. Thus values for m and k could be obtained for any type of round from a series of simple, controllable experiments.

5.5 LOCATING OF THE TRAJECTORY OF A SHELL

5.5.1 General

In a previous section, a relationship between the period of the N-wave and the distance from the flight path of the round was established. In this section one of the ways in which this information can be used will be explored. For the purpose of the mathematical analysis, it will be assumed that the distance estimates derived from these periods are accurate.

5.5.2 The Basic Measuring Problem

If only one sensor is used, which can provide a signal from which a distance estimate, r, can be made, then the best estimate of actual location of the source of the phenomenon sensed by the sensor is that it must lie on the surface of a sphere of radius r. This simple case is shown below in Figure 19.

This type of measurement is applied in Scalar UDI systems, generally with one or two thresholds for values of r, yielding very near-miss, near-miss and miss-indication.

In commercial systems for which information is available use is generally made of an amplitude-range equation.

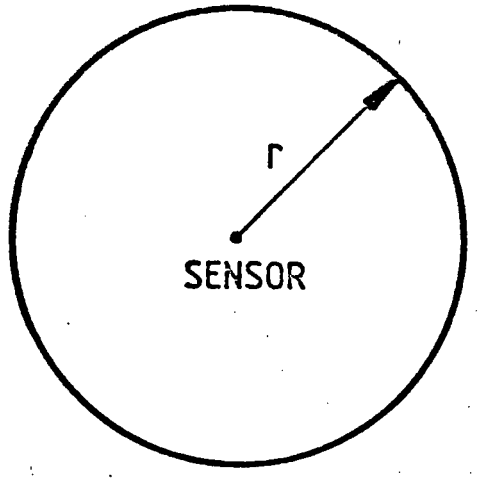

FIGURE 19: Resolution of a single sensor.

If two sensors are used which provide estimates r_1 and r_2 of the range of the disturbing phenomenon then the best estimate of location is that the phenomenon exists on the circle common to the two spheres as shown in Figure 20 below.

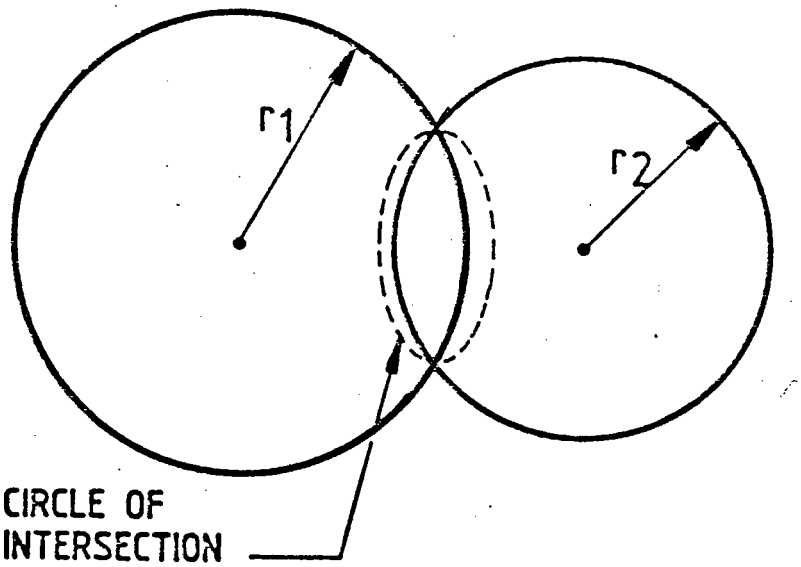

FIGURE 20 : Resolution of two sensors.

If a third sensor is added to the array, three estimates r_1, r_2 and r_3 of the distance to the disturbing phenomenon may be made. This situation is shown in Figure 21 below. For clarity, the estimates are shown as radii only, and not as spheres.

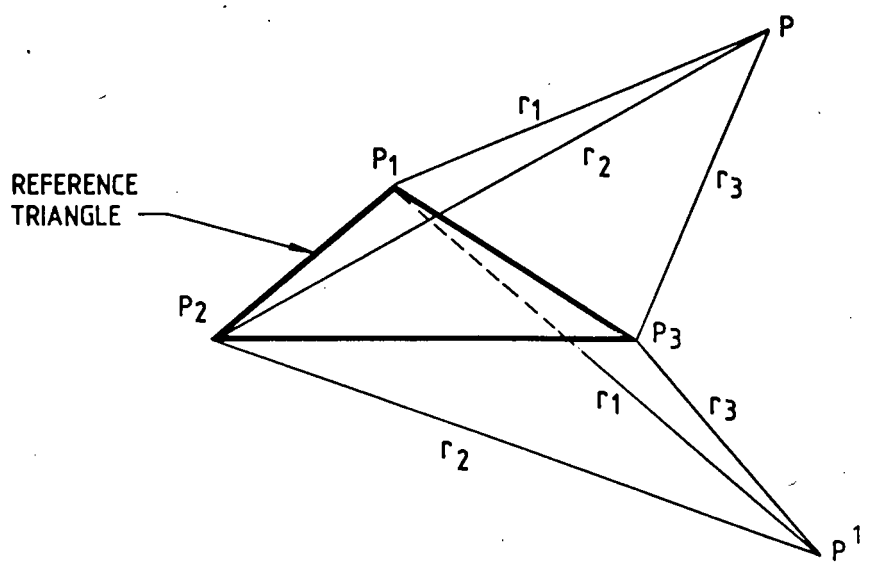

FIGURE 21 : Estimate of location by means of three sensors.

The sensors are located at P_1, P_2 and P_3 and supply estimates r_1, r_2 and r_3 respectively. Provided certain basic geometric criteria are met, the estimates imply the existence of two possible points P and P'.

The two solutions arise because of the nature of the equations describing the situation, viz the equations of the three spheres:

$$(x - x_1)^2 + (y - y_1)^2 + (z - z_1)^2 = r_1^2$$

$$(x - x_2)^2 + (y - y_2)^2 + (z - z_2)^2 = r_2^2$$

$$(x - x_3)^2 + (y - y_3)^2 + (z - z_3)^2 = r_3^2$$

The centres of the three spheres are located at:

P_1 ; (x_1, y_1, z_1)
P_2 ; (x_2, y_2, z_2)
P_3 ; (x_3, y_3, z_3)

respectively.

This ambiguity was recognised by the author and resolved in August 1982 by including a fourth sensor at P_4 supplying an estimate r_4 of the distance to the disturbing phenomenon.

The four sensors could be located anywhere in space and provided that the measurements (or deduction) of r_1, r_2, r_3 and r_4 were sufficiently accurate, the ambiguity could be resolved.

By adding a fourth sensor, not co-planar with the other three, a three-dimensional array is formed which has four triangular sides. Each triangle yields the locations of both an actual point P and a virtual point P'.

The hypothesis was then proposed by the author that:
the real point of location of the disturbing phenomenon would be where four of the points coincided.

A second hypothesis was also proposed by the author that:
if four of the implied points did not coincide, then the centre of gravity (COG) of the four points closest together would be the most likely estimate of the location of the disturbing phenomenon.

The application of these two theorems became known at NIAST as the "Method of Four Triangles". (See Appendix V for details).

The method is dealt with at some length because it has a bearing on several classes of estimation problem such as:

- Acoustic MDI
- Sonar location
- Ground impact scoring

In Ref 7, p 148 the use of a "string computer" to solve a ground scoring problem is described. The method of Four Triangles is a computational implementation of this method.

A string computer would be applied to this location problem by

(i) Drawing a triangle to scale representing P_1, P_2 and P_3.

(ii) Cutting lengths of string proportional to r_1, r_2 and r_3.

(iii) Securing one end of each string to the appropriate point (ie (P_1,r_1), (P_2,r_2), (P_3,r_3)).

(iv) Tying the three ends together and pulling the strings to ensure equal tension in each.

(v) Measuring the coordinates of the knot of (iv) above.

No standard method of solving the problem analytically could be found and the author was thus obliged to develop the method shown in Appendix V during April 1983.

Although the method could be applied to any four, non-coplanar points, it was decided for brevity and symmetry to use an array of sensors arranged to coincide with the four apices of a regular tetrahedron of side a. There is no theoretical reason why the sensors should be arranged to form a tetrahedron. Practical experience indicates that the sensors should be arranged:

- as far apart from each other as possible
- so as to prevent or avoid masking by the supporting structure.

5.5.3 Constraints and Sensitivity of the Method

Given the three points in space

$$P_1 : (x_1, y_1, z_1)$$
$$P_2 : (x_2, y_2, z_2)$$
$$P_3 : (x_3, y_3, z_3)$$

and the lengths r_1, r_2 and r_3, the r_i will only coincide if:

(a) they are long enough to reach from the apices to the centroid of the triangle (minimum lengths of r_i)

(b) any line, r_i, is long enough to reach from its particular origin, P_i, to the point of intersection acquires complex coordinates and has no real significance.

This constraint implies that the sensors should be arranged so that their separation is greater than the greatest expected error.

5.5.4 Introducing the Fourth Point

A fourth point (P_4; (x_4, y_4, z_4) is introduced and all the points P_1 to P_4 chosen to lie on the apices of a regular tetrahedron of side a.

Solving the triangles successively for two implied points each, yields:

for triangle $P_1P_2P_3$ the points P_a and P'_a

for triangle $P_2P_3P_4$ the points P_b and P'_b

for triangle $P_3P_4P_1$ the points P_c and P'_c

for triangle $P_4P_1P_2$ the points P_d and P'_d

Theoretically, only two triangles need to be used to resolve the dilemma inherent in the use of a single triangle. However, the addition of the fourth point to the array creates four triangles and there is no fundamental means of choosing between them.

Each triangle provides two estimates of the location of possible points. Hence four triangles provide 2^4 ie 16 possible groups of 4 points each as shown in Table 10.

GROUP NO	1	2	3	4	5	6	7	8	9	10	11	12	13	14	15	16
POINTS IN GROUP	P_a	P'_a	P_a	P_a	P_a	P'_a	P'_a	P'_a	P_a	P_a	P_a	P'_a	P'_a	P_a	P'_a	P'_a
	P_b	P_b	P'_b	P_b	P_b	P'_b	P_b	P_b	P'_b	P'_b	P_b	P'_b	P'_b	P'_b	P_b	P'_b
	P_c	P_c	P_c	P'_c	P_c	P_c	P'_c	P_c	P'_c	P_c	P'_c	P'_c	P_c	P'_c	P'_c	P'_c
	P_d	P_d	P_d	P_d	P'_d	P_d	P_d	P'_d	P_d	P'_d	P'_d	P_d	P'_d	P'_d	P'_d	P'_d

TABLE 10: Sixteen groups of four points each

The centre of gravity of each of the 16 clusters of points is:

$$\left[\frac{1}{4} \sum_{i=1}^{4} x_i \ , \ \frac{1}{4} \sum_{i=1}^{4} y_i \ , \ \frac{1}{4} \sum_{i=1}^{4} z_i \right] = (\bar{x} \ , \ \bar{y} \ , \ \bar{z})$$

The Variance of each cluster of four points is, h

$$h^2 = \frac{1}{4}\sum_{i=1}^{4}(\bar{x} - x_i)^2 + \frac{1}{4}\sum_{i=1}^{4}(\bar{y} - y_i)^2 + \frac{1}{4}\sum_{i=1}^{4}(\bar{z} - z_i)^2$$

As stated earlier, in paragraph 5.5.2, the author contended that the Centre of gravity of the cluster of points with the smallest variance provided the best estimate of a point through which the projectile passed at supersonic speed.

Again making use of a computer, it is a straight forward task to calculate the COG and variance of each cluster of four points and then to select the COG of the cluster with the smallest variance.

Because of masking, interference or equipment malfunction it is possible that not all four sensors will respond for each shot. It is very easy to include redundant timers in such a way that no four are co-planar. The likelihood, say, that four out of six readings will be valid, is considered to be greater than that four out of four will be valid.

5.6 SPECIFICATION AND DESIGN OF HARDWARE TO MEASURE THE REQUIRED TIMES.

(i) Time of flight

It has been shown that the instantaneous velocity can be deduced from the time of flight by making use of equation 5.3.2. The first requirement was thus to detect the exit of the shell from the muzzle of the gun and start a timer which was stopped when the shell passed the sensor.

The times of flight are referred to as t_i in what follows.

The time t_i was measured in practice by placing a microphone of medium quality (bandwidth 30-20 000 Hz) about 3 m from the muzzle.

When the gun is fired, the microphone produces a large noisy output with at least one large positive voltage spike close to the start of the output. This spike is easy to detect and is used as the starting pulse, t_o.

A timing error of 1-5 micro seconds may occur in detecting this pulse. Because the expected value of t_i is about 0,6 s for a range of 500 m and 1,2 s for a range of 1000 m, this error is negligible.

The start pulse t_o is used to trigger a tone burst of 5400 Hz which is applied to the input of a 179 MHz transmitter mounted near the gun. The arrangement is shown schematically in Figure 22. In practice the detector used could detect the first large positive or negative signal and prevent subsequent pulses from reaching and retriggering the threshold detector.

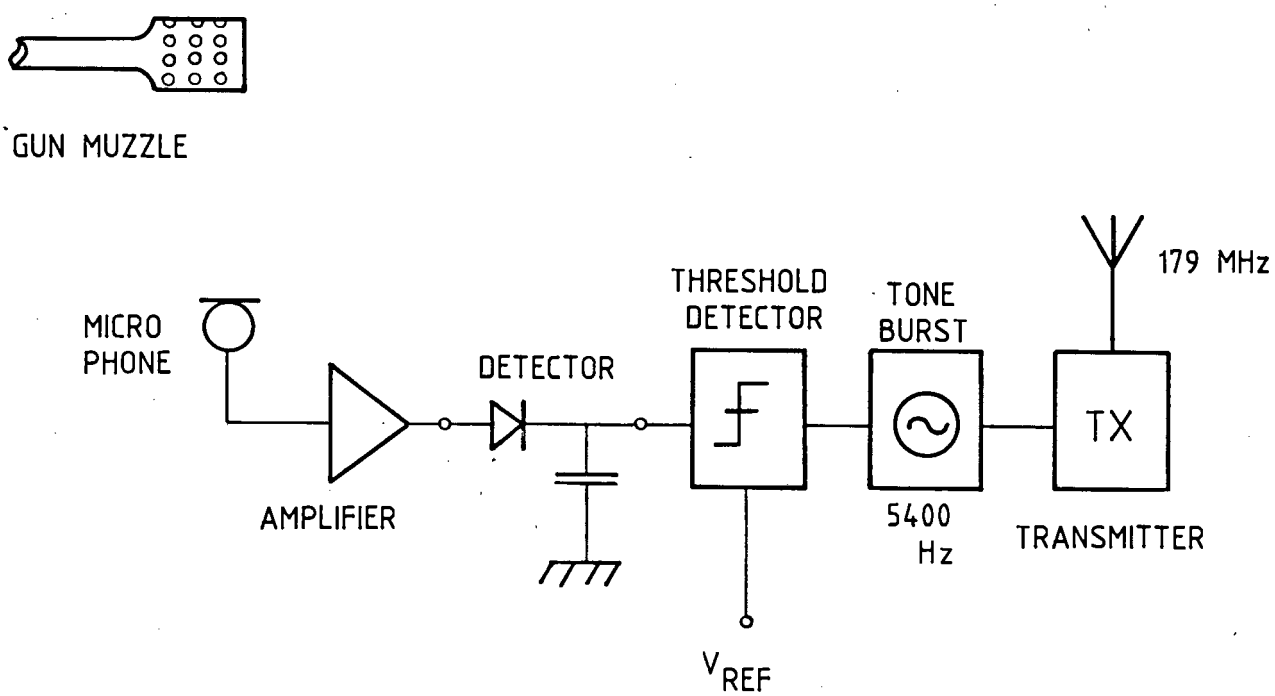

FIGURE 22: Diagram of muzzle blast detector.

A receiver may be positioned down-range at say 500 m. This receiver will detect the tone burst and start a timer.

A processing delay is incurred because of the rise times of receiver I/F circuits and output filters. The tone decoder used to decode the 5400 Hz burst also contributes delay. The time of flight measurement could be in error by up to 5 ms.

Using 5.3.1 for S(t), the error on distance computed at 500 m is about 4 m on slant range.

Solving 5.3.2 for $\nu(t)$, the velocity error caused is about 2,3 ms^{-1}. This causes an error of about 0,04° in the estimate of θ, the half-angle of the shock cone.

Because the method proposed by the author uses **relative** differences, these seemingly large errors do not affect calculation of miss distance.

The counters at the receiver are thus started within 5 ms of the muzzle blast.

The shell reaches the vicinity of the receiver about 0,6 sec after the muzzle blast and, moving in excess of mach 1,0, causes an N-wave which can be detected, and used to stop the counters.

The situation is shown diagrammatically in Figure 23.

The tone decoder is a phase-locked-loop (PLL) tuned to 5400 Hz.

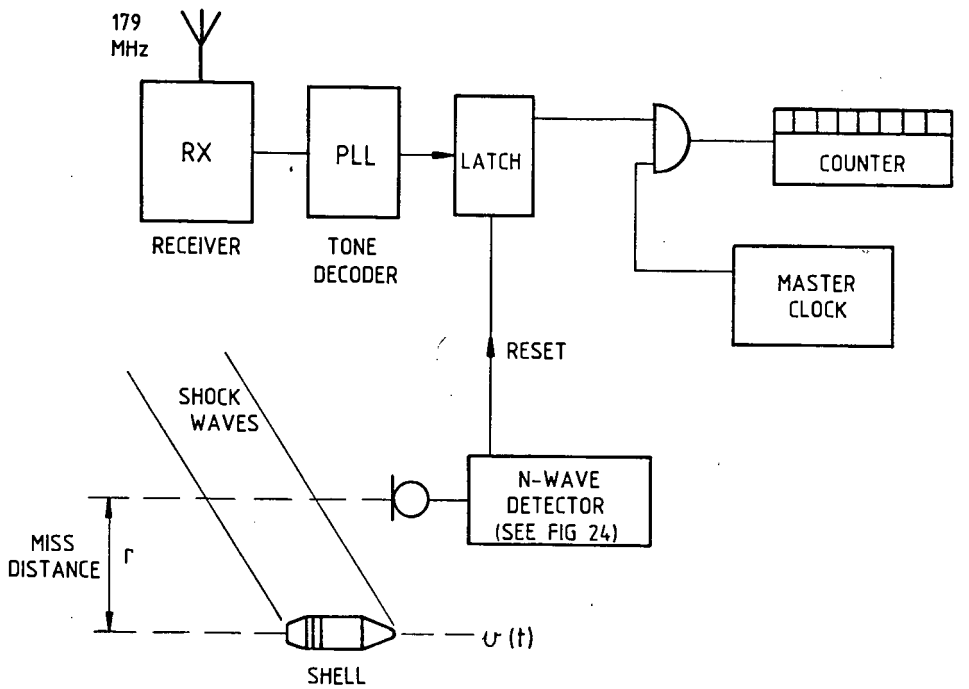

FIGURE 23: Receiver stage of time of flight measurement

Note:

(a) The means of detecting that the disturbance at the sensor was caused by an N-wave and not noise is dealt with subsequently and described in great detail in Ref 19.

(b) Because the shell may be past the microphone when the shock wave reaches it, estimates of S(t) must be corrected by adding $\frac{r}{\tan\theta}$ to S(t) where r and θ are as previously defined.

(ii) Measurement of the Period of the N-Wave

Examination of the N-waves shown in Appendix III shows that while some exhibit the theoretically predicted features, others are severely distorted as discussed in paragraph 3.2 (v).

In 1981 the author developed circuitry which detected the amplitude of an N-wave and established that the amplitude had been present for at least some minimum time, say 75% of the theoretically expected duration.

Experiments in 1983 were called off because wind, gusting at up to 10-15 kts (very mild) was disturbing the microphones. The author made recordings of the effect of this wind and after examining these on a spectrum analyzer found that almost all of the energy was below 600 Hz.

Accordingly a wind-noise filter was introduced into the signal path.

The final part of the circuit was a rate detector Ref 19 which detects the two positive flanks of the N-wave. These are characterized by rise times of about 200 kv/sec. A circuit was developed which

(i) detected this slope when +ve
(ii) ignored it when -ve
(iii) ignored it when slower than a given rate, derived from detailed observations of many N-waves.

The detector was thus designed to detect a specific non-linear event. The reference rates in the N-wave detectors were set at 180 kV/sec.

The microphones have a 3 dB point at 30 kHz. This implies a step response which is a ramp of slope $2\pi f\hat{A}$, where $\hat{A}$ is the peak amplitude of the step. Using the stated values the slope is 188 kV/sec for a 1 voltstep.

All the subsequent circuitry has design bandwidth greater than 30 kHz.

Note: Other microphone properties are shown on page 70.

The final arrangement is shown in Figure 24.

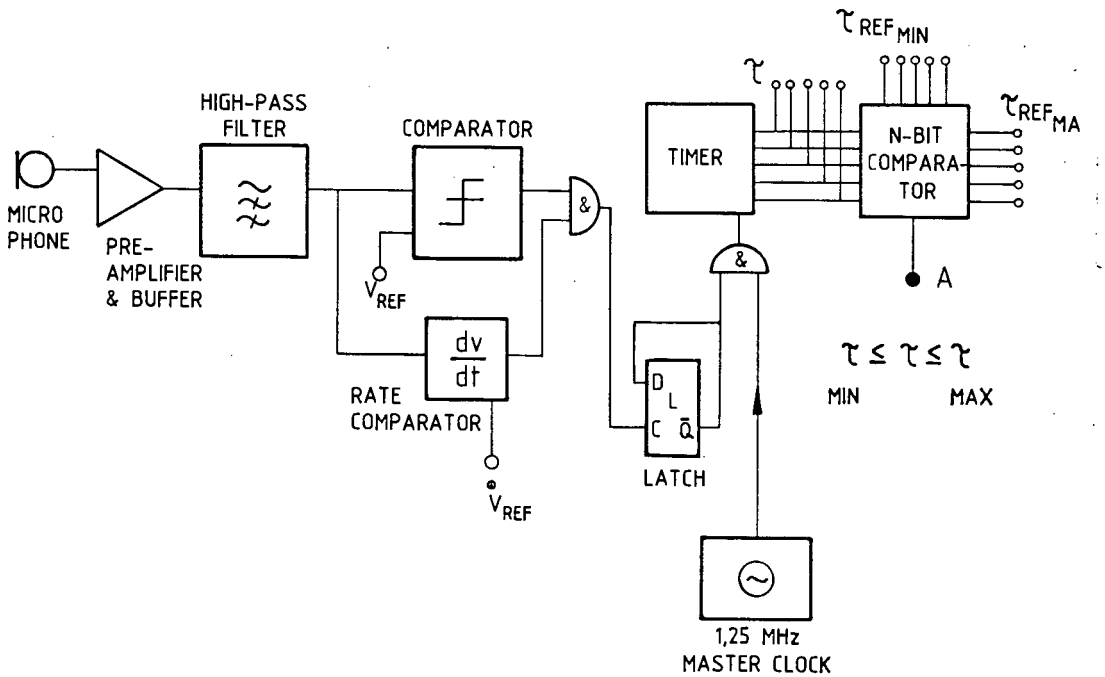

FIGURE 24: N-wave detector

In operation, if both the reference voltage, 4,7 V, and the rate, 200 kv/sec are exceeded, the latch, L, is set and clock pulses are admitted to the timer.

The output of the times is compared, in an N-bit comparator, against τ_{min} and τ_{max} the minimum and maximum expected N-wave periods respectively.

If no second pulse arrives, τ_{max} is exceeded and the counter and latch reset by supervisory circuitry not shown here.

If the second pulse arrives too soon, τ_{min} is not exceeded and again a reset takes place.

If the second pulse arrives in the time window τ_{min} to τ_{max} (in practice 400 - 800 μs) a valid N-wave is deemed to have occurred. In this case the latch is reset, the counter stopped and the count read out to buffering and printer stages for permanent record.

Supervisory circuitry is arranged to print specific messages such as:

- WILD SHOT (Muzzle blast but no N-wave)
- NOISE (N-wave but no muzzle blast)
- RESET (In event of manual reset or after printing valid N-wave times)

In addition a digital multiplexer is arranged to perform the following functions:

- Print N-wave time and time of flight in a pre-set format for each microphone
- Read the buffered information to the printer

The combined system diagram which includes features of Figures 23 and 24 is shown in Figure 25 together with the supervisory and multiplexer circuits. For the experiments conducted by the author five microphones were used.

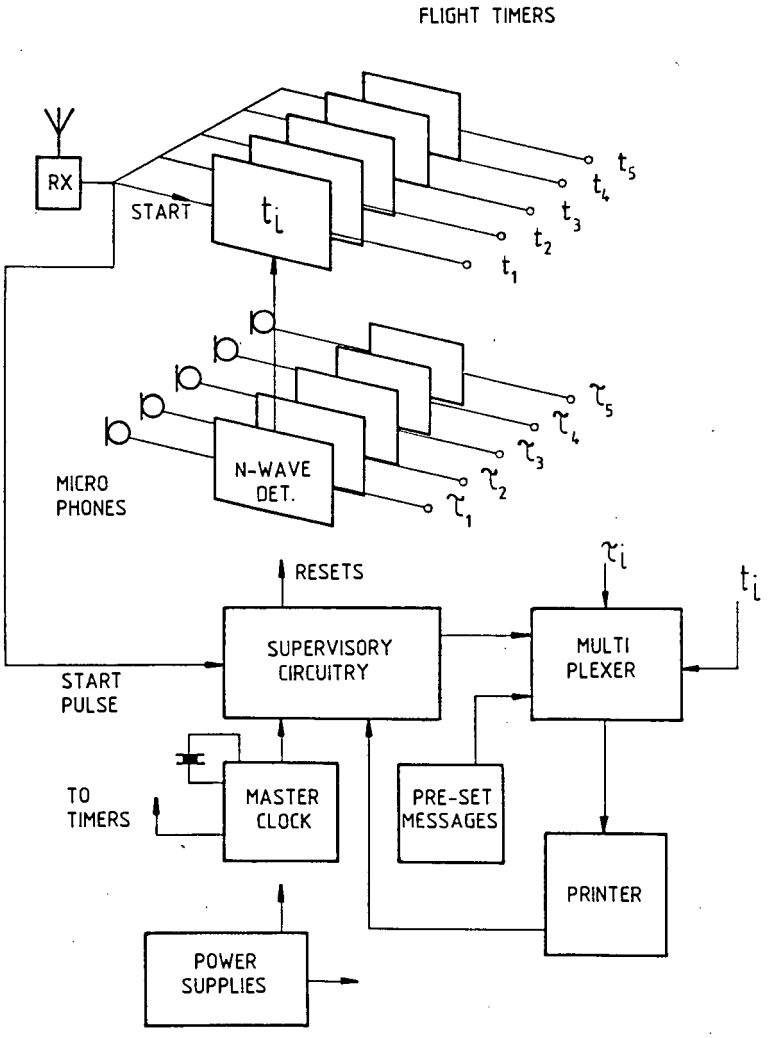

FIGURE 25: Target system block diagram

In the experiments performed by the author, the link between the printer and the target system was a 50 m cable. It is intended to replace this table with a radio link from the airborne target.

(iii) Microphones used in Experiments

Because no data was available which accurately described the frequency components of an N-wave, the author decided that experiments should be conducted with microphones that had a frequency response as wide as possible.

At a later stage of the work, the performance could be reduced by including filters of lower and lower cut-off frequency until performance, under known conditions, of the whole system, could be seen to be affected. A lower cost microphone could then be specified. This part of the work has not yet been addressed.

Details of the microphones used in the experiments are as follows:

- diameter 3 mm
- length 3 mm
- preamplifier B & K 2639 T
- bandwidth ~30 kHz

Note: These microphones are expensive and for cost effectiveness, a cheaper type will have to be used operationally.

Spectra of the N-waves show a peak at about 2200 Hz and harmonics at integral multiples of this extending to 20 kHz and beyond, at about 16 dB below the peak.

5.7 EXPERIMENTAL PROCEDURE

5.7.1 The Microphone Array

The array is shown in Figure 26. The locations of the microphones, described by the axes shown remains fixed.

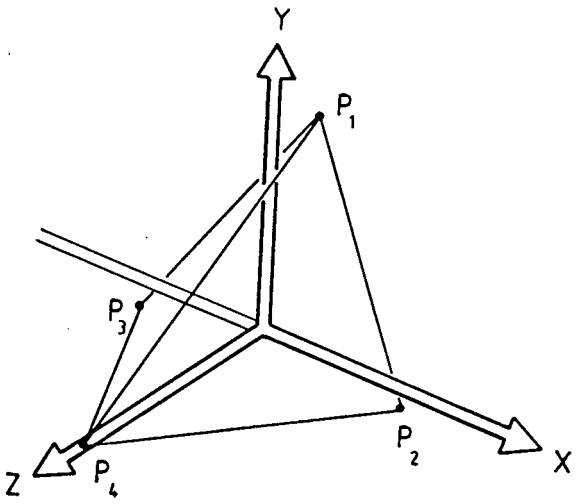

FIGURE 26: The Reference Axes and Microphone Locations

The location of the tetrahedron array of microphones in the axes is arbitrary.

The microphone array was arranged to be in a given orientation relative to the gun and the line of fire.

The array was arranged at a height of 4m above the ground for all experiments.

The orientations used were those set out below. In this context vertical and horizontal refer to true, fixed terrestrial directions relative to which the target axes might move. The figures are diagrammatic and are not to scale.

(i) Orientation I (See Figure 27)

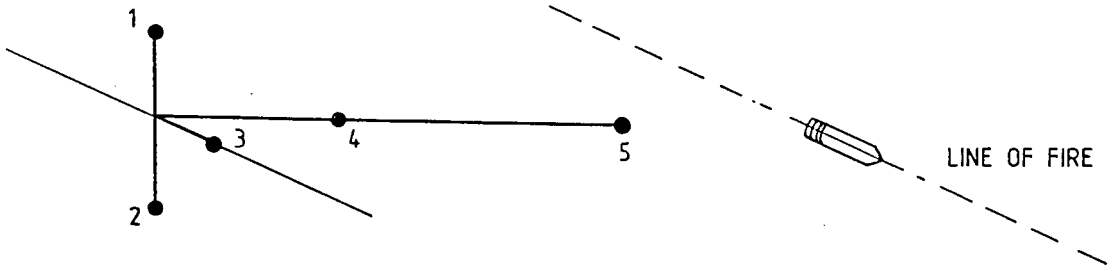

FIGURE 27: Orientation I

Microphones:
- 1, 2 Vertical; 1 above
- 3 horizontal pointing down range
- 4, 5 horizontal at right angles to line of fire.

(ii) Orientation II (See Figure 28)

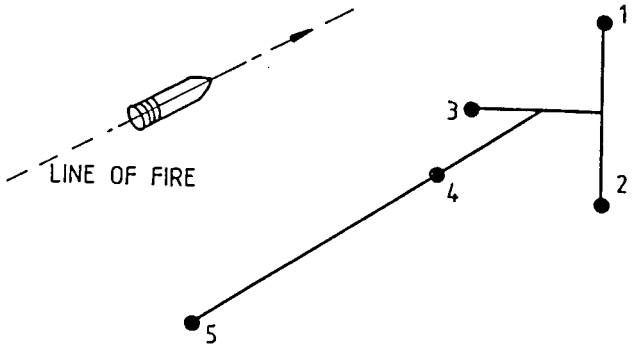

FIGURE 28: Orientation II

Microphones:
- 1, 2 vertical; 1 above
- 3 horizontal pointing at right angles to line of fire
- 4, 5 parallel to line of fire pointing towards gun.

(iii) Orientation V (See Figure 29)

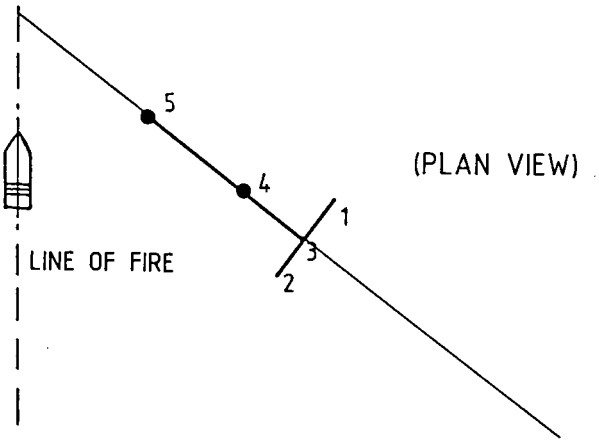

FIGURE 29: Orientation V

Microphones:
- 1, 2 horizontal below
- 3 vertical above
- 4, 5 pointing down range making an acute angle of 45° with the line of fire.

(iv) Orientation VIII (See Figure 30)

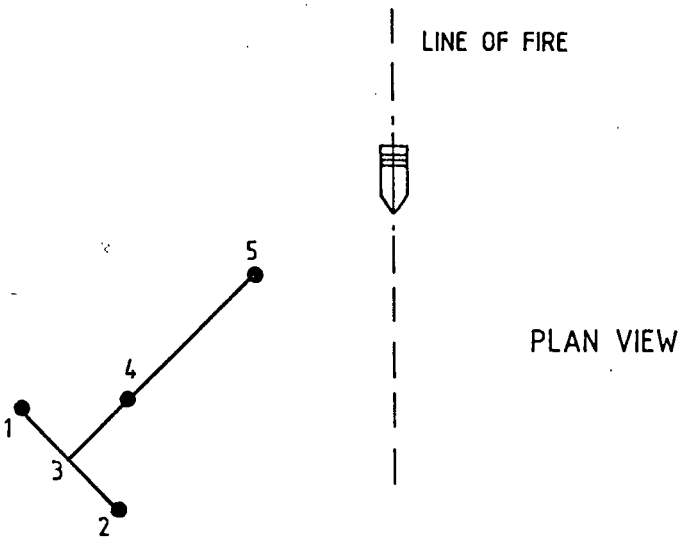

FIGURE 30: Orientation VIII

Microphones:
- 1, 2 horizontal below (1 closer to gun)
- 3 vertical upper
- 4, 5 horizontal pointing up range towards gun making an angle of 135° with the line of fire.

(v) Orientation IX (See Figure 31)

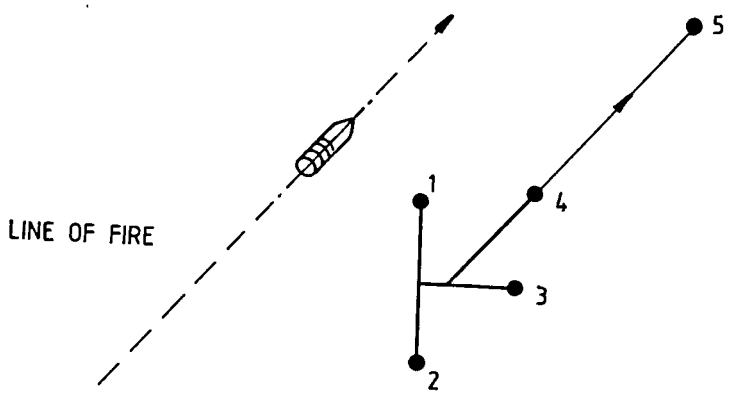

FIGURE 31: Orientation IX

Microphones:
- 1, 2 vertical; 1 above
- 3 horizontal pointing at right angles away from line of fire
- 4, 5 horizontal pointing downrange, parallel to line of fire.

(vi) Orientation X (See Figure 32)

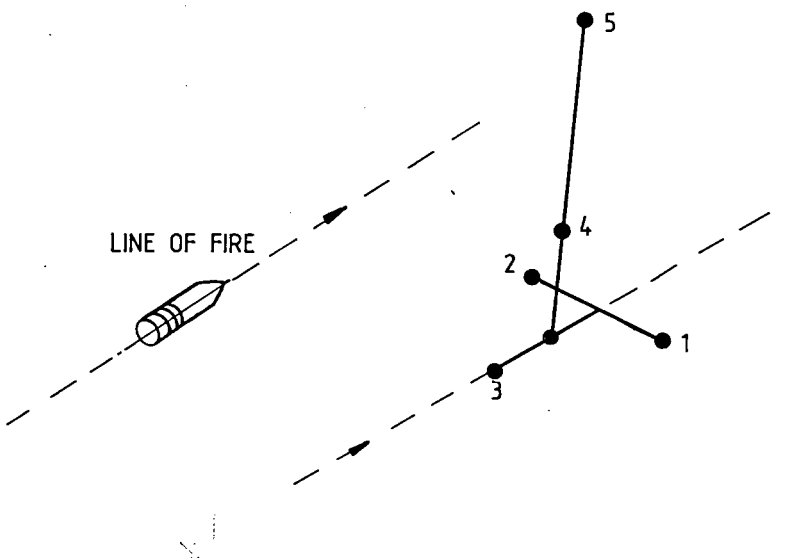

FIGURE 32: Orientation X

Microphones:
- 1, 2 horizontal at right angle to line of fire, 2 being closer
- 3 horizontal pointing up range parallel to line of fire
- 4, 5 vertical

(vii) Orientation XV (See Figure 33)

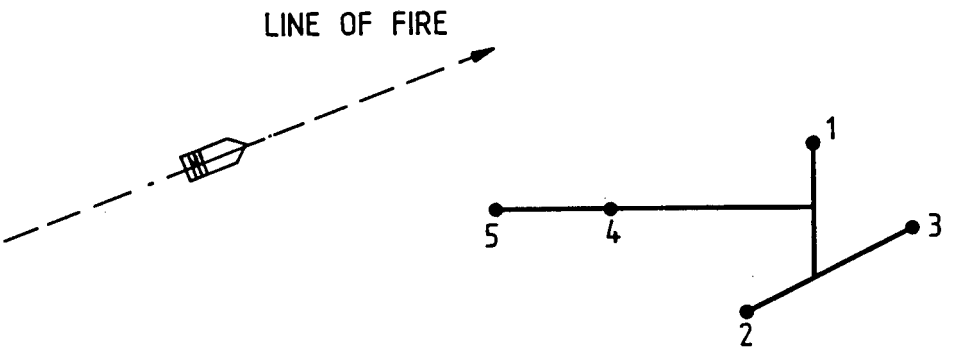

FIGURE 33: Orientation XV

Microphones:
- 2, 3 horizontal parallel to line of fire; 3 down range
- 1 vertical
- 4, 5 horizontal at rt angles to line of fire

(viii) Orientation XVI (See Figure 34)

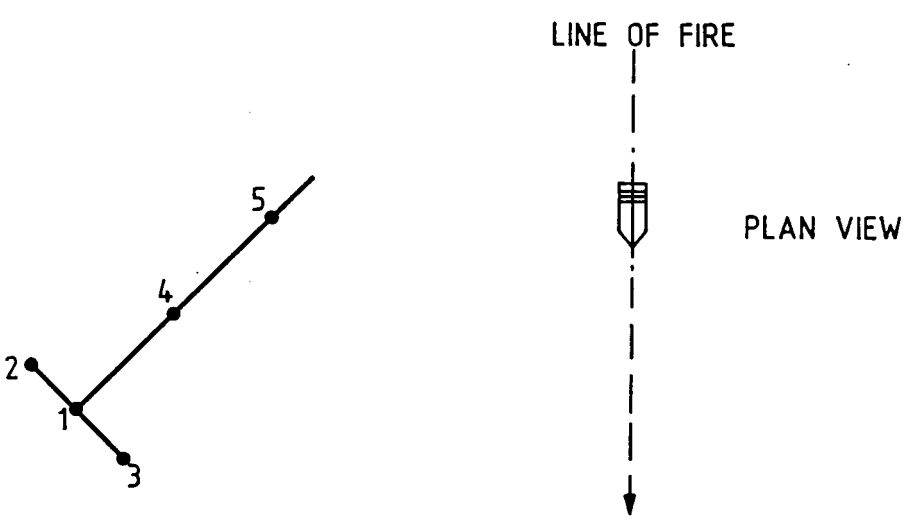

FIGURE 34: Orientation XVI

Microphones:
- 2, 3 horizontal at 45° to line of fire; 3 down range
- 1 vertical
- 4, 5 horizontal at an angle of 45° to line of fire 5 up range

(ix) Orientation XVII (See Figure 35)

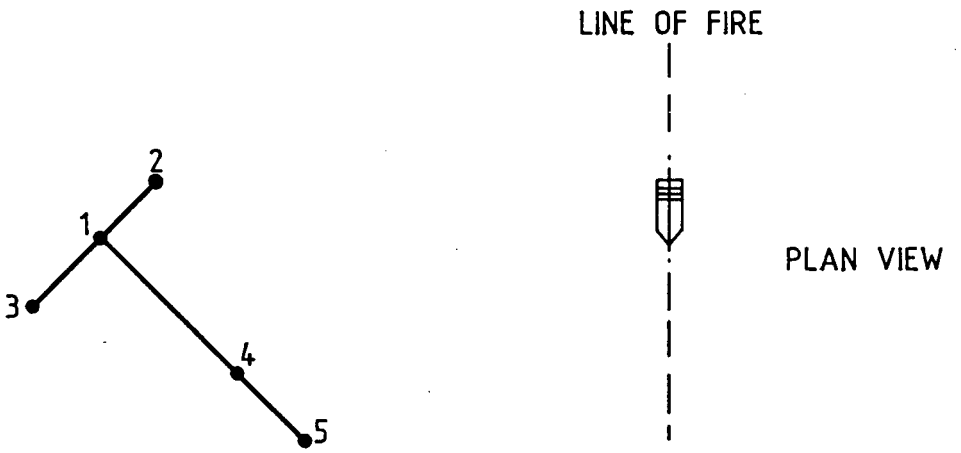

FIGURE 35: Orientation XVII

Microphones:
- 2, 3 horizontal, at 135° to line of fire; 3 down range
- 1 vertical
- 4, 5 at an angle of 45° to line of fire, 5 down range

(x) Orientation XVIII (See Figure 36)

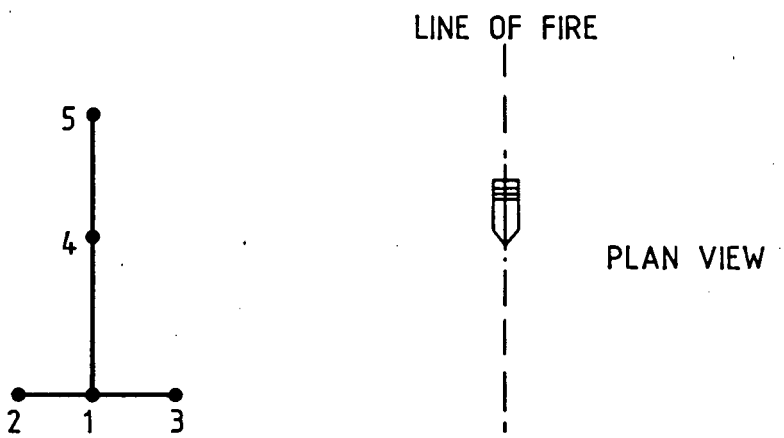

FIGURE 36: Orientation XVIII

Microphones:
- 2, 3 horizontal at right angles to line of fire; 3 being closer
- 1 vertical
- 4, 5 horizontal pointing up range

Note: An infinite number of orientations of the target relative to the line of fire is possible. Ten were chosen in an arbitrary way. Systematic prescription of orientations will be necessary to analyze error of measurement of minimum vectors in terms of masking and mathematical sensitivity. This work is intended for the future.

5.7.2 Aiming Procedure

The target was set up at 4m above the ground at a given range (500 or 1000m). To the left and right of the target were placed flags at 2,5m above the ground. The flags were spaced 5, 10 and 15m left and right of the target as seen by the gunner. The gunner could thus use his sight graticule to aim 5,10 or 15m left or right and interpolate to aim at elevations of zero, (in line with target) 1, 2 or 5m above it.

A code was derived which describes the aim. Thus

- 5L0 means 5m left of target, elevation 0
- 0H5 means 5m above the target
- 15R1 means 15m right of target, elevation 1m.

These descriptions, together with the orientation and range allow each aimed point to be expressed in either target or range coordinates.

For each shot it is necessary to calculate in target coordinates the point through which the shot should have passed as well as the point through which it actually passed.

Two procedures were adopted to relate aimed and measured miss vector. In early experiments it was important to establish that scalar miss-distance was measurable and that misses to left and right could be distinguished from each other. At that stage of development, no actual verification of a point on the trajectory was deemed necessary by the author. Accordingly total reliance was placed on the ability

of the gunner to fire a shell over a given flag (see Figure 37). During experiments on 29th January 1985 it was verified that

- the sequence of stimulations of the microphones was as expected from inspection of the reference axes in the various orientations;

- the scalar miss distance as measured was generally within ± 15% of that aimed;

- misses to left and right more distinguishable from each other.

In subsequent experiments on 18th June 1985 plywood screens 2400 mm x 1200 mm were erected so that the exact miss distance could be measured. The centres of these screens were horizontally in line with the centroid of the microphone array and set at 5, 10 and 15 meters left of the array.

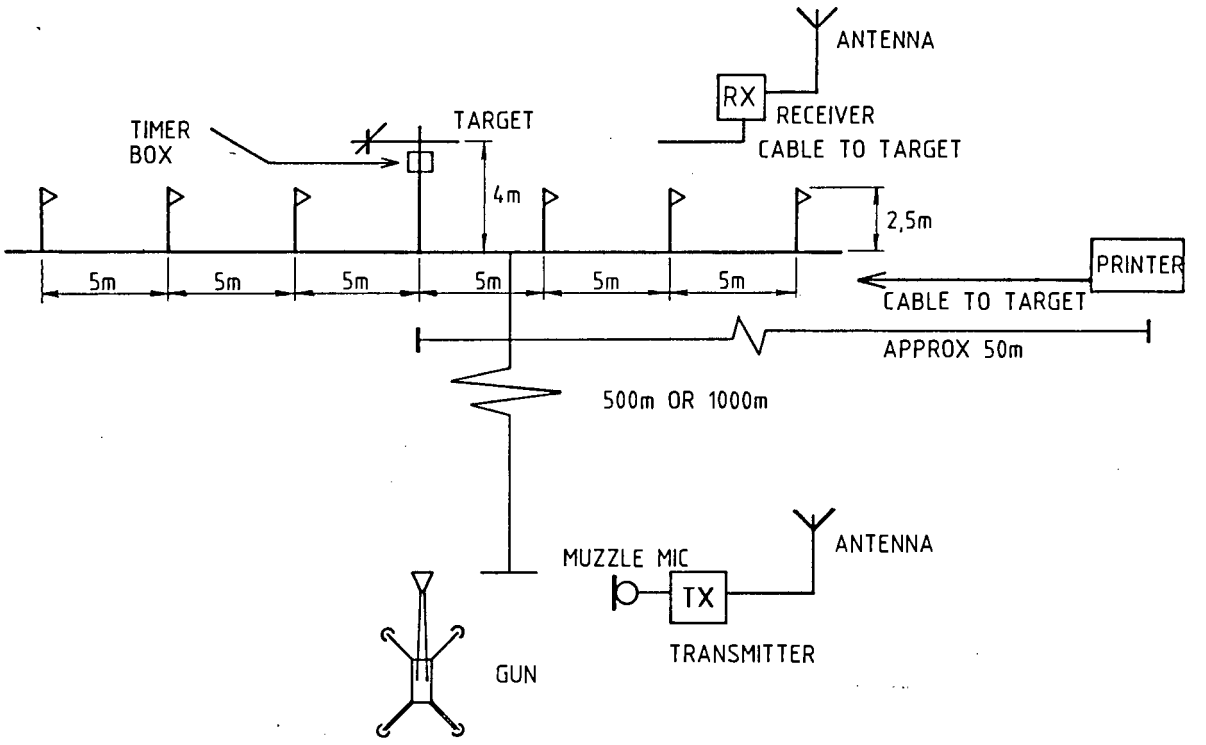

FIGURE 37: Set up at Shooting Range

Throughout these experiments range safety officers were present and due attention was paid to safety procedure.

6 CONCLUSIONS

The literature survey of Chapter 2 shows that acoustic measurements have been used to determine Miss Distance but have been limited in all but one case to zone and sector indication. All but two of the systems reviewed make use of the amplitude of the supersonic shockwave, despite the relative ease of measuring its period. The vector system described in this thesis represents an advance over available systems. Acoustic measurement of Miss Distance is attractive because it entails no modification of the typically small anti-aircraft rounds.

A simple empirical relationship between N-wave period and miss distance is developed in Chapter 5 (paragraph 5.4) and verified by practical measurements, the results of which are summarised in Appendix VIII.5. It is shown that the error in this estimate is systematic and reducible to less than 18%.

It is shown in Section 5.5 that four estimates of the distances from an array of sensors to the path of the shell are sufficient to estimate the miss vector. The results of measurements are shown in Appendices VIII.6 and VIII.7. The error on the magnitude of the vector is about ±15% at most and that on the angle about ±10°.

The computation of the vector is sensitive to errors in the basic estimates of distance. It is shown in Appendix VIII that the errors are reduced by increasing the dimensions of the array of sensors.

From the measured periods shown in Appendix IX.1 it can be seen that failure by one sensor out of five, to detect a shockwave occurs in about 20% of cases. These failures are ascribed to masking of sensors by the structure of the array and imply that redundant sensors should be included in any practical design.

7 REFERENCES

[1] "Data Reduction and Analysis Techniques for Miss Distance Indicator and Scoring Systems". Document 130-75; August 1975, White Sands Missile Range, New Mexico 88002, New Mexico, USA.

[2] Bello, R C - "Miss Distance Indicators". Paper presented at the Naval Air Development Centre, Warminster, PA USA, 1981.

[3] Brondstatter, W W and Ford, J - "Report on Results of Concept Formulation Activities for an Armed Aircraft Qualification Range Scoring System". NAVTRADEVCEN 69-C-0178-1, Orlando, Florida, April 1970.

[4] Gander, T J - "WILDCAT twin 30 mm SPAAG firing trials". International Defence Review, Vol 4, No 2, 1983.

[5] Article - "The MAE 15 Automatic Scoring System for Air Targets". International Defence Review, May 1975.

[6] Swedair Trade Literature (1982) - "Miss Distance Calculator MDC80 ATA/GTA". Swedair AB, Stockholm, Sweden.

[7] Chubb, T W - "Gun harmonization using the Sector Miss Distance Indicator". Royal Aircraft Establishment Farnborough, England.

[8] Sedivec, D F, Lloyd, BV and Dawes, DL - "Concept Formulation Study for an Armed Aircraft Qualification Range Scoring System". Report 69-C-0179-1, Naval Training Device Centre, Orlando, Florida, USA, 1970.

[9] Société Européenne de Propulsion Trade Literature -"Acoustic Scoring System". SEP, Paris, 1981.

[10] Sellman, UCI - "Projectile Miss Distance Device for use on a Target or the like". US Patent: 3 217 290; 9 Nov 1965.

[11] SFENA - "System for Acoustical Detection of Projectiles Passing in the Vicinity of an Airborne Target". British Patent 2089/60, 902756 of 20 Jan 1960.

[12] Mattei, J I, Vincennes, J B and Manganne, R - "Acoustical Firing Indicator". US Patent 2925582, 16 Feb 1960, US Patent Office.

[13] Snow, W B - "Survey of Acoustic Characteristics of Bullet Shock Waves". IEEE Transactions on Audio and Electroacoustics, Vol Au-15, No 4, December 1967.

[14] Du Mond, J W M, Cohen, E R, Panofsky, W K H and Deeds, E - "A Determination of the Wave Forms and Laws of Propagation Dissipation of Ballistic Shock Waves". Journal of the Acoustical Society of America, Vol 18, No 1, July 1946.

[15] Contraves, A G, Trade Literature - "Skytrack". International Defence Review, Vol 15, No 11, November 1982.

[16] Smith, A T - "Miss Distance Measurement using one Camera". Royal Aircraft Establishment, Farnborough, England, 1973.

[17] Mermagen, W H - "Measurements of the Dynamical Behaviour of Projectiles over long Flight Paths". Journal of Spacecraft, USA, Vol 8, No 4, April 1971.

[18] Klug, J and Whittle-Bennets, D - "Derivation of Equations of Motion for a 20 mm Round". Internal NIAST Publication, May 1983.

[19] Bruël and Kjaer, Master Catalogue, 980, p 110.

[20] Kappetijn, H - Internal NIAST Report, 1985.

APPENDICES

		PAGE
I	SCHLIEREN PHOTOGRAPHS OF 20 MM ROUNDS FOR VARIOUS MACH NUMBERS.	A.2
II	DIMENSIONS OF 20 MM ROUND USED IN EXPERIMENTS	A.9
III	PHOTOGRAPHS OF RECORDED N-WAVES	A.11
IV	SPECIFICATION OF REFERENCE - AXES OF THE TARGET SYSTEM	A.15
V	MATHEMATICAL ANALYSIS: ESTIMATING THE COORDINATES OF TWO POSSIBLE POINTS (THE METHOD OF FOUR TRIANGLES)	A.19
VI	EXAMPLES OF CALCULATIONS USING THE METHOD OF APPENDIX V	A.25
VII	MATHEMATICAL ANALYSIS (ALTERNATIVE METHOD)	A.29
VIII	DISCUSSION OF RESULTS	A.34
IX	EXPERIMENTAL READINGS	A.54

APPENDIX I: SCHLIEREN PHOTOGRAPHS OF 20 MM ROUNDS FOR VARIOUS MACH NUMBERS.

The following pages show photographs taken in the High Speed Wind Tunnel of the National Institute for Aeronautics and Systems Technology. The author gratefully acknowledges the permission to use these facilities and the assistance of the Wind Tunnel Staff in producing the photographs.

Features which are significant to the discussions elsewhere in this thesis include the following:

(i) the nose wave is very sharply defined;

(ii) the geometric apex of the nose cone is located somewhat ahead of the nose of the round;

(iii) there is no very clearly defined base shock cone but rather a series of cones;

(iv) the last cone at the base is some distance behind the base of the round;

(v) the dense black line attached to the base of the round is the support (sting) on which the round was supported in the tunnel.

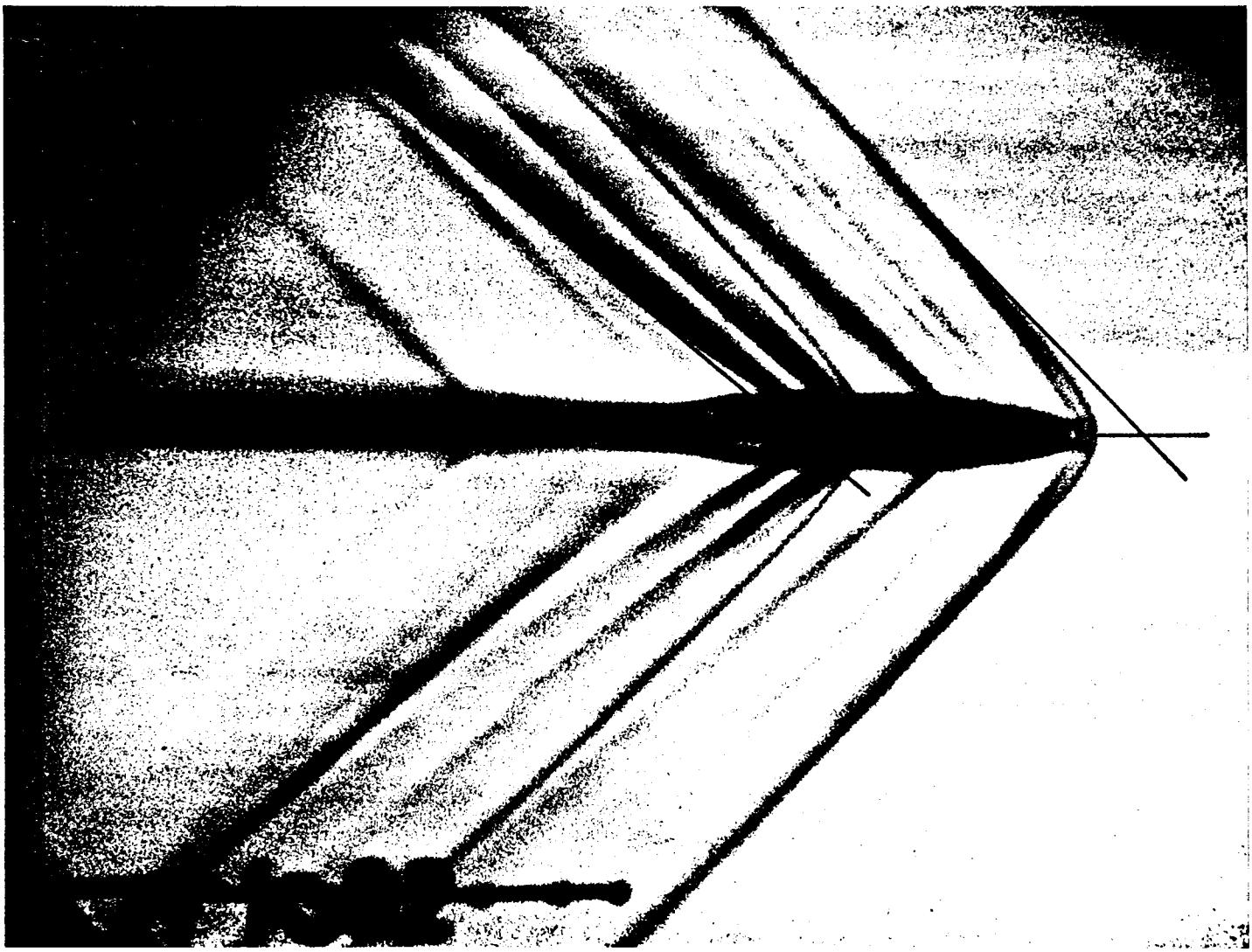

$\theta_1 = 46°$

$\theta_2 = 40°$

$\sin^{-1} \frac{1}{M_0} = 42° 30'$

FIGURE I.1: Round at M = 1,48

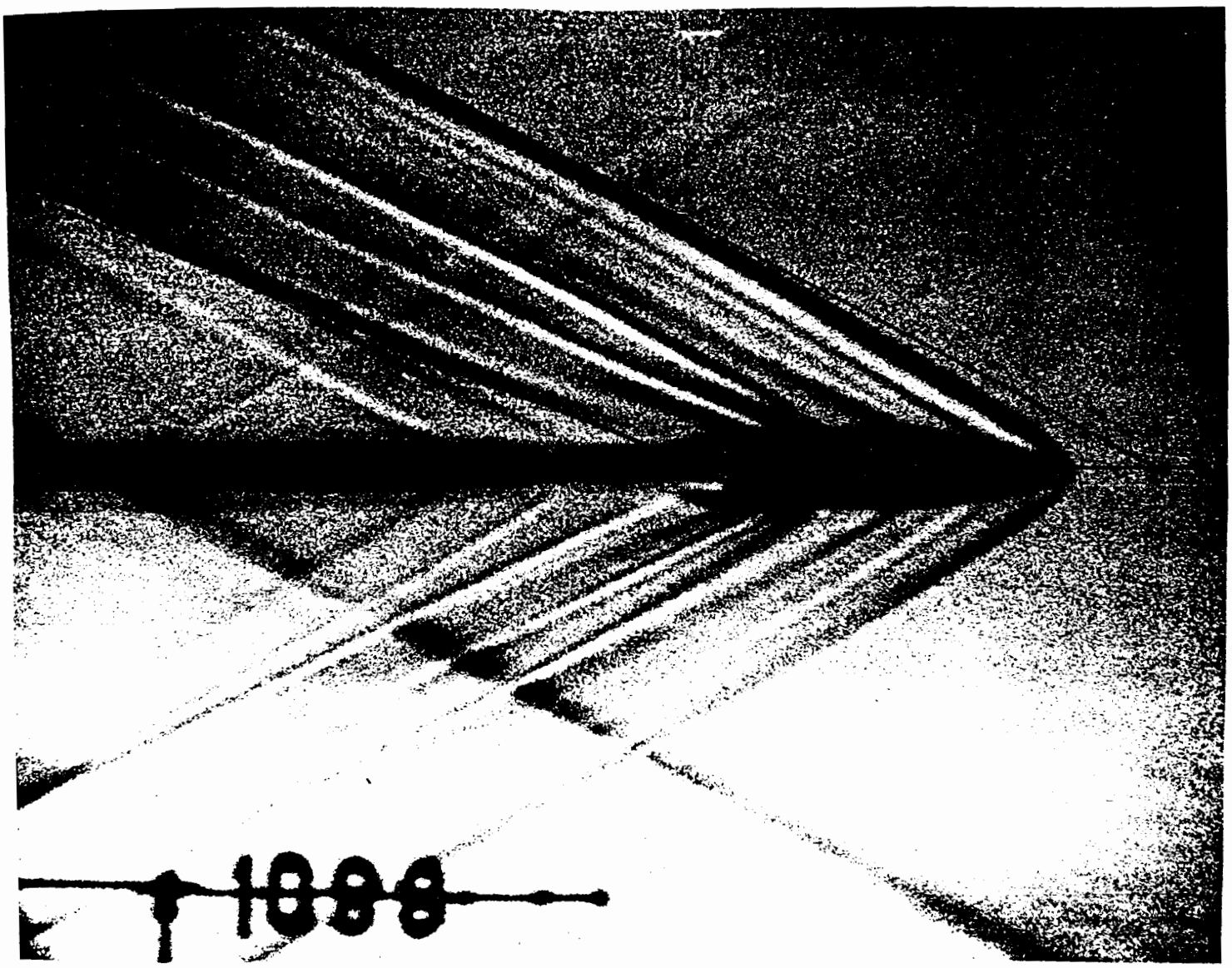

$\theta_1 = 27,7°$

$\theta_2 = 21\frac{1}{2}°$

$\sin^{-1} \frac{1}{M_0} = 27° 2'$

FIGURE I.2: Round at M = 2,20

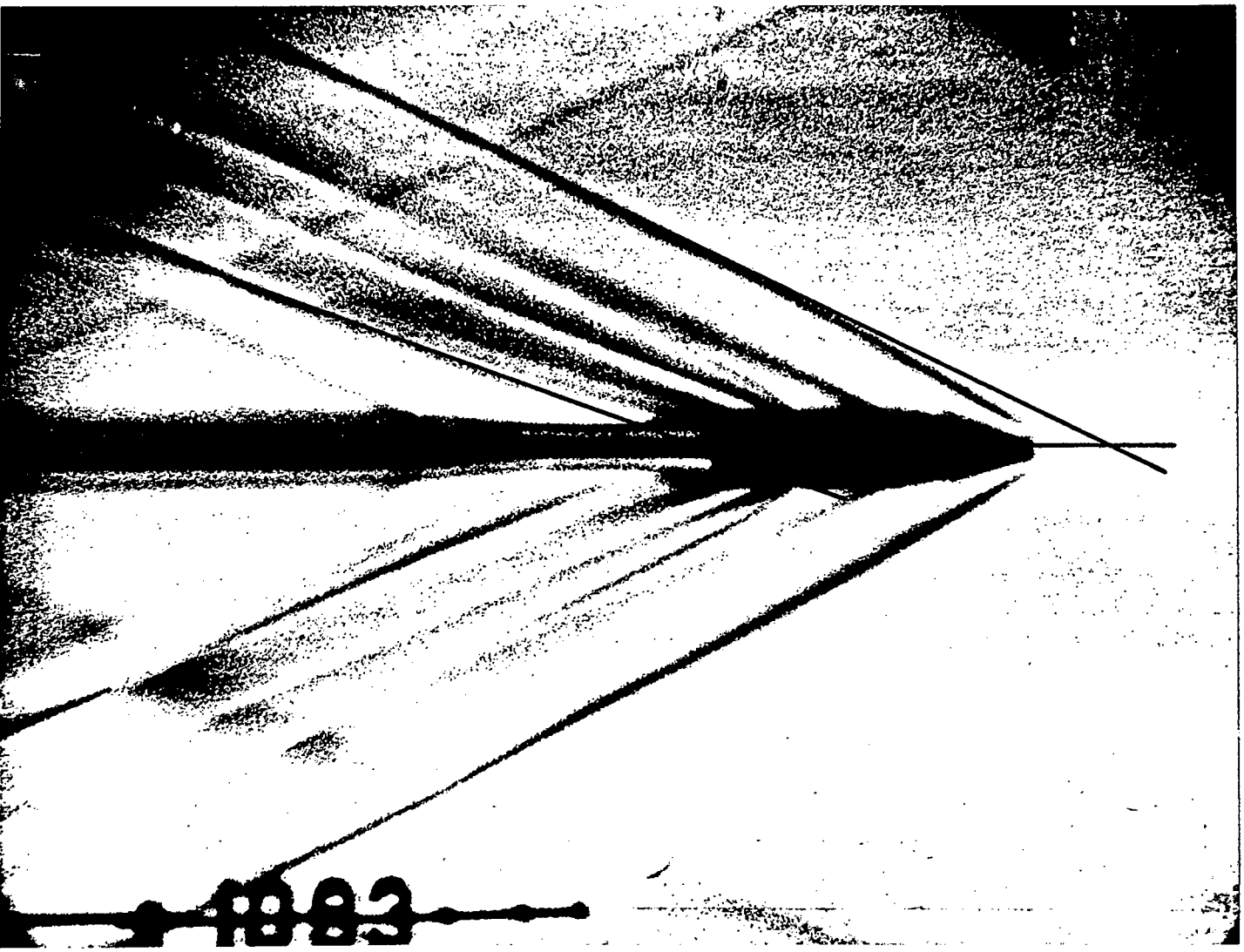

$\theta_1 = 25,5°$

$\theta_2 = 19,7°$

$\sin^{-1} \frac{1}{M_0} = 23,3°$

FIGURE I.3: Round at M = 2,52

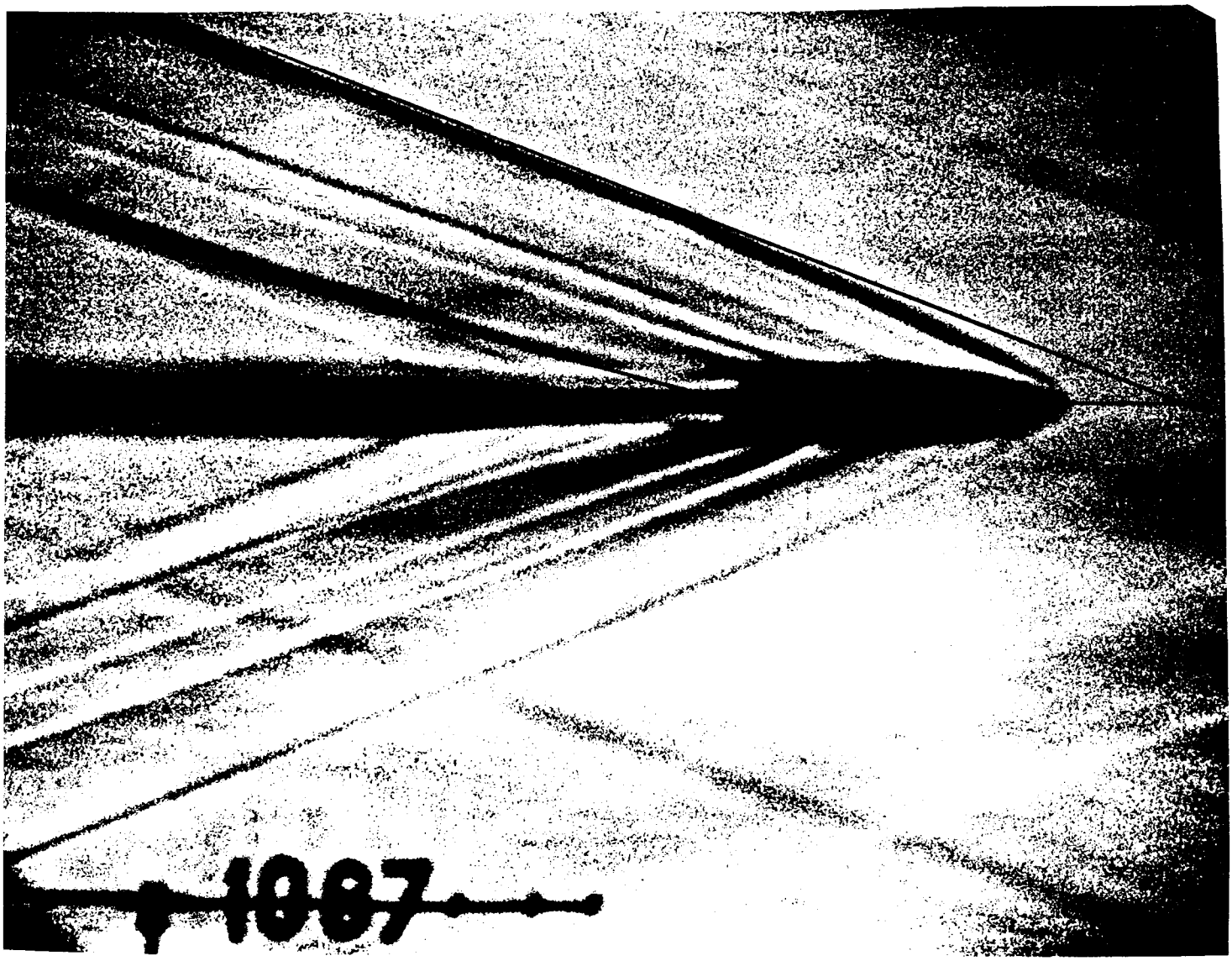

$\theta_1 = 21°$

$\theta_2 = 16\frac{1}{2}°$

$\sin^{-1} \frac{1}{M_0} = 19{,}6°$

FIGURE I.4: Round at M = 2,97

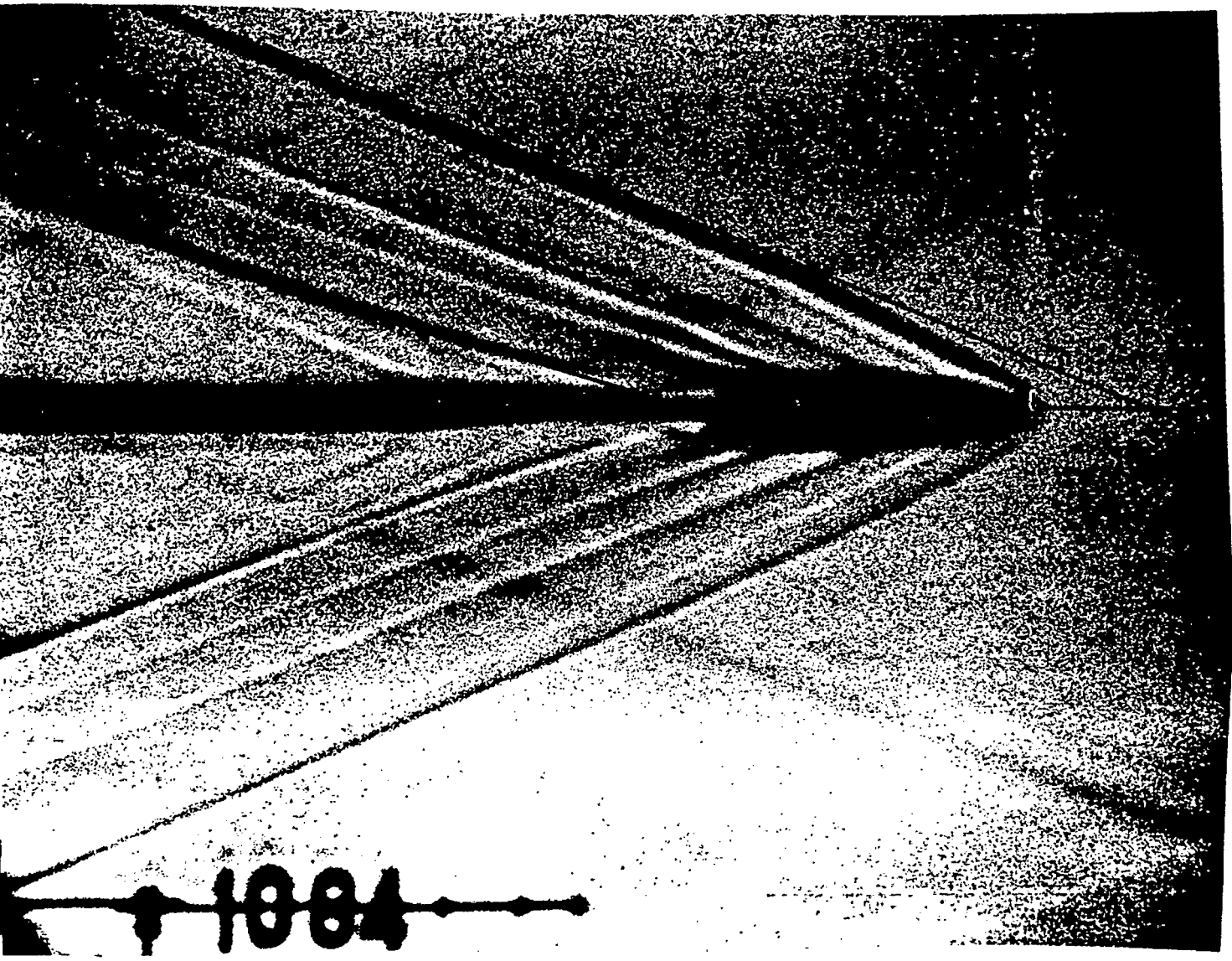

$\theta_1 = 22°$

$\theta_2 = 17\frac{1}{2}°$

$\sin^{-1} \frac{1}{M_0} = 19{,}47°$

FIGURE I.5: Round at M = 3,0

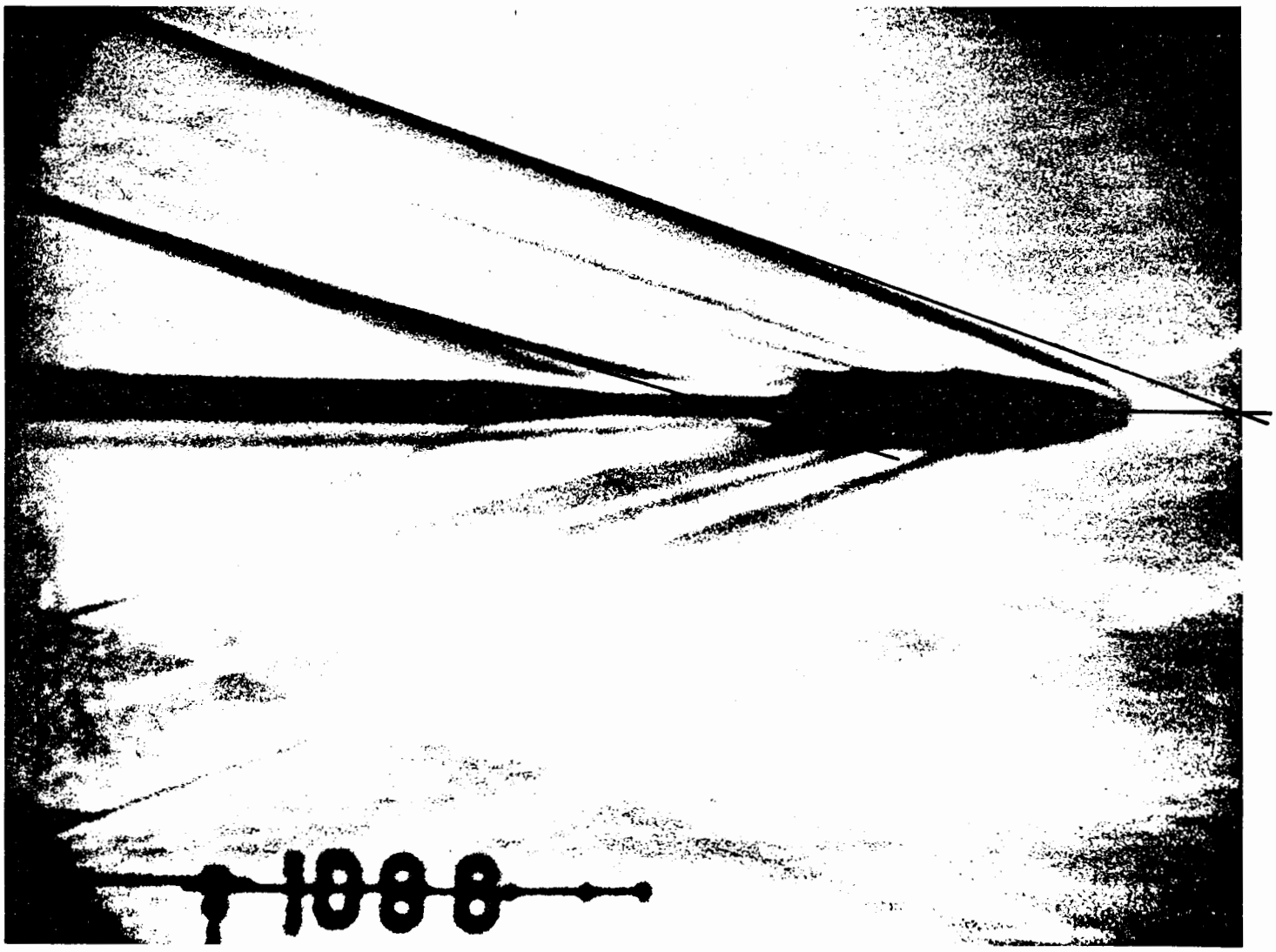

$\theta_1 = 19°$

$\theta_2 = 16°$

$\sin^{-1} \frac{1}{M_0} = 18,2°$

FIGURE I.6: Round at M = 3,20

APPENDIX II: DIMENSIONS OF THE 20 mm ROUND USED IN ALL THE EXPERIMENTS

It should be noted that the shell has many discontinuities of its surface corresponding to features such as driving bands, seals, changes of taper etc. Each of these discontinuities causes a separate shock wave at supersonic speed.

DIMENSIONS OF 20mm ROUND

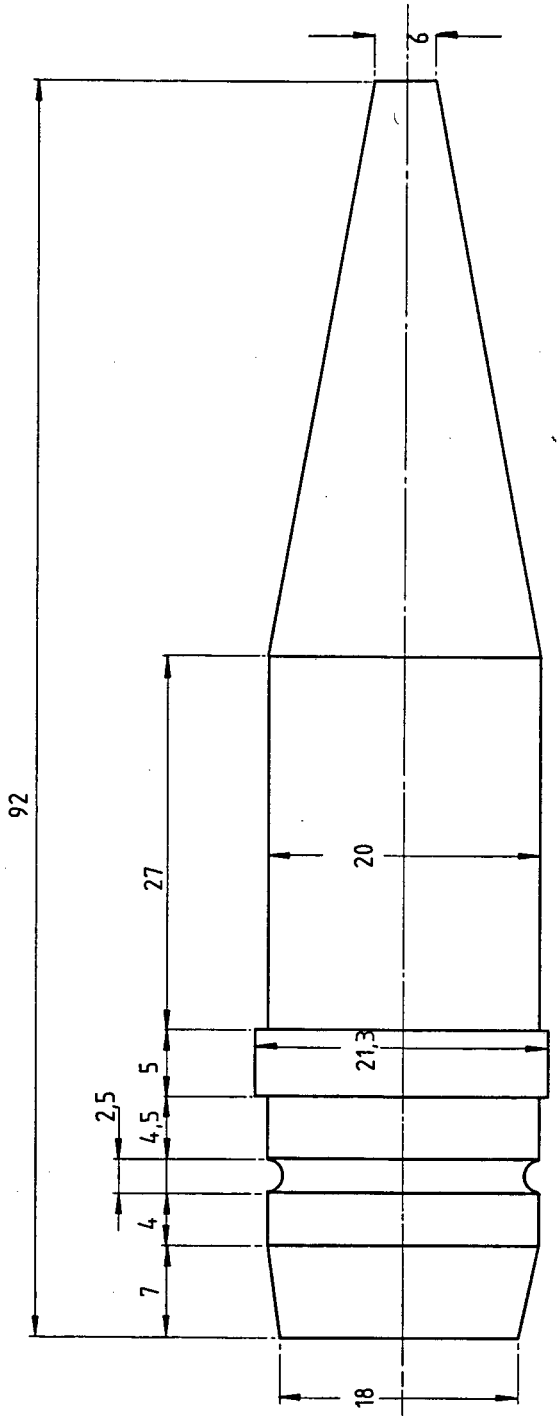

ALL DIMENSIONS IN mm.

APPENDIX III: PHOTOGRAPHS OF RECORDED N-WAVES

The following pages show N-waves measured at distances of 5,10 and 15 m from the flight path of the shell.

In all cases the horizontal scale is 125 μsec per cm. The vertical scale is 100 mV per cm for the N-waves at 5 m, and 50 mV per cm for those at 10 and 15 m.

Features to observe are the following:

(i) the very sharp rise (approximately 200 kV/s) at the start of the N-wave;
(ii) the sharp rise corresponding to the base shock cone;
(iii) generally erratic behaviour after the base transient; and
(iv) other randomly occurring peaks and dips along the slower transitions.

The design of the N-wave detector depended on knowledge of the N-wave as detected by the microphones actually used. The design used the effects:

- amplitude threshold exceeded;
- threshold exceeded for a given time; and
- sharp positive transients at start and end of N-wave.

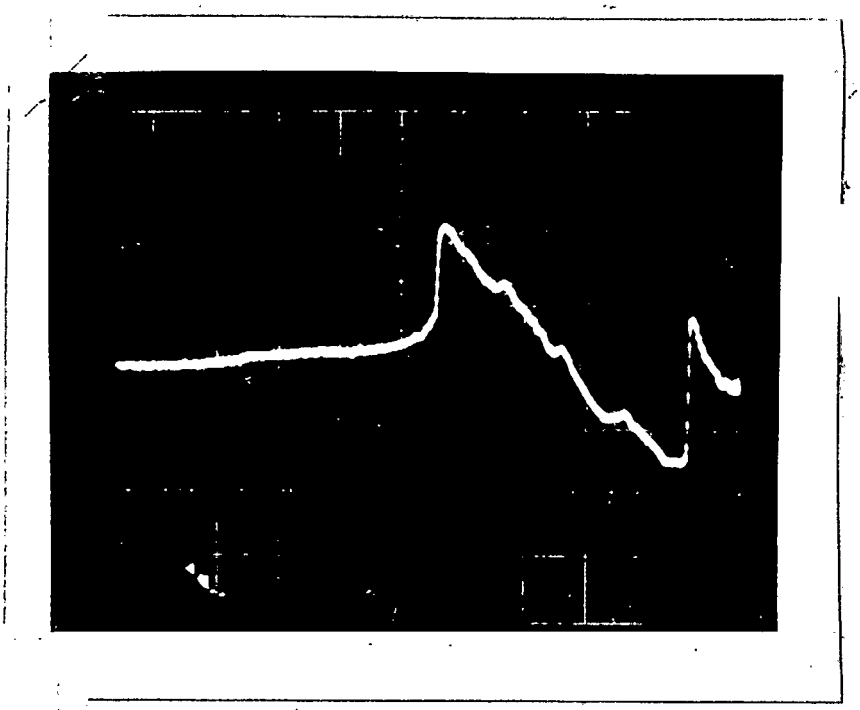

Scale
H: 125 µs/cm
V: 100 mV/cm

FIGURE III.1: N-wave at 5 m

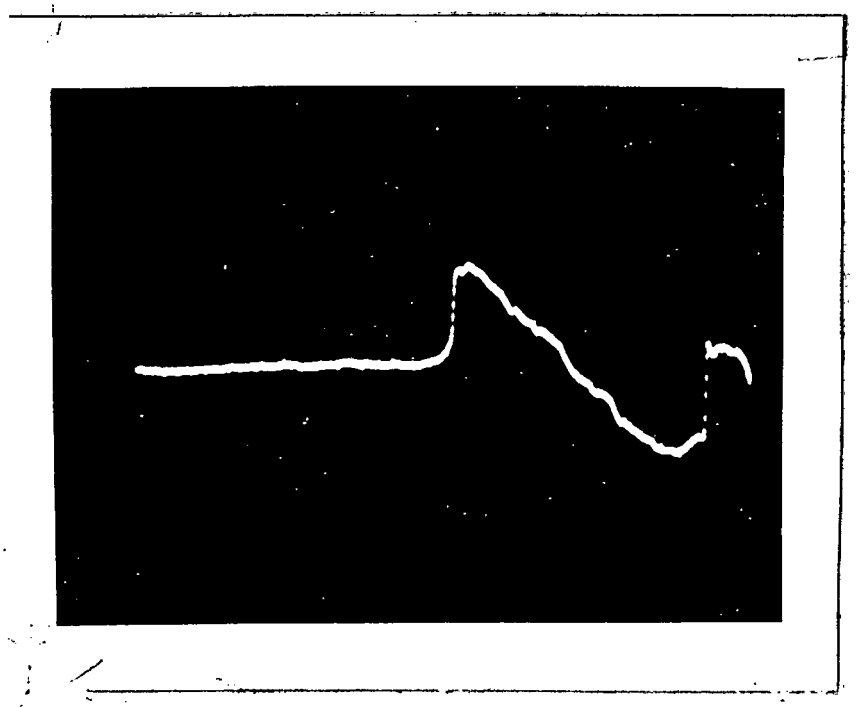

FIGURE III.2: N-wave at 5 m

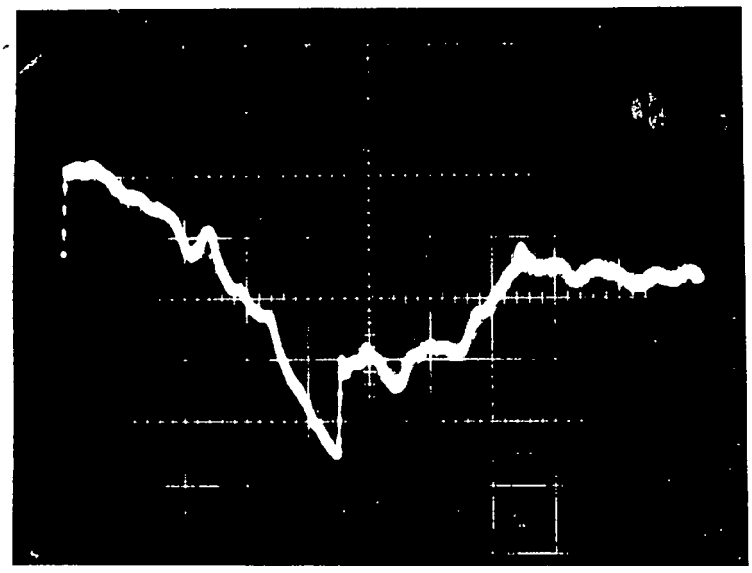

Scale
H: 125 µs/cm
V: 50 mV/cm

FIGURE III.3: N-wave at 10 m

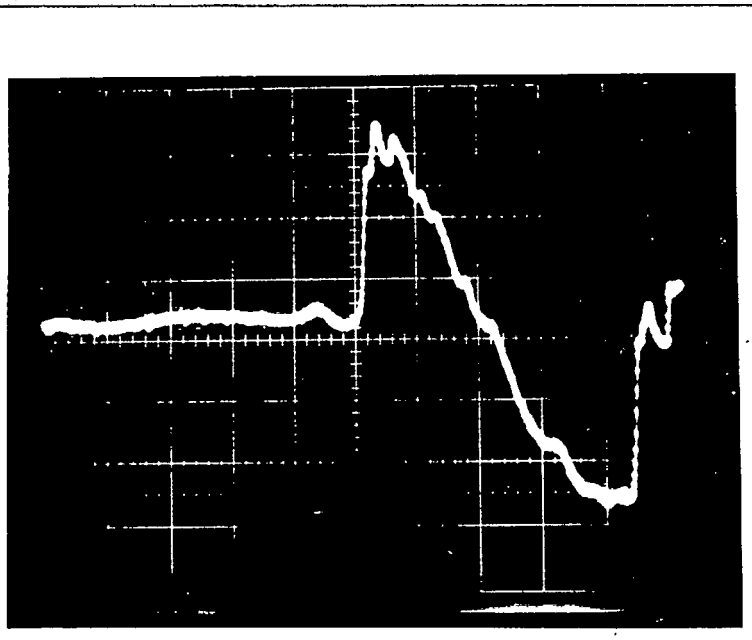

FIGURE III.4: N-wave at 10 m

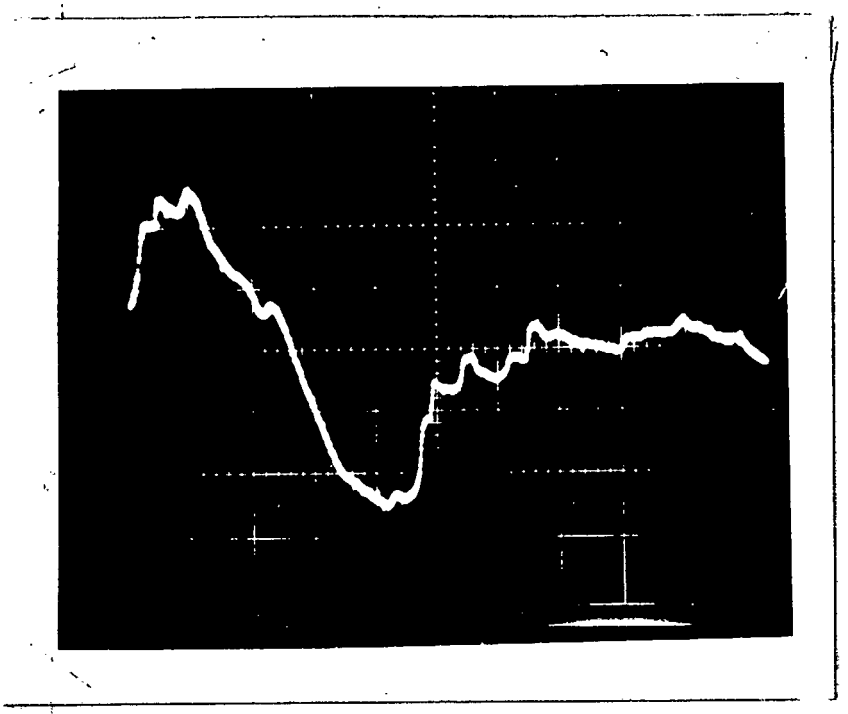

Scale
H: 125 µs/cm
V: 50 mV/cm

FIGURE III.5: N-wave at 15 m

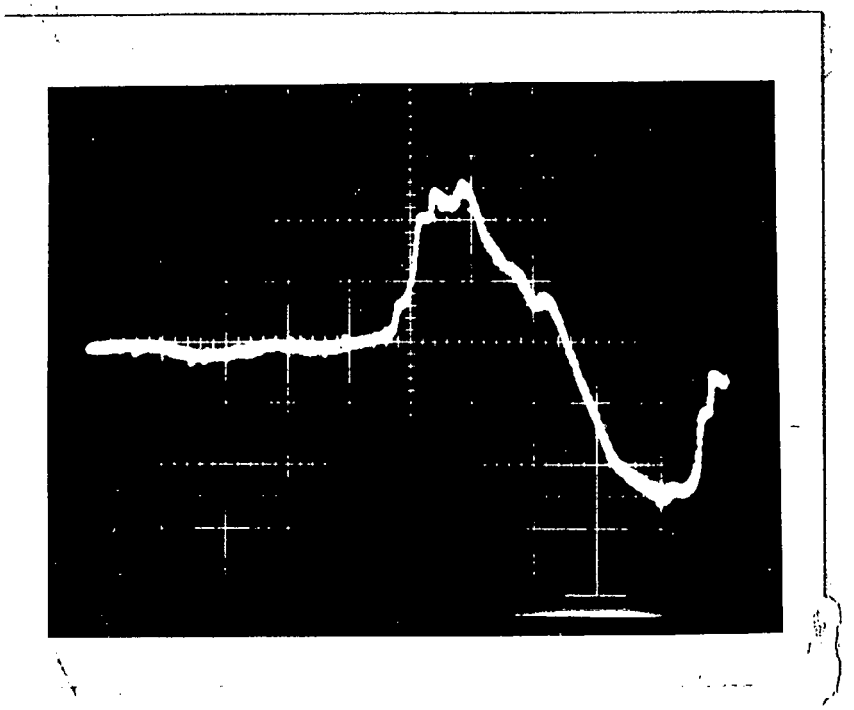

FIGURE III.6: N-wave at 15 m

APPENDIX IV: SPECIFICATION OF REFERENCE - AXES OF THE TARGET SYSTEM

In Section 5.5.2 it was stated that the locations of the four microphones were chosen to coincide with the four apices of a regular tetrahedron.

Let the sides of the tetrahedron be of length a as shown in Figure IV.1 below.

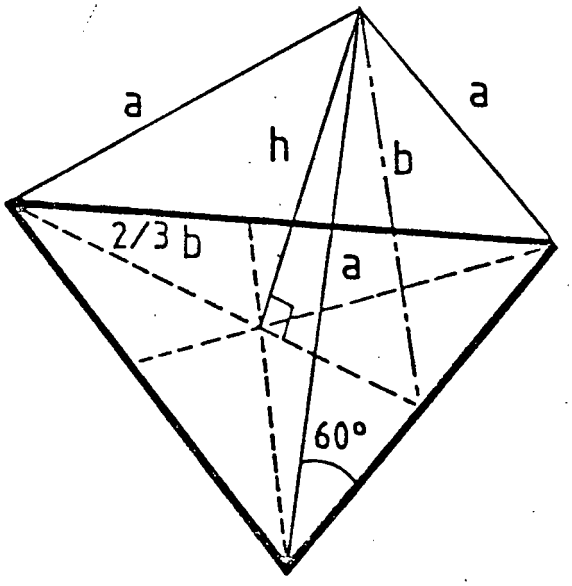

FIGURE IV.1: A Regular Tetrahedron

$$b = \frac{\sqrt{3}\, a}{2}$$

$$h^2 = b^2 - \left(\frac{1}{3}\, b\right)^2$$

$$h = \sqrt{\frac{3}{4}\, a^2 - \frac{1}{9}\,\frac{3}{4}\, a^2}$$

$$= a \sqrt{\frac{3}{4} - \frac{1}{12}}$$

$$= 0{,}81849\ a$$

A basic property of a tetrahedron is that its centre of gravity is located above the centroid of the base, at a height equal to one quarter of the altitude of the tetrahedron.

Then if the origin of the axes is co-incident with the COG of the tetrahedron, and the base is parallel to the X-Y plane, is its condusive to symmetry to rotate the base so that one side of it is parallel to the X-axis. This situation is shown in Figure IV.2 where the apices are identified.

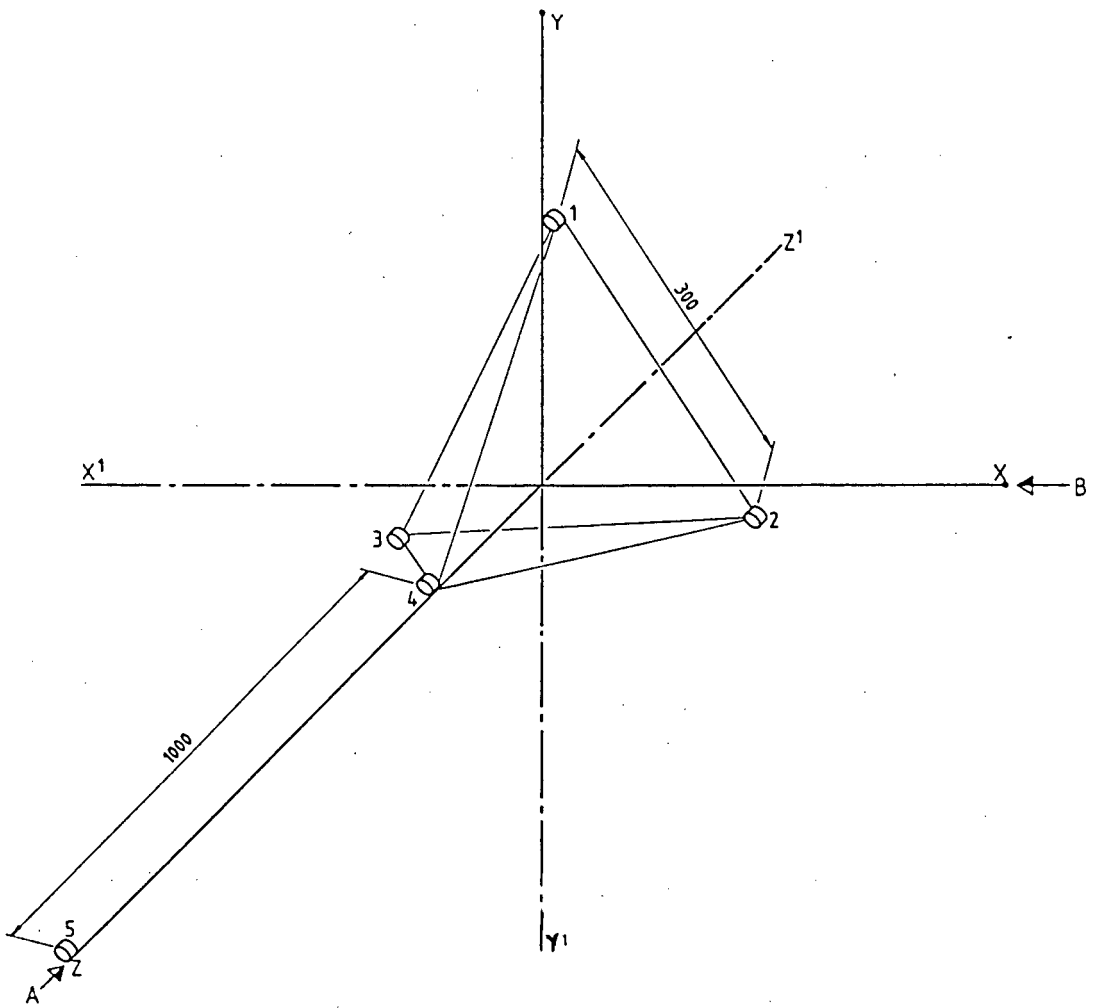

FIGURE IV.2: The choice of Axes

From Figure IV.2 it is clear that:

$$z_1 = z_2 = z_3 = -\frac{1}{4} \times 0{,}81649\ a$$

$$= -\ 0{,}81649\ a$$

Then $$z_4 = 3 \times 0{,}2049\ a$$

$$= 0{,}61236\ a$$

$$y_1 = \frac{2}{3}\ b$$

$$= \frac{2}{3} \times \frac{\sqrt{3}}{2}\ a$$

$$= 0{,}5773\ a$$

$$y_2 = -\frac{1}{3}\ b = y_3$$

$$= -\ 0{,}28865$$

If the side is unity, the apices are:

$$P_1 = (\ 0\ ,\ 0{,}5773\ ,\ -0{,}204\ )$$

$$P_2 = (\ 0{,}5\ ,\ -0{,}28867\ ,\ -0{,}204\ )$$

$$P_3 = (\ -0{,}5\ ,\ -0{,}28867\ ,\ -0{,}204\ )$$

$$P_4 = (\ 0\ ,\ 0\ ,\ +0{,}61236\ )$$

The origin is at (0, 0, 0).

In practice, the author initially selected sides of a = 0,3 meters, a choice based on compromise, bearing in mind that the final system would have to be fitted to a towed target. Subsequent experience showed that this dimension was too small and that a side of 1,0 m gave more accurate results.

The final coordinates used in the programme were thus:

$$\bar{P_1} = (\ 0\ ,\ 0{,}173\ ,\ -0{,}0612\ )$$

$$P_2 = (\ 0{,}15\ ,\ -0{,}0866\ ,\ -0{,}612\ )$$

$$P_3 = (\ -0{,}15\ ,\ -0{,}0866\ ,\ -0{,}612\ )$$

$$P_4 = (\ 0\ ,\ 0\ ,\ 0{,}1837\ )$$

$$P_5 = (\ 0\ ,\ 0\ ,\ 1{,}000\ )$$

Note: (i) The point P_5 was included, at 1 m from P_4 so that under certain circumstances it could be used to easily measure the velocity of the passing round.

(ii) P_5 plays no essential rôle in the projectile locating procedure which is based on four triangles. If any of the essential four microphones mal-functions, P_5 provides redundancy so that a valid reading may still be made.

V MATHEMATICAL ANALYSIS: ESTIMATING THE COORDINATES OF TWO POSSIBLE POINTS

Note: The author is indebted to Mr P Swart of the University of Pretoria for his assistance in obtaining an elegant solution to this problem by means of vector analysis.

PROBLEM STATEMENT

Given: (i) 3 points P_i, with coordinates (x_i, y_i, z_i)
(ii) 3 lines of length ℓ_i originating from the P_i.

Required: If the ℓ_i converge, the coordinates of the points of convergence P and P^1.

Solution: Let the P_i be P_1, P_2 and P_3 as shown below.

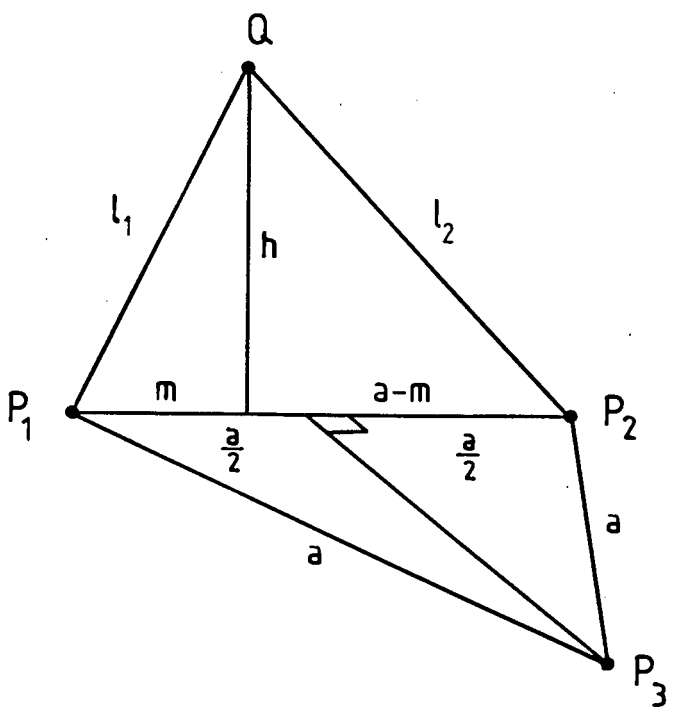

FIGURE V.1: Simplified Geometry

Consider only ℓ_1 and ℓ_2 (avoiding the trivial cases) where:

$$(\ell_1 + \ell_2) < a$$
$$\text{or} \quad (\ell_1 + a) < \ell_2 \qquad \text{(V.1)}$$
$$\text{or} \quad (\ell_2 + a) < \ell_1$$

for which convergence at a point not on P_1P_2 is impossible. Let ℓ_1 and ℓ_2 converge at a point Q. From the figure:

$$\cos\phi = \frac{\ell_1^2 - \ell_2^2 + a^2}{2a\,\ell_1} \qquad \text{(V.2)}$$

$$m = \ell_1 \cos\phi \qquad \text{(V.3)}$$

$$= \frac{\ell_1^2 - \ell_2^2 + a^2}{2a} \qquad \text{(V.4)}$$

$$h = \sqrt{\ell_1^2 - m^2} \qquad \text{(V.5)}$$

Solution of the problem consists of allowing the line h to rotate towards P_3 until line $P_3\,Q = \ell_3$, when Q = P, the point sought.

Since rotation could be towards or away from P_3, two solutions are possible viz: one above the plane $P_1\,P_2\,P_3$ and are below it.

Define a set of convenient axes (X, Y, Z) as shown below.

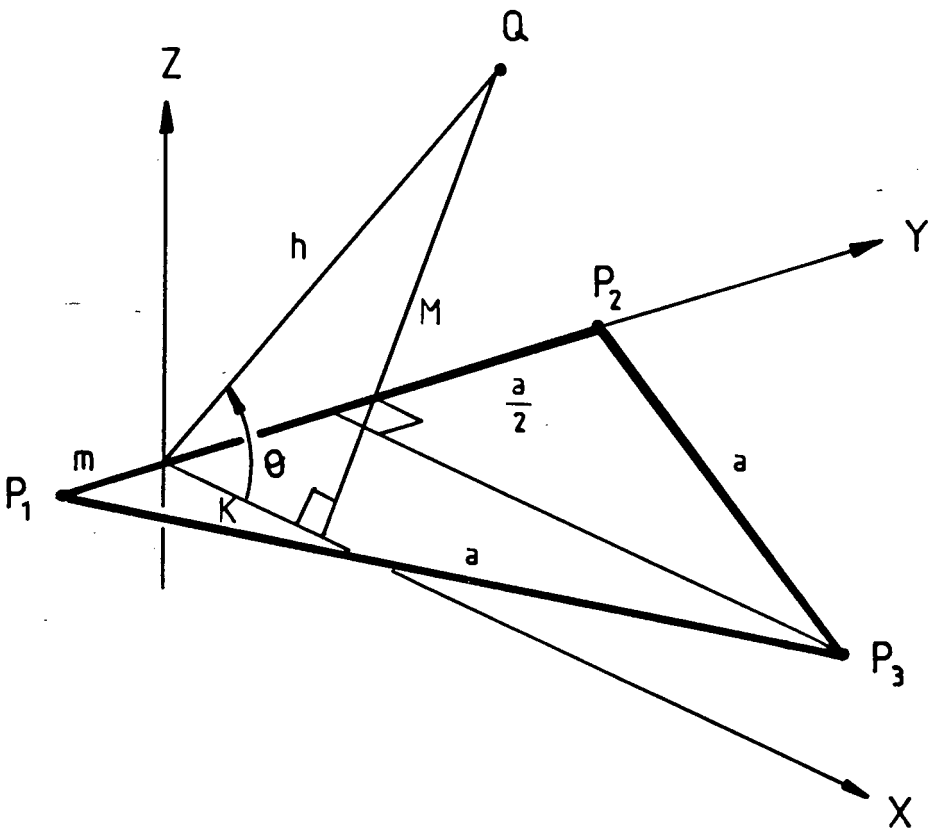

FIGURE V.2: Line h rotated through angle θ

Because Δ P_1 P_2 P_3 is equilateral and of side a, lying on the X-Y plane, the coordinates of P_3 are:

$$\left(\frac{\sqrt{3}\,a}{2}\ ,\quad \frac{a}{2} - m\ ,\quad 0\right)$$

let $$L^2 = |\,Q\,P_3|^2 \qquad (V.6)$$

$$= \left((h\cos\theta - \sqrt{\frac{3}{2}}a)^2 + (\frac{a}{2} - m)^2 + h^2\sin^2\theta\right)$$

$$= h^2 + a^2 - am + m^2 - \sqrt{3}\,ah\cos\theta$$

$$= \ell_3^{\,2} \text{ for a possible solution}$$

$$\text{thus } \cos\theta = \frac{h^2 + (m - \frac{a}{2})^2 + \frac{3}{4}a^2 - \ell_3^2}{\sqrt{3}\, a\, h} \qquad (V.7)$$

K is the X-coordinate of P (Q)

i.e. $K = h\cos\theta$

$$= \frac{h^2 + (m - \frac{a}{2})^2 + \frac{3}{4}a^2 - \ell_3^2}{\sqrt{3}\, a} \qquad (V.8)$$

and M is the Z-coordinate of P

i.e. $$M = \sqrt{h^2 - K^2} \qquad (V.9)$$

The problem is thus solved for conveniently chosen axes. The axes must now be translated to the general set (X, Y, Z) for any points P_1, P_2, P_3 located in X Y Z.

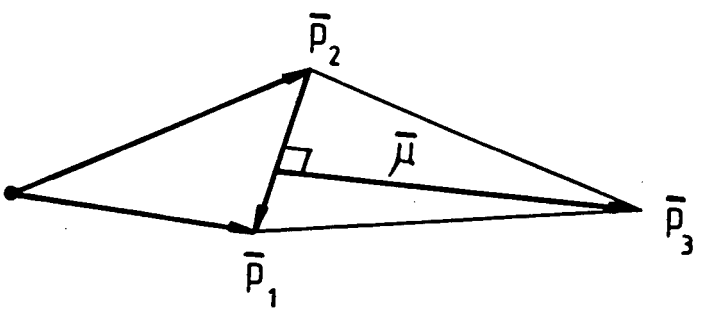

FIGURE V.3: Vector diagram

for P_1, P_2, P_3 points on an equilateral triangle:

$$\bar{\mu} \perp \bar{P}_1 - \bar{P}_2 \qquad (V.10)$$

where $\bar{\mu}$ is a unit vector.

thus $\bar{\mu} = \dfrac{\bar{\mu}'}{|\bar{\mu}'|}$ (V.11)

where $\bar{\mu}' = \bar{p}_3 - \frac{1}{2}[\bar{p}_1 + \bar{p}_2]$ (V.12)

find a vector $\bar{\lambda}$ so that

$$\bar{\lambda} \perp \Delta P_1 P_2 P_3$$

if λ is as defined, then

$\bar{\mu} \times (\bar{p}_2 - \bar{p}_1)$ lies along $\bar{\lambda}$

and $\frac{1}{a}\bar{\mu} \times (\bar{p}_2 - \bar{p}_1)$ is a unit vector $\parallel \bar{\lambda}$

thus $\bar{p}$, the vector to the unknown point P is

$$\bar{p} = \bar{p}_1 + \frac{m}{a}(\bar{p}_2 - \bar{p}_1) + K\bar{\mu} \pm M\bar{\lambda} \quad \text{(V.13)}$$

where m, a, K and M are as previously defined

i.e. $$\begin{pmatrix} x \\ y \\ z \end{pmatrix} = \begin{pmatrix} x_1 \\ y_1 \\ z_1 \end{pmatrix} + \frac{m}{a} \begin{pmatrix} x_2 - x_1 \\ y_2 - y_1 \\ z_2 - z_1 \end{pmatrix} + \bar{K}\mu \pm \bar{M}\lambda \quad \text{(V.14)}$$

where $$\bar{\mu} = \begin{pmatrix} x_3 \\ y_3 \\ z_3 \end{pmatrix} - \frac{1}{2} \begin{pmatrix} x_1 + x_2 \\ y_1 + y_2 \\ z_1 + z_2 \end{pmatrix} \quad \text{(V.15)}$$

and $\bar{\lambda} = \frac{1}{a}\bar{\mu} \times (\bar{p}_1 - \bar{p}_2)$

$$= \frac{1}{a} \begin{pmatrix} x_3 - \frac{1}{2}(x_1 + x_2) \\ y_3 - \frac{1}{2}(y_1 + y_2) \\ z_3 - \frac{1}{2}(z_1 + z_2) \end{pmatrix} \times \begin{pmatrix} x_1 - x_2 \\ y_1 - y_2 \\ z_1 - z_2 \end{pmatrix} \qquad (V.16)$$

Equation V.15 expresses the coordinates of the fourth point P or P' in terms of the known values:

- the lengths ℓ_1, ℓ_2, ℓ_3

- the coordinates (x_i, y_i, z_i) of the points P_i

Equation V.14 is solved successively for $P_1\ P_2\ P_3$, $P_2\ P_3\ P_4$, $P_3\ P_4\ P_1$ and $P_4\ P_1\ P_2$ to yield the eight possible points as discussed elsewhere in this thesis. (Paragraph 5.5.3)

Solution of the equations, V.14, V.15 and V.16 was implemented by computer and details of two calculations are shown in Appendix VI.

VI EXAMPLES OF CALCULATIONS

A VERIFICATION OF METHOD OF COMPUTATION

A point P_5: (15, 15, 15) was chosen for case of calculation.

thus $P_{51} = 25,9166$
$P_{52} = 25,980$
$P_{53} = 26,152$
$P_{54} = 25,875$

Using the theory developed in Appendix V, four pairs of possible points are calculated to be:

$P_A = (14,944, \quad 14,954, \quad 15,099)$

$P'_A = (14,944, \quad 14,954, \quad -15,222)$

$P_B = (14,944, \quad -2,5169, \quad 21,156)$

$P'_B = (14,944, \quad 15,141, \quad -14,9119)$

$P_C = (16,336, \quad 14,151, \quad 14,407)$

$P'_C = (13,1923, \quad 15,966, \quad 15,690)$

$P_D = (15,000, \quad 14,993, \quad 15,000)$

$P'_D = (-24,606, \quad -7,874, \quad -1,173)$

Sixteen calculations are performed, corresponding to the 16 possible groupings shown in Table 10 of paragraph 5.5.4.

Each calculation performed found average values for the x, y and z coordinates of P_5.

i.e. $$\left(\frac{1}{4}\sum_{i=1}^{4} x_i \;,\; \frac{1}{4}\sum_{i=1}^{4} y_i \;,\; \frac{1}{4}\sum_{i=1}^{4} z_i\right) = (x_5, y_5, z_5)$$

The variance, defined by the author for ease of calculation to be:

$$\bar{h}^2 = \sum_{i=1}^{4} (\bar{x} - x_i)^2 + \sum_{i=1}^{4} (\bar{y} - y_i)^2 + \sum_{i=1}^{4} (z - z_i)^2$$

was also calculated for each of the 16 groups of points. the results are shown in Table VI.1

TABLE VI: Results of calculations

Group No	$\bar{x}$	$\bar{y}$	$\bar{z}$	h^2	
1	15,306	10,395	16,415	254,409	
2	15,306	10,395	8,835	1023,76	
3	15,306	14,809	14,850	2,298	(lowest value)
4	14,520	10,849	16,736	267,56	
5	5,405	,67	12,372	1878,98	
6	15,306	14,809	7,24	674,0	
7	14,520	10,84	9,156	1056,35	
8	5,404	4,678	4,792	2403,15	
9	15,520	15,263	15,175	3,40	
10	5,404	9,093	10,811	1778,27	
11	4,61	5,132	12,693	1860,97	
12	14,520	15,263	7,595	697,557	
13	5,404	9,093	3,230	2207,77	
14	4,618	9,546	11,132	1748,25	
15	4,618	5,132	5,11	2404,61	
16	4,618	9,546	3,551	2197,22	

The smallest variance is 2,298 which corresponds to a calculated point (15,306, 14,809, 14,850) which agrees well with the selected point (15, 15, 15).

The method of calculation was thus deemed to be correct.

B APPLICATION TO MEASURED DATA

Shot No 10 indicated estimated distances of

ℓ_1 = 11,92 m

ℓ_2 = 11,85 m

ℓ_3 = 11,71 m

ℓ_4 = 11,85 m

The possible pairs of points are:

P_a = (-5,497, -6,376, 8,243)

P'_a = (-5,497, -6,376, -8,366)

P_b = (-5,497, -10,496, 0,345)

P'_b = (-5,497, 8,265, -6,289)

P_c = (2,14, -10,876, -4,23)

P'_c = (-11,419, -2,957, 1,306)

P_d = (10,307, 2,748, 5,34)

P'_d = (-8,358, -8,028, -2,281)

The calculated points and variances are shown in Table VI.2.

TABLE VI: Results of calculations

Group No	$\bar{x}$	$\bar{y}$	$\bar{z}$	h^2	
1	0,363	-6,227	2,42	381,261	
2	0,363	-6,227	-1,728	394,877	
3	0,363	-1,537	-1,904	533,526	
4	-3,026	-4,270	3,806	394,86	
5	-4,303	-8,920	0,519	164,122	
6	0,363	-1,537	-3,386	504,203	
7	-3,026	-4,27	-0,343	454,454	
8	-4,303	-8,921	-3,633	114,449	
9	-3,026	0,420	2,150	504,205	
10	-4,304	-4,231	-1,139	404,344	
11	-7,692	-6,964	1,903	114,463	
12	-3,026	0,420	-2,002	508,703	
13	-4,303	-4,231	-5,291	299,579	
14	-7,692	-2,274	0,245	299,608	
15	-7,692	-6,964	-2,249	110,763	(lowest h^2)
16	-7,692	-2,274	-3,907	240,816	

The lowest variance occurred for group 15 i.e. 110,763 corresponding to P_s = (-7,692, -6,963, -2,249) compared with an aimed point of (-8,6, -5,0, -1).

The greatest source of error is the z-coordinate i.e. -2,25 versus 0.

The aimed point lay in the x-y plane and the expected value of z was thus zero.

In the discussion of results the problems caused by the 0,3 m measuring base are discussed.

The error of 2,25 m corresponds to an angle-error of less than 11° at a distance of 11,75 m from the target which is close to the design target figure of 10°.

APPENDIX VII: MATHEMATICAL ANALYSIS ALTERNATIVE METHOD (MMD METHOD)

The analysis in this appendix is a non-rigorous summary of work described in a confidential report produced by another department of CSIR. In the discussion of results and elsewhere, this is referred to as the MMD method.

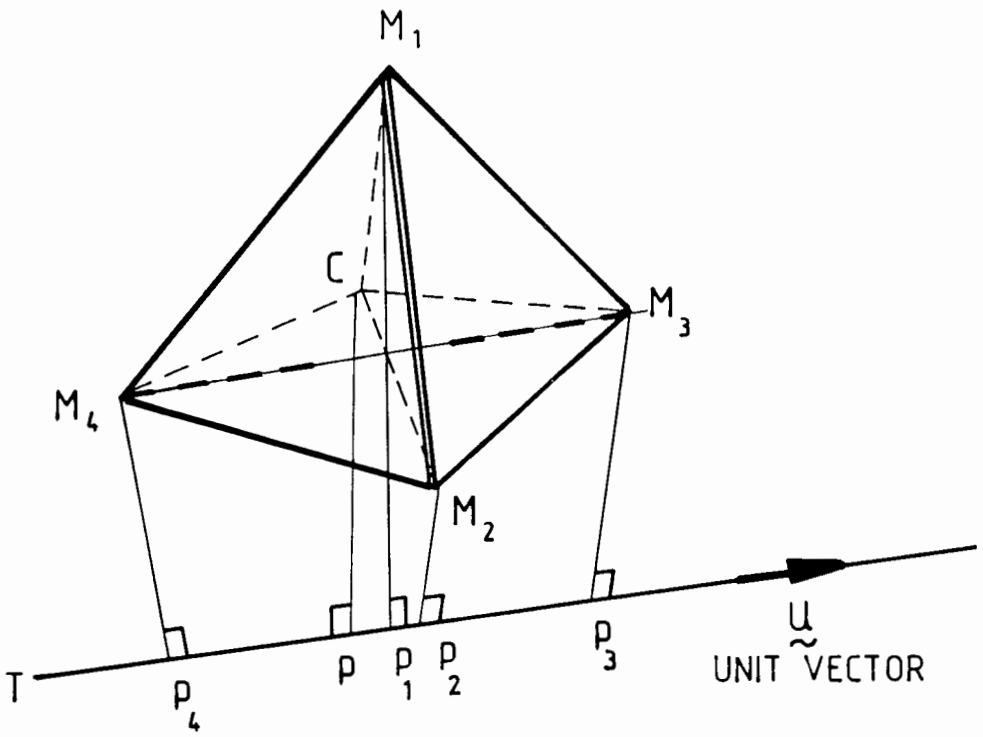

FIGURE VII.1: Diagram of Round passing a Tetrahedral Array

The centroid of the microphone array is located at C. The Tetrahedral array is of side d. The four microphones are designated M_i (i = 1, 2, 3, 4).

Because of symmetry,

$$\Sigma_i \, \tilde{CM}_i = 0 \qquad \text{(VII.1)}$$

The miss distance is the line joining the centroid C to the point of closest approach of the round to the array, P.

It is shown in the report mentioned that

$$\tilde{CP} = \tilde{R} + \tilde{r} \qquad \text{(VII.2)}$$

where $\tilde{R}$ is shown to be

$$\tilde{R} = - \sum_i \left(\frac{L_i}{d}\right)^2 \tilde{CM}_i \qquad \text{(VII.3)}$$

where $L_i = L_1, L_2, L_3, L_4$

are the perpendicular distances from the M_i to the trajectory TT of the round.

Further it is shown that

$$|r| \leq \frac{d}{\sqrt{24}} \leq 0{,}21 \; d$$

since d = 0,3 m, $|r|$ = 0,0612 and R is typically 5 m or greater, R may be used as a good approximation of the miss vector.

The coordinates of the array are

$$\tilde{CM}_1 = d\left(0, \frac{1}{\sqrt{3}}, - \frac{1}{2\sqrt{6}}\right)$$

$$\tilde{CM}_2 = d\left(\frac{1}{2}, - \frac{1}{2\sqrt{3}}, - \frac{1}{2\sqrt{6}}\right)$$

$$CM_3 = d(-\frac{1}{2}, -\frac{1}{2\sqrt{3}}, -\frac{1}{2\sqrt{6}})$$

$$\tilde{C}M_4 = d(0, 0, \frac{1}{2}\sqrt{\frac{3}{2}})$$

Using equation VII.3 it can be shown that the cartesian coordinates of the closest point P are:

$$x_p = (\frac{L_3^2 - L_2^2}{2d})$$

$$y_p = (\frac{L_2^2 + L_3^2 - 2L_1^2}{\sqrt{12}\, d}) \qquad \text{(VII.4)}$$

$$z_p = (\frac{L_1^2 + L_2^2 + L_3^2 - 3L_4^2}{\sqrt{24}\, d})$$

An <u>independent</u> estimate for the distance $\tilde{C}p$ is also found i.e.

$$|\tilde{C}p|^2 = \frac{1}{4}\Sigma_i L_i^2 - \frac{1}{4}d^2 \ldots. \qquad \text{(VII.5)}$$

$|\tilde{C}p|$ is thus the RMS value of the estimates L_i, corrected by $\frac{1}{4}d^2$ to account for the fact that the L_i are measured from the M_i and not from the centroid C.

This independent estimate of $|\tilde{C}p|$ is useful when "adjusting" the L_i to account for random error.

It can be shown that, from VII.4,

$$|\tilde{R}|^2 = \Sigma_i (\frac{L_i^4 - L^4}{2d^2})$$

where $L^2 = \frac{1}{4} \sum_i L_1^2$

But from VII.5

$$|\tilde{C}p|^2 = L^2 - \tfrac{1}{4}d^2$$

so that $\sqrt{\Sigma_i (L_i^4 - L^4)/2d^2}$ should not differ from $\sqrt{L^2 - \frac{1}{4}d^2}$ by more than $d/\sqrt{24}$.

The ratio:

$$\frac{|R| - \sqrt{L^2 - \frac{1}{4}d^2}}{d/\sqrt{24}} = f_0$$

is used as a figure of merit which should not be greater than unity.

When $f_0 > 1$, the L_i are marginally adjusted subject to the conditions:

(i) $\sum_i L_i'^2 = \sum_i L_i^2$

(where L_i' are the new values for the L_i)

(ii) $\sqrt{\sum_i (L_i'^4 - L^4)/2d^2} - \sqrt{L^2 - \frac{1}{4}d^2} < \frac{d}{\sqrt{24}}$

(iii) $\sum_i (L_i'^2 - L_i^2)^2$ is minimised.

The report verifies the findings obtained by the method of four triangles that the miss distance is fairly insensitive to errors in the L_i, but that the vector described by VII.4 is very sensitive.

It is shown that a 1% error in L_i is magnified by 46 times in $\tilde{R}$ but $|\tilde{C}p|$ is only affected by 1%.

When the adjustments (i), (ii) and (iii) above are made the error magnification is reduced to about half i.e. to 24 times.

Calculations performed by the author confirm this error multiplication. In an example, in two dimensions X and Y, when no error is present a miss vector points to (-0,15 , 9,99). A 1% error on one length estimate causes the vector to point to (-3,499 , 9,474) i.e. an error vector of $|\tilde{E}V|$ = 3,38 m.

The crucial factor is the length of the side of the tetrahedron. In all the early experiments performed this was set at 0,3 m. If it is increased, the reduction in error magnification is very significant. It can be shown in the above example that increasing the length of the base to 1,0 m reduces the error vector $|EV|$ from 3,38 m to 1,0 m a reduction in error magnification from 33 to 10 times.

APPENDIX VIII: DISCUSSION OF RESULTS

VIII.1 RELATIONSHIP BETWEEN N-WAVE PERIOD AND MISS DISTANCE

The relationship shown in equation 5.12 provides adequate accuracy for the intended application. In its simplified form, equation 5.10, it has been tested for other calibers and the two constants m and k are readily calculated.

Because of the signal conditioning and detection applied as described in section 5.6, noise immunity should be adequate. In laboratory tests the N-wave detector is unaffected by sine-waves. (Detailed noise measurements of wind and engine noise at a towed target have yet to be performed. At the time of writing an approved target was not yet available).

The effect of altitude on Mach Number can easily be taken into account in the empirical relationships deduced by the author.

The fact that a simple device has been developed which enables miss distance (scalar) to be measured is itself of immediate practical use. By eliminating the step transitions from one zone to another, direct improvement in the usefulness of acoustic MDI is possible.

The accuracy obtainable from this method is limited by the noisy nature of the shock-wave at the base of the round. The clock period used in the system was 0,8 micro seconds. At the velocities encountered at the target, the round may move less than 1 mm in this interval.

In flight the attitude of a shell varies with time as it precesses and nutates. Such motion has slow and rapid components. The author has shown that, for motion past sensors that is not parallel to the line between the sensors, (i.e. the general case) the time between

stimulation of the sensors is dependent on:

- velocity
- angle between trajectory and sensor axis
- shock wave angle.

The shockwave angle is thus inherently subject to random variation of a sort which, while it does not influence the practical miss distance by significant amounts, does affect direction measurement adversely in a system which magnifies errors by forty fold.

The conclusion is thus that the relationship between N-wave period is useful and predictable, but that it must be judiciously applied. The implication for the MDI system described is that a larger measuring base must be used.

VIII.2 MATHEMATICAL WORK

No rigourous proof is available for the method of Four Triangles developed by the Author. In practice it is robust and an answer can always be obtained; (provided that the difference between the lengths estimated never exceeds the side of the triangle between their origins).

Whereas the method is sensitive, it is marginally less so than the method described in Appendix VII.

A detailed discussion of the results follows in paragraphs VIII.2 onwards.

VIII.3 NUMBER OF VALID READINGS

For the method of four triangles or the MMD method to solve the location problem the following are necessary conditions:

(i) at least four values of τ, the N-wave period;

(ii) the difference between any two calculated lengths (r_i) must not exceed the measuring base (300 or 1000 m);

(iii) a value for the time of flight from which the velocity can be calculated.

Because of the noisy nature of the N-wave, (ii) above was often violated in the 300 mm case. This led to a very high rejection rate amongst sets of data used in the calculations (77,9)%.

Increasing the measuring base to 1000 mm reduced the rejection rate from 77,9% to 11,9%, and this is seen as a clear design guideline.

Readings including two or more failures to recognize N-waves (4 out of 5 readings must be valid) dropped from 12,2% to 9,4% which also increased the effectiveness of the system by 22,9%.

The improvements in (i) and (ii) above brought about by increasing the measuring base from 300 to 1000 mm increased the useful readings from 19,4% of shots fired to 79,8% of shots fired.

VIII.4 MMD METHOD IMPROVEMENT

With the 300 mm measuring base the MMD method failed in 26,3% of all cases. When the base was increased to 1000 mm this failure rate dropped to 8,8% an improvement of 66,5%.

In all cases where condition (ii) of VIII.1 was satisfied the method of four triangles obtained a solution, demonstrating the robustness of this method.

VIII.5 INDICATED MISS DISTANCE (SCALAR)

Histograms of the results for the two measuring bases are shown in Figures VIII.1 and VIII.2, overleaf.

For a 300 mm base the average error estimated at 8.7% ±32,74%. This estimate is not verified because no target was used to trace the actual miss distance.

For the 1000 mm base the calculated error is shown to be 18,3% ±17,2%. This result consists of two components

(i) an average error of +10,5% ±12,6% for a range of 500 m;

(ii) an average error of +37,85% ±10,1% for a range of 1000 m.

Because the error is positive in 51 out of 55 cases at 500 m and in all readings at 1000 m it is systematic and easily corrected.

The systematic nature of the errors and the fact that the standard deviation is reduced by a factor of about 2,6 indicates that the method is under control.

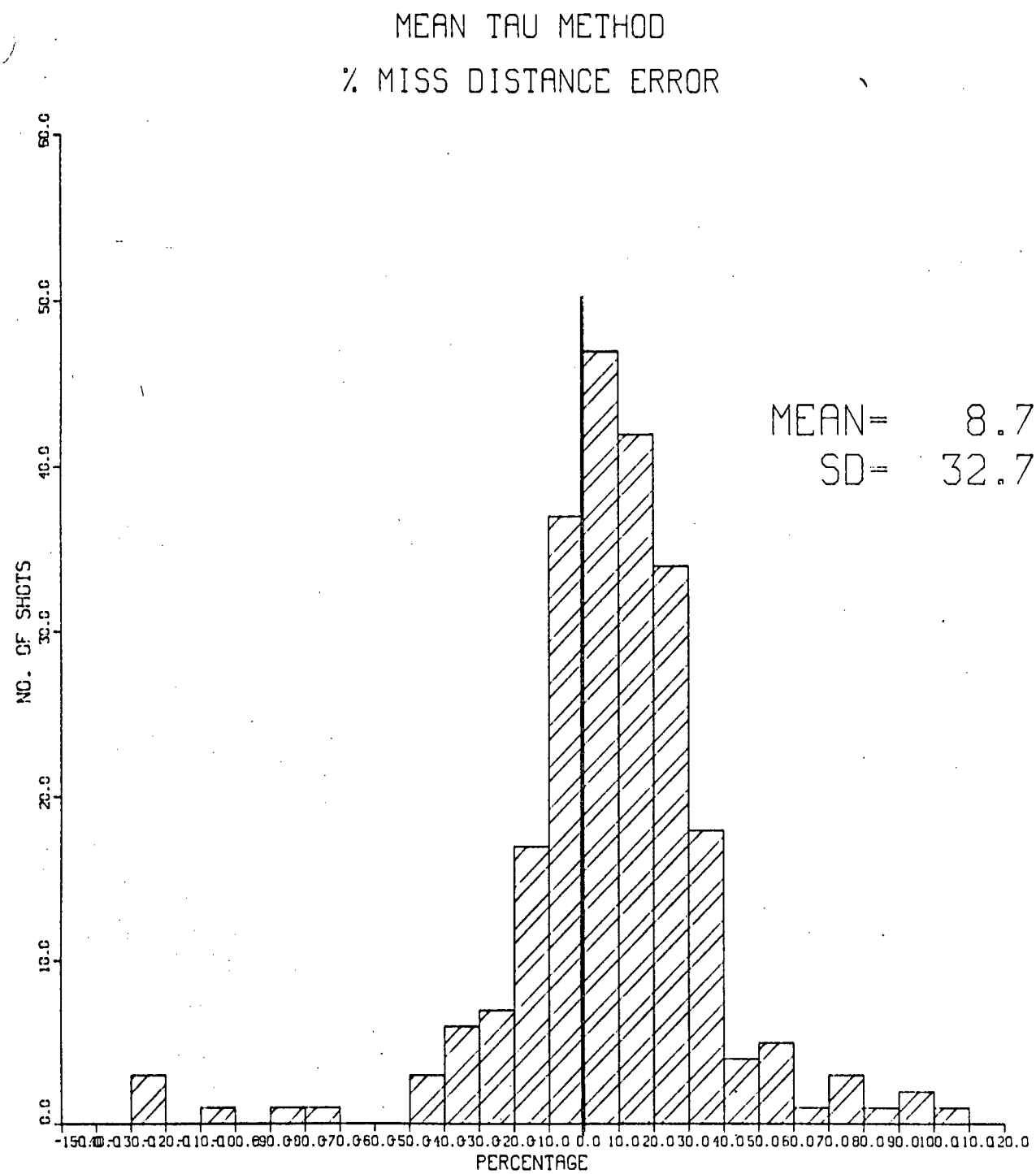

FIGURE VIII.1: Histogram of average error for 300 mm base (Scalar Miss Distance)

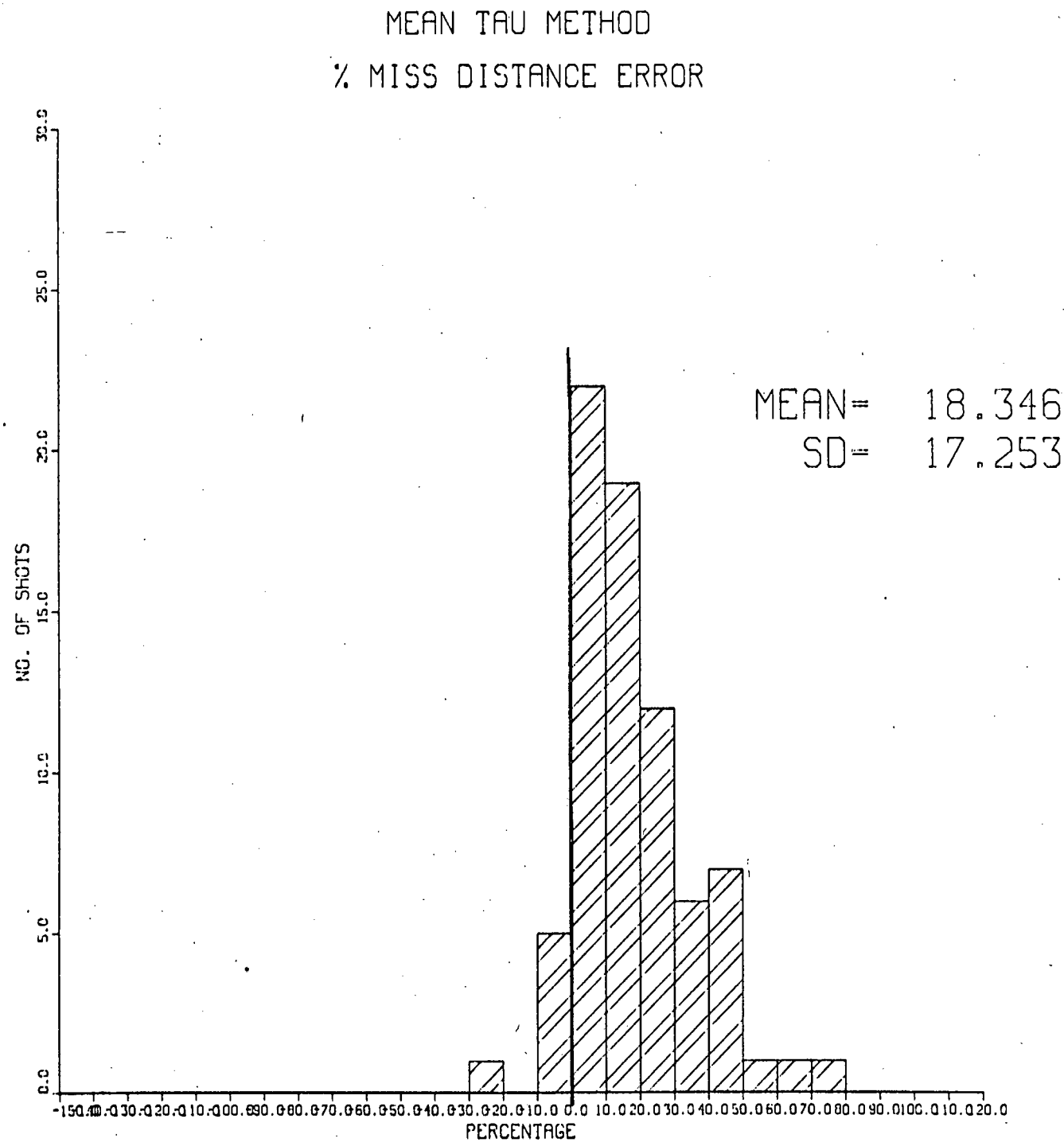

FIGURE VIII.2: Histogram of average error for 1000 mm base (Scalar Miss Distance)

VIII.6 INDICATED MISS DISTANCE (VECTOR)

Histograms of the average % error are shown in Figures VIII.3 and VIII.4 overleaf.

(i) Method of Four Triangles

For the 300 mm base, the estimated average error is +1,52 ±15,8% and for the 1000 mm base the measured average error is -9,03% ±16,5%. These readings indicate

(a) that the gunner's grouping is good even when the exact passage of the round is unknown.

(b) that control and repeatability are high.

(ii) MMD Method

This method shows a trend similar to that in (i) above i.e. the average error rises from 8,5% to 14,9% and the standard deviation stays more or less the same 12,3% for 300 mm base and 11,40% for the 1000 mm base.

The miss distance measured by the two methods is sufficiently accurate to provide useful information to both operating and gun system maintenance crews.

The % distance error for the 300 and 1000 mm bases for the MMD method are shown in Figures VIII.5 and VIII.6 respectively.

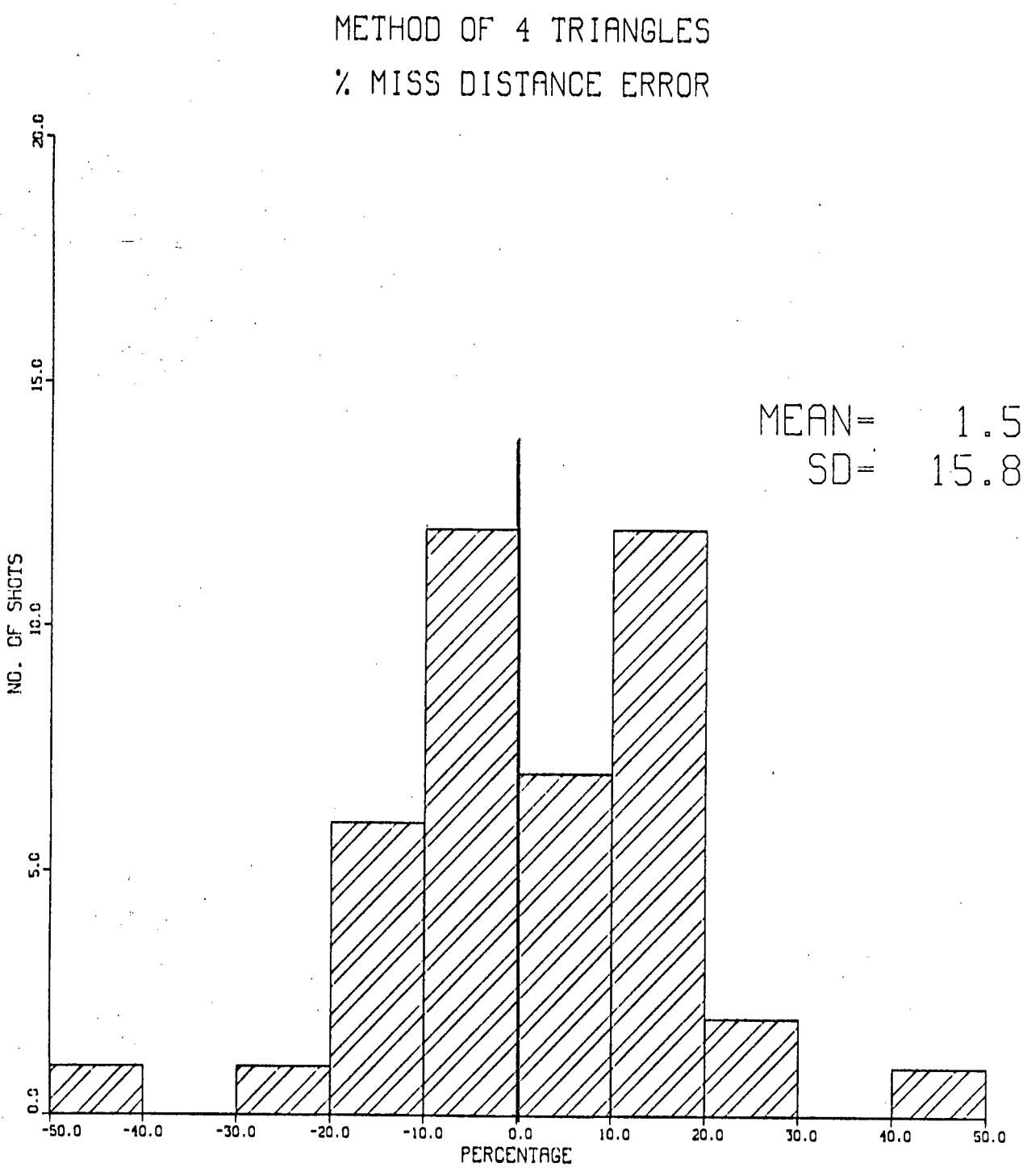

FIGURE VIII.3: Average % distance error for 300 mm (Four Triangles)

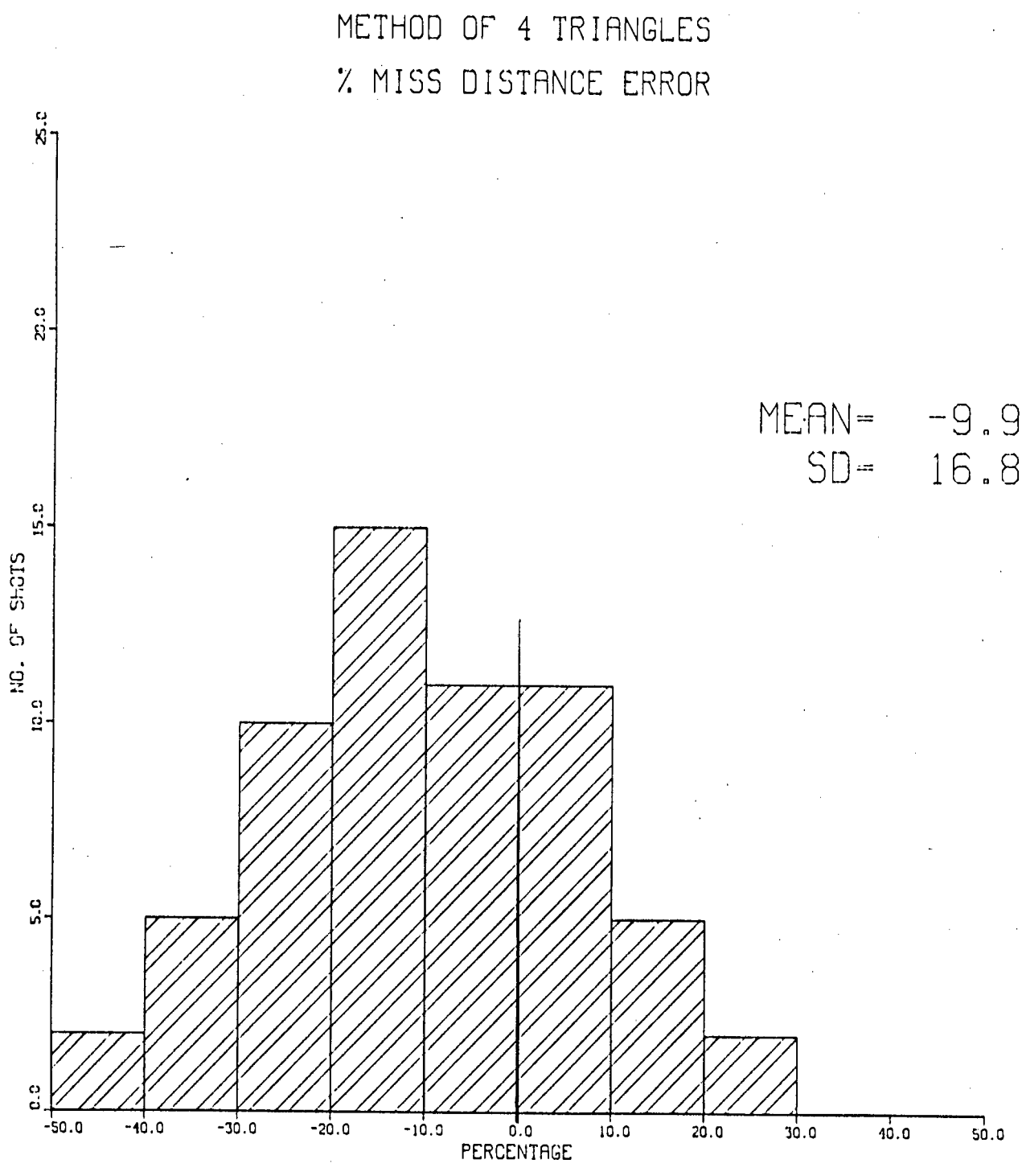

FIGURE VIII.4: Average % distance error for 1000 mm
(Four triangles)

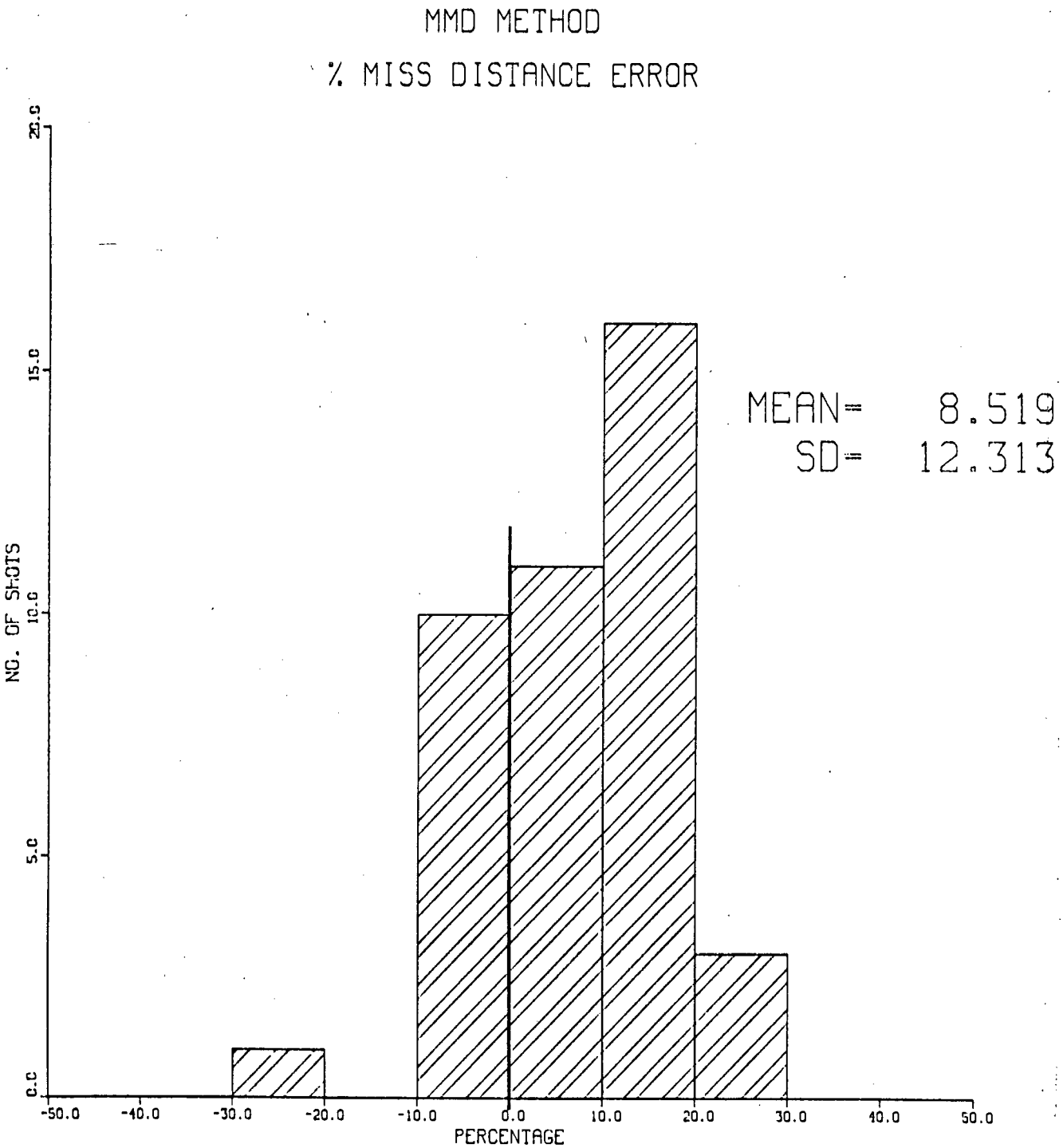

FIGURE VIII.5: Average % distance error for 300 mm base (MMD method)

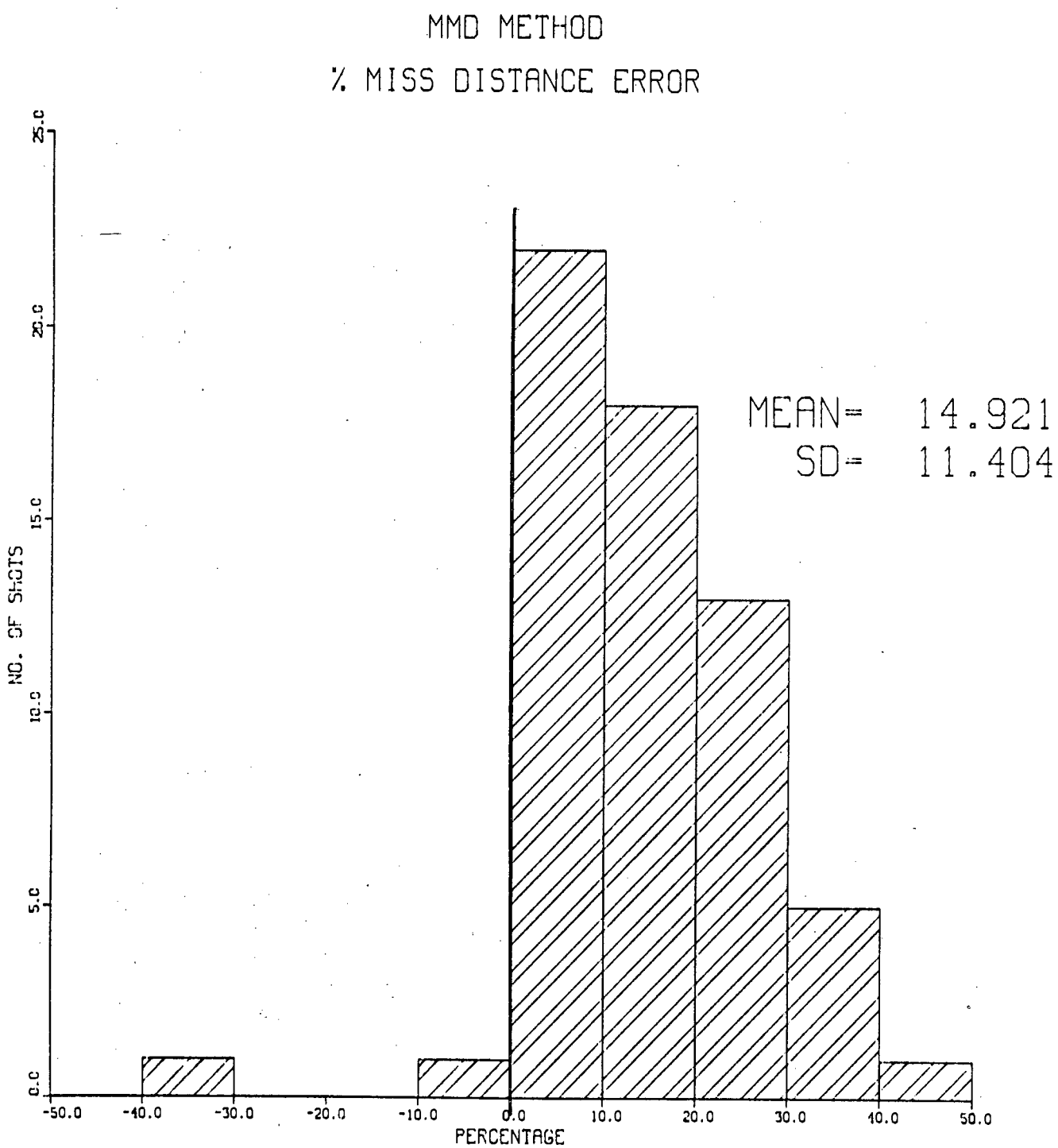

FIGURE VIII.6: Average % distance error for 1000 mm base (MMD method)

VIII.7 ANGULAR ERROR

Histograms of the average angular error (degrees) are shown in Figures VIII.7 and VIII.8 overleaf for the 300 and 1000 mm measurement bases for the method of four triangles and in VIII.9 and VIII.10 for the MMD method.

(i) Method of Four Triangles

The average error for 300 mm base is 7,28° ±21,3° which, for the 1000 mm base, reduces to an average of 0,072° ±34,2. The reduction in error for a larger measuring base is expected and predicted in Appendix VII. The increase in standard deviation is contrary to what would be expected.

(ii) MMD Method

The change in angular error results is not as marked as in the previous case. The standard deviation is reduced from ±30,6° to ±25,2° although in a small sample this might not convey very much. It is however a change constant with the increase in measuring base.

The average error changes from 2,58° to -3,3° which is not regarded as very significant and is unexpected given the 3,33-fold increase in measuring base.

The angular error in both cases (i) and (ii) above is regarded by the author as satisfactory given the inherent noisiness of the phenomenon on which it is based. The large standard deviation is a direct result of the error multiplication inherent in the dependence described in V and VI. The angular error histogram for the MMD method shows an improvement in the grouping (spread) of data from the 300 to 1000 mm base. Whereas the method fails to provide answers 13% more often than the more robust method of four triangles, the answers it provides are better. This can also be seen from the fact that the MMD method achieves 36 out of 60 readings in the range ±10% while the method of 4 triangles yields only 1 result in his range.

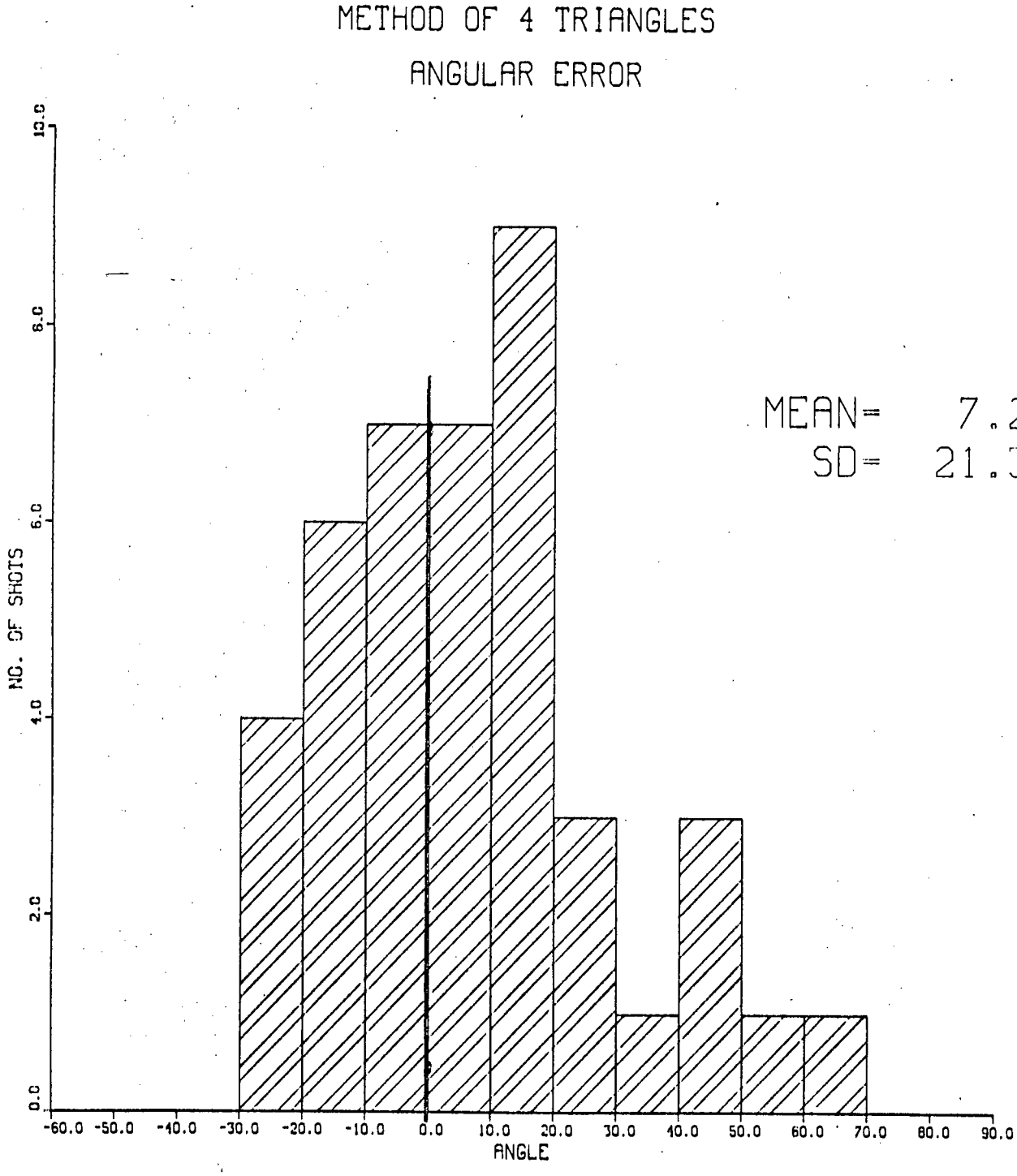

FIGURE VIII.7: Average angular error (degrees) for 300 mm base (Four Triangles

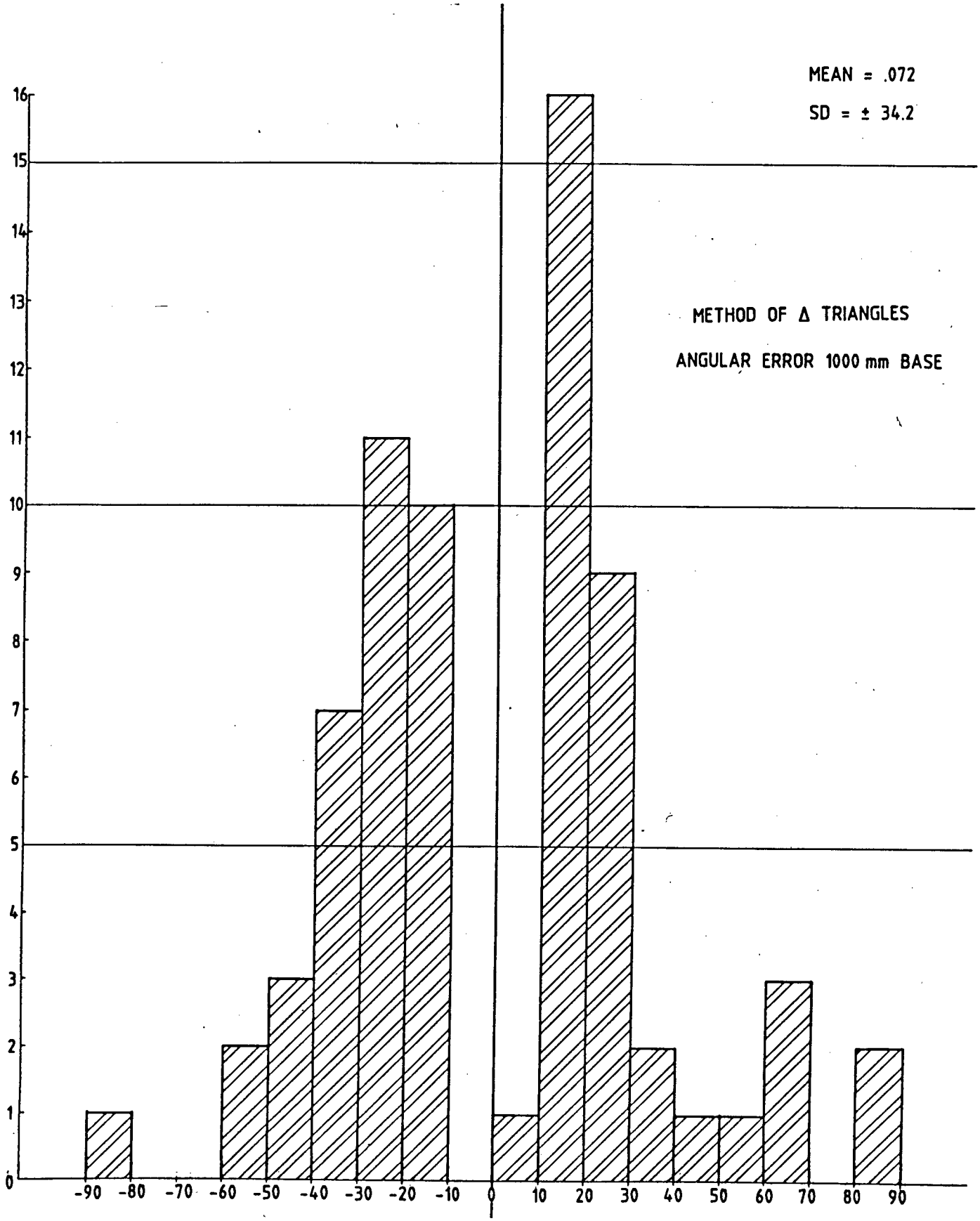

FIGURE VIII.8: Average angular error (degrees) for the 1000 mm base (Four Triangles)

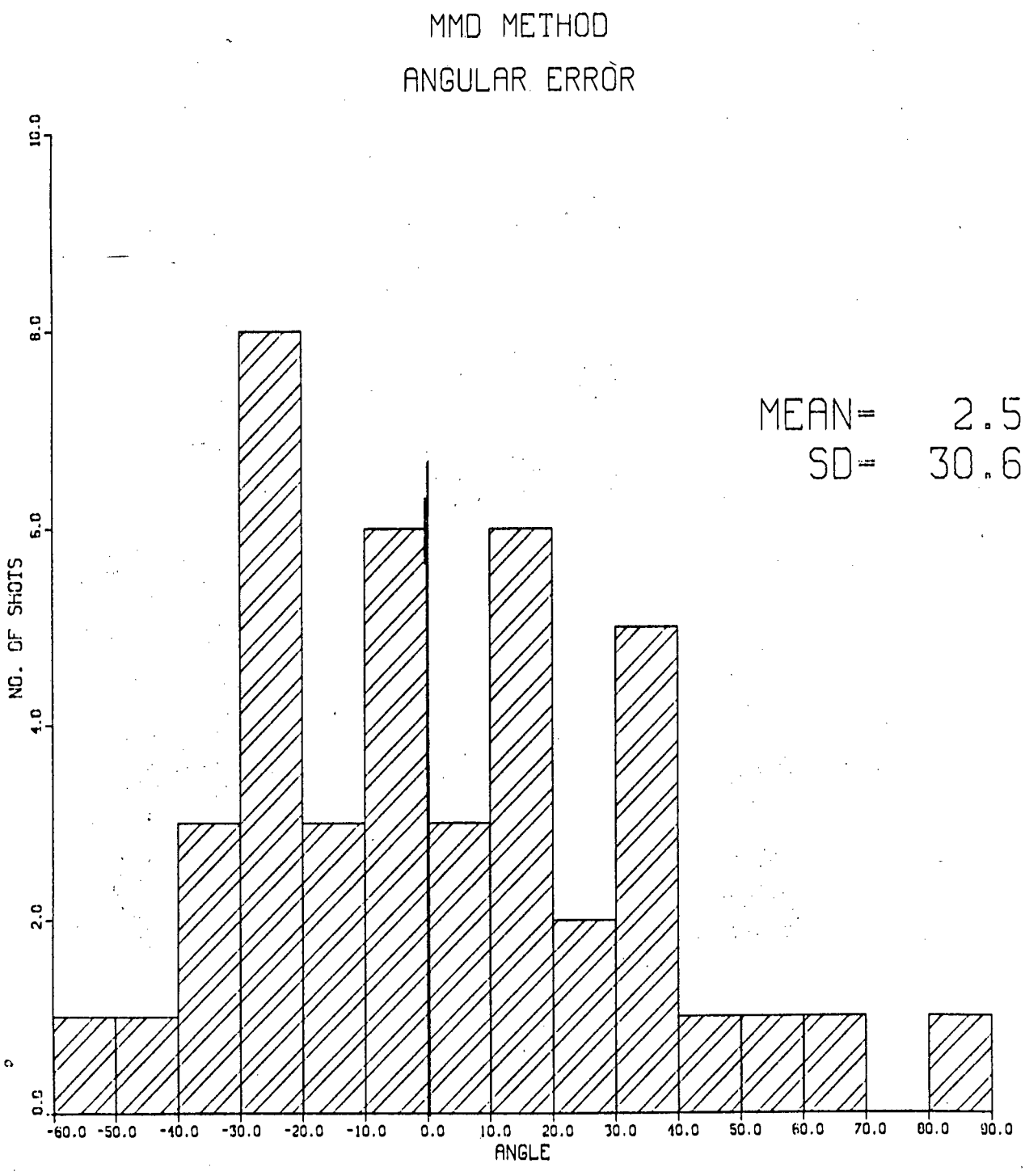

FIGURE VIII.9: Average angular error (degrees) for the 300 mm base (MMD method)

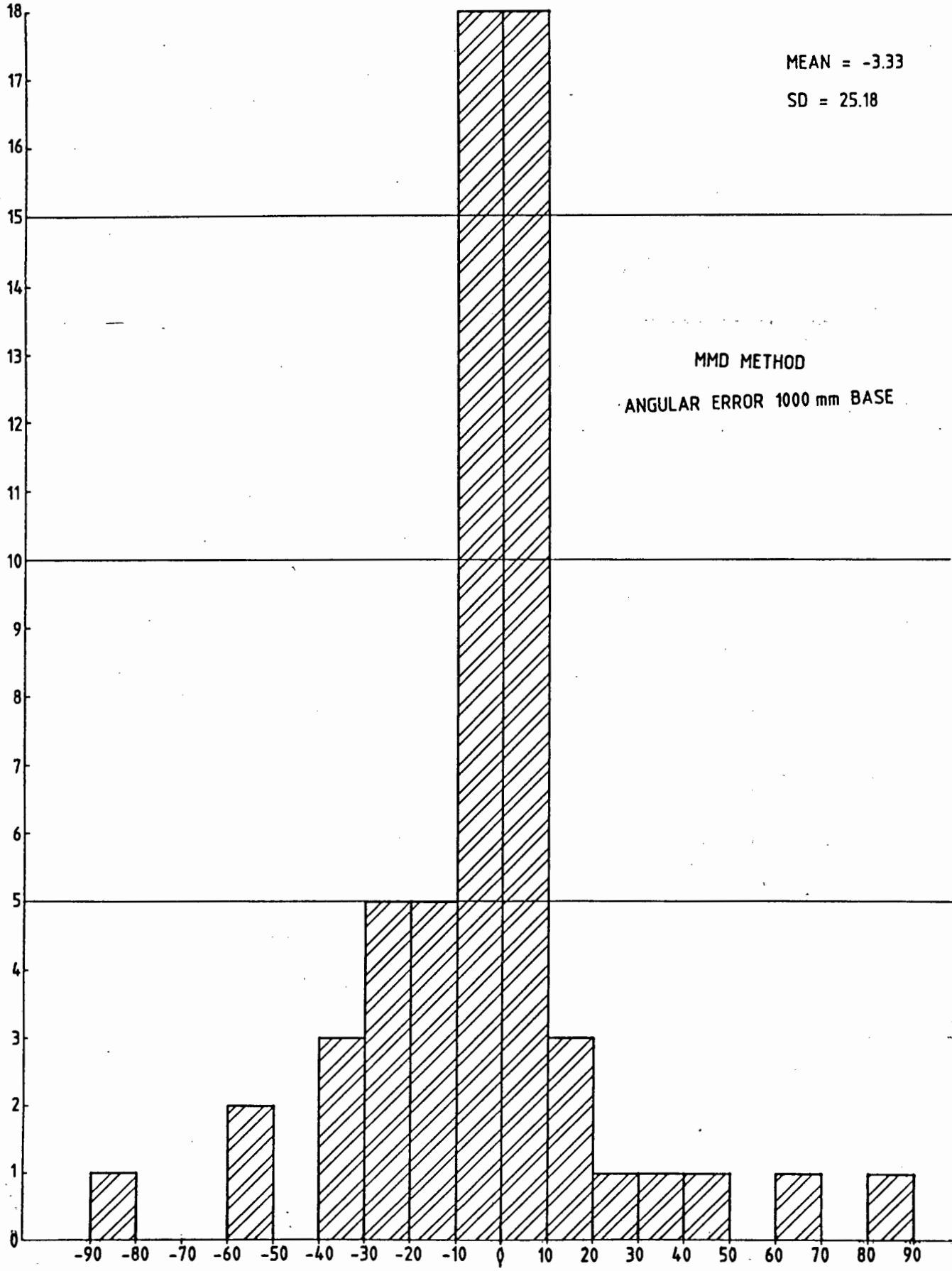

FIGURE VIII.10: Average angular error (degrees) for the 1000 mm base (MMD Method)

VIII.8 LIMITS TO ACCURACY

The measuring clock rate is 1,25 MHz implying a resolution of ±0,8 μs on any reading.

A typical N-wave has a duration of 530 μs. The % error in any reading is thus

$$100 \times \frac{0,8}{530} = 0,15\%$$

The error multiplication (amplification) in the vector calculation is shown to be between 30 and 46 times implying a probable range of error of 4,5% to 6,9%. These values are lower than those measured i.e. 9-11% for the two methods and represent theoretically noiseless limits.

The noisy nature of the measured times can be seen by comparing N-wave periods at identical miss distances.

In Orientation XV sensors 1, 2 and 3 are at identical distances from the passage of the round. The sensors and all signal processing stages are identical.

For the first few readings of orientation XV, the range of the readings has an average of 10,4 ±4,4 micro-seconds.

For orientation XVIII the average difference between sensors 5 and 4 is 3,12 ±2,72 μs.

Equation 5.10 relates miss distance to N-wave period

i.e $$r = \frac{\tau\, v(t) - m\ell o}{(k-1)\sqrt{Mo^2 - 1}}$$

for some v(t)

$$\frac{\delta r}{\delta \tau} = \frac{\tau \, v(t)}{(k-1)\sqrt{Mo^2 - 1}}$$

Typically at 500 m say,

$$k - 1 = 4{,}84 \times 10^{-3}$$
$$v(t) = 834{,}0 \text{ ms}^{-1}$$
$$c = 346{,}0 \text{ ms}^{-1}$$

hence

$$\frac{\delta r}{\delta \tau} = 7{,}85 \times 10^{4} \text{ ms}^{-1}$$

errors of 3 μs result in length errors of 0,235 meters i.e. at 10 m an error of 2,35%.

It is clear that the trailing shock cone is changing dimension or angle very rapidly and that these changes are reflected in the small differences detected at different sensors.

For a typical barrel design, the shell could be rotating at up to 180 000 RPM at its exit from the muzzle. At 500 m this rotation will be somewhat slower say 144 000 RPM.

This rotational speed implies a period of 416 μs per revolution.

At a velocity of 834 ms^{-1}, the shell takes 1,19 ms to cover 1 m; the distance between two sensors in the 1000 mm base system. Thus during that time it rotates 2,85 times. Thus the aspect of the shock wave which stimulated the first microphone is unlikely to be the same as that which stimulates the second sensor.

In view of these sources of error, it is unlikely that accuracies of ±10% will be bettered in systems which depend on N-wave period as a means of measuring miss distance. Whereas this is acceptable for estimating the modulus of the miss vector, error multiplication makes the argument of such a vector highly suspect.

It is not possible to derive the miss distance from a sequence of stimulations of sensors. It is however possible in principle to derive the direction from which the stimulations emanated. Using the distance law for modulus and a sequence relationship (as yet to be developed) it should be possible to improve the angular resolution to close to 10°, more than satisfying the requirements for training and evaluation.

APPENDIX IX: EXPERIMENTAL READINGS

The data are grouped as follows:

1 Measured times (τ_i and t_i) in microseconds for the 300 mm base system.

2 Calculated miss vectors for 300 mm base

3 Measured times for the 1000 mm base system

4 Calculated miss vectors for 1000 mm base

Note: The orientations of the microphones are as described in Chapter 5.7.

IX.1 MEASURED TIMES

T1 - T5 times of flight

TAU 1 - TAU 5 N-Wave periods

300 mm Measurement Base

Date of Test 29-1-85

500 METRES

SHOT NO.	AIM		T(1)	T(2)	T(3)	T(4)	T(5)	TAU(1)	TAU(2)	TAU(3)	TAU(4)	TAU(5)	V(T)	AIMED MISS DISTANCE	MEASURED MISS DISTANCE	XERROR
							ORIENTATION II									
1	5L	0	498247.2	498263.2	497568.8	497770.4	496665.6	443.2	441.6	436.8	442.4	443.2	842.8	5.0	5.5	10.4
2	5L	0	498336.8	498344.8	497666.4	497346.4	496724.8	436.0	435.2	430.4	434.4	435.2	842.8	5.0	4.9	-2.2
3	5L	0	484873.6	484948.8	484228.8	484430.4	483339.2	448.8	448.0	442.4	448.0	444.8	847.6	5.0	6.0	19.8
4	5L	0	496608.0	496598.3	495919.2	496112.0	495003.2	445.6	443.2	439.2	446.4	444.0	843.4	5.0	5.7	14.5
5	5L	0	494060.0	494126.4	493418.4	493603.2	492504.8	444.0	444.0	439.2	442.4	442.4	844.3	5.0	5.6	12.4
6	10L	0	514860.0	514867.2	480000.0	514363.2	513192.8	520.8	517.6	.0	517.6	512.8	837.1	10.0	12.2	21.8
7	10L	0	508451.2	508516.8	507812.0	507993.6	506866.4	510.4	509.6	508.0	511.2	509.6	839.3	10.0	11.5	15.1
8	10L	0	501424.8	501454.4	500760.0	500948.0	499824.8	512.8	512.0	509.6	512.8	514.4	841.7	10.0	11.7	17.3
9	10L	0	511416.8	511493.6	510787.2	510957.6	509820.8	508.8	506.4	505.6	506.4	506.4	838.2	10.0	11.2	12.5
10	10L	0	508072.8	508130.0	507464.0	507629.6	506453.6	514.4	513.6	512.0	513.6	505.6	839.4	10.0	11.7	17.0
11	10L	0	501587.2	501755.4	501016.0	501196.8	500096.0	501.6	500.8	498.4	502.4	501.6	841.6	10.0	10.7	7.4
12	10L	0	511322.4	511468.0	510732.0	510901.6	509740.8	508.0	507.2	504.8	506.4	504.0	838.2	10.0	11.2	11.9
13	15L	0	524565.6	524670.4	523954.4	524124.8	522976.0	550.4	550.4	548.0	551.2	555.2	833.7	15.0	15.2	1.4
14	15L	0	520972.0	521051.2	520342.4	520524.8	519375.2	548.8	549.6	546.4	551.2	544.8	834.9	15.0	14.9	-.4
15	15L	0	521058.4	521109.6	520423.2	520586.4	519428.8	547.2	548.0	545.6	547.2	545.6	834.9	15.0	14.8	-1.3
16	15L	0	521077.6	521145.6	520448.0	520620.8	519471.2	540.0	540.0	537.6	542.4	552.8	834.9	15.0	14.4	-3.7
							ORIENTATION I									
18	20L	0	545546.4	545500.8	545792.0	544961.6	542275.2	627.2	627.2	625.6	624.8	616.8	826.4	20.0	21.9	9.5
19	20L	0	539949.6	508462.4	486884.0	539359.2	536679.2	615.0	.0	619.2	614.4	613.6	833.2	20.0	21.0	4.9
20	15L	0	522914.4	522792.0	523119.2	522296.0	519620.8	561.6	560.0	560.0	559.2	548.0	834.2	15.0	15.8	5.3
21	15L	1	511704.8	511646.4	511943.2	511113.6	508424.0	554.4	554.4	556.0	553.6	547.2	838.1	15.0	15.3	2.1
22	15L	1	533520.8	533408.0	533732.8	532908.0	530244.8	608.0	608.0	610.4	607.2	604.8	830.5	15.0	20.3	35.1
23	15L	1	706032.8	705918.4	675168.8	705436.8	671708.0	606.4	604.8	604.8	603.2	599.2	777.1	15.0	21.0	39.6
24	5R	0	495874.4	496505.6	496560.8	495811.2	494578.4	435.2	432.8	440.8	436.0	436.0	843.5	5.0	5.1	1.3
25	5R	0	482164.8	482130.4	482816.8	482068.0	480861.6	429.6	428.0	436.8	431.2	433.6	848.4	5.0	4.7	-5.3
26	5R	0	499081.6	499036.0	480000.0	498977.6	497722.4	428.8	427.2	.0	434.4	432.8	842.6	5.0	4.6	-8.2
27	10R	0	507907.2	507874.4	480000.0	507796.8	506549.6	502.4	501.6	.0	503.2	502.4	839.5	10.0	10.9	8.7
28	10R	0	509364.0	509300.0	480000.0	509231.2	507955.2	494.4	492.0	.0	495.2	493.6	839.0	10.0	10.1	1.1
29	10R	0	494237.6	494142.4	480000.0	494108.8	492876.8	496.8	495.2	.0	499.2	494.4	844.3	10.0	10.3	3.3
30	10R	0	491608.8	491549.6	480000.0	491497.6	490256.8	497.6	495.2	.0	499.2	498.4	845.2	10.0	10.4	4.4
31	15R	0	521507.2	521434.4	480000.0	521387.2	520125.6	555.2	552.8	.0	556.0	547.2	834.8	15.0	15.4	2.4
32	15R	0	536176.0	536125.6	480000.0	536028.0	534682.4	548.8	548.0	.0	548.8	544.0	829.7	15.0	14.9	-.5
33	15R	0	525561.6	525516.0	480000.0	525436.8	524097.6	564.0	562.4	.0	563.2	551.2	833.4	15.0	16.0	6.8
34	15L	0	521928.8	521896.0	522178.4	521352.0	518658.4	559.2	558.4	559.2	557.6	547.2	834.5	15.0	15.7	4.5
35	10L	0	506968.8	506944.8	507216.0	506391.2	503687.2	500.8	499.2	500.0	498.4	484.8	839.7	10.0	10.4	3.6
37	5RT	0	481303.2	481228.0	481584.0	481998.0	484554.4	418.4	416.8	418.4	424.8	443.2	848.7	5.0	4.1	-18.2
38	10R	0	506234.4	506191.2	506557.6	506934.4	509473.6	496.0	494.4	496.8	498.4	504.0	839.9	10.0	10.5	4.7
39	15R	0	511006.4	510977.6	511332.8	511712.0	514249.6	544.0	544.0	544.0	546.4	552.8	838.2	15.0	14.7	-1.7
40	15L	5	523316.0	523424.8	523635.2	522815.2	520161.6	551.2	552.0	552.0	550.4	541.6	834.0	15.8	15.1	-4.7
41	10LT	5	503316.8	503503.2	503674.4	480000.0	500256.8	508.0	507.2	508.0	.0	494.4	841.2	11.2	11.0	-1.3
42	10L	5	510164.8	510388.0	510539.2	509736.8	507166.4	513.6	513.6	512.8	511.2	498.4	838.6	11.2	11.5	3.1
43	5L	5	481819.2	482236.8	482280.0	481559.2	479400.8	441.6	443.2	442.4	440.0	424.0	848.5	7.1	5.3	-25.2
44	0L	5	480000.0	490843.2	490750.4	490472.0	490463.2	.0	441.6	440.8	440.8	438.4	845.4	5.0	5.5	9.1
45	0L	10	480000.0	505392.8	505299.2	505043.2	504996.8	.0	510.4	508.8	510.4	508.8	840.3	10.0	11.5	15.0
48	10R	5	509552.0	509308.0	510023.2	510362.4	512771.2	505.6	505.6	505.6	508.8	516.8	838.7	11.2	11.4	2.0
49	15RT	5	512304.0	512478.4	512733.6	513097.6	515580.8	548.0	548.0	548.0	550.4	557.6	837.7	15.8	15.1	-4.4
50	15R	5	520077.6	520244.8	520306.4	520868.8	523350.4	557.6	557.6	556.0	560.0	568.8	835.0	15.8	16.0	1.1

500 METRES

SHOT NO.	AIM		T(1)	T(2)	T(3)	T(4)	T(5)	TAU(1)	TAU(2)	TAU(3)	TAU(4)	TAU(5)	V(T)	AIMED MISS DISTANCE	MEASURED MISS DISTANCE	XERROR
							ORIENTATION V									
52	10L	0	496045.6	496772.8	496376.8	496048.8	494628.8	491.2	492.8	492.0	490.4	476.8	843.4	10.0	9.7	-3.4
56	5R	0	488980.0	488794.4	488957.6	489591.2	492395.2	432.0	429.6	432.8	437.6	444.8	846.0	5.0	5.0	.4
57	10R	0	500797.6	500623.2	500759.2	501412.8	504238.4	496.8	495.2	496.8	501.6	508.0	841.8	10.0	10.6	6.2
58	15R	0	519963.2	519785.6	519894.4	520557.6	523390.4	556.8	556.0	556.8	559.2	563.2	835.1	15.0	15.8	5.7
59	15L	5	510822.4	511544.0	510995.2	510811.2	509427.2	548.0	548.8	477.6	545.6	528.0	838.3	15.8	13.3	-16.1
60	10L	5	505070.4	505775.2	505214.4	551680.0	503776.0	496.0	496.8	496.0	.0	483.2	840.4	11.2	10.0	-10.2
61	5L	5	496914.4	497556.0	496838.4	480000.0	495982.4	436.8	437.6	434.4	.0	422.4	843.2	7.1	4.8	-32.5
62	0L	5	494475.2	494719.2	493924.8	494575.2	495592.8	452.8	451.2	448.0	453.6	454.4	844.1	5.0	6.5	29.1
							ORIENTATION VIII									
67	15L	0	516504.0	516112.8	516254.4	515675.2	513110.4	540.0	536.8	537.6	538.4	533.6	836.5	15.0	14.0	-6.9
68	10L	0	497715.2	497304.0	497556.0	496914.4	494368.0	494.4	492.0	493.6	492.0	482.4	843.1	10.0	9.9	-1.5
70	5L8	0	495561.6	495148.0	495485.6	494796.0	492270.4	433.6	425.6	431.2	428.8	413.6	843.8	5.0	4.2	-15.4
71	5R	0	494751.2	495572.0	495232.0	480000.0	495974.4	448.0	450.4	452.0	.0	460.0	843.8	5.0	6.5	30.1
72	5R	0	486589.6	487412.8	487056.0	487172.8	487834.4	444.0	446.4	447.2	449.6	458.4	846.7	5.0	6.2	24.4
73	10RT	0	492759.2	493576.0	493246.4	493342.4	493979.2	506.4	509.6	509.6	509.6	516.0	844.5	10.0	11.5	15.4
74	10RB	0	506861.6	507684.8	507309.6	507432.0	508051.2	500.0	502.4	502.4	505.6	510.4	839.6	10.0	11.0	10.2
75	15R	0	519099.2	519923.2	519533.6	519656.8	520247.2	552.8	555.2	554.4	555.2	558.4	835.3	15.0	15.6	3.7
76	15L	5	517935.2	517556.0	517586.4	517092.8	514601.6	554.4	552.8	552.8	552.0	546.4	836.0	15.8	15.2	-3.6
77	10L	5	503307.2	502939.2	502884.0	502464.0	500063.2	504.0	500.8	501.6	500.8	493.6	841.1	11.2	10.7	-4.6
78	5L	5	493652.0	493402.4	493074.4	492879.2	490894.4	436.0	428.8	429.6	430.4	421.6	844.5	7.1	4.5	-36.7
79	0L	5	491839.6	492144.8	491342.4	480000.0	491038.4	422.4	420.8	415.2	.0	421.6	845.1	5.0	3.7	-26.6
80	0L	10	498410.4	498640.0	497857.6	498100.0	497369.6	487.2	486.4	484.0	487.2	488.8	842.7	10.0	9.5	-5.1
81	5R	5	493805.6	494520.8	493784.0	480000.0	494592.0	453.6	455.2	452.8	.0	460.0	844.2	7.1	6.8	-4.5
82	10R	5	507132.8	507936.0	507352.0	480000.0	508224.0	511.2	513.6	512.0	.0	518.4	839.5	11.2	11.9	6.2
83	15R	5	513310.4	514115.2	513536.8	513787.2	514374.4	556.0	557.6	556.0	556.8	561.6	837.4	15.8	15.8	-.4

1000 METRES

SHOT NO.	AIM		T(1)	T(2)	T(3)	T(4)	T(5)	TAU(1)	TAU(2)	TAU(3)	TAU(4)	TAU(5)	V(T)	AIMED MISS DISTANCE	MEASURED MISS DISTANCE	%ERROR
							ORIENTATION II									
137	15L	1	1115627.2	1115671.2	1114959.2	1115210.4	1114321.6	544.0	543.2	541.6	543.2	543.2	665.4	15.0	15.3	1.9
138	10L	1	1116363.2	1116438.4	1120000.0	1115956.8	1115052.0	492.0	492.0	.0	492.8	492.0	665.3	10.0	8.6	-14.4
139	10LT	1	1095252.0	1095310.4	1040000.0	1094849.6	1094004.0	498.4	497.6	.0	498.4	500.0	670.2	10.0	9.5	-5.1
140	10L	1	1114209.6	1114256.8	1120000.0	1113786.4	1112879.2	491.2	490.4	.0	491.2	490.4	665.8	10.0	8.4	-16.1
141	5L	1	1088017.6	1088184.8	1040000.0	1087662.4	1086792.0	416.0	416.0	.0	415.2	418.4	671.9	5.1	-1.1	-121.4
143	5R	1	1090517.6	1090608.8	1040000.0	1090290.4	1088414.4	460.8	460.0	.0	462.4	455.2	671.4	5.1	4.5	-11.9
144	10R	1	1113119.2	1113230.4	1040000.0	1112893.6	1110992.0	511.2	511.2	.0	512.8	510.4	666.1	10.0	11.2	10.9
146	15R	1	1126618.4	1126736.0	1127216.0	1126390.4	1124474.4	561.6	561.6	562.4	562.4	559.2	662.8	15.0	17.8	18.2
147	15RT	1	1118498.4	1118609.6	1120000.0	1118274.4	1116382.4	564.8	564.8	.0	564.0	560.0	664.8	15.0	18.0	19.8
148	15R	1	1119745.6	1119874.4	1120000.0	1119527.2	1117628.0	562.4	563.2	.0	563.2	560.0	664.5	15.0	17.9	18.8
149	15L	5	1117552.0	1117812.0	1117032.0	1117242.4	1116314.4	561.6	562.4	559.2	561.6	561.6	664.9	15.8	17.7	12.2
150	10L	5	1126746.4	1127011.2	1126231.2	1126436.8	1125500.8	553.6	553.6	551.2	553.6	556.8	662.8	11.2	16.7	49.8
151	10LT	5	1106826.4	1107134.0	1106392.8	1106579.2	1105670.4	527.2	528.0	526.4	528.0	528.0	667.4	11.2	13.3	18.8
152	10L	5	1127664.0	1123062.4	1127272.0	1127432.0	1126466.4	523.2	524.0	521.6	523.2	524.8	662.6	11.2	12.7	13.5
153	5L	5	1122298.4	1122853.6	1122102.4	1120000.0	1121100.8	490.4	492.8	489.6	.0	492.8	663.8	7.1	8.5	19.7
155	5L	5	1099218.4	1099823.2	1099096.0	1040000.0	1098079.2	486.4	488.8	486.4	.0	489.6	669.2	7.1	8.1	14.7
156	0L	5	1113619.2	1114333.6	1113796.8	1120000.0	1112306.4	469.6	472.8	471.2	.0	470.4	665.8	5.0	5.8	16.3
157	0L	5	1118406.4	1119127.2	1118634.4	1120000.0	1117057.6	460.8	463.2	462.4	.0	462.4	664.7	5.0	4.6	-7.6
159	5R	5	1108554.4	1109105.6	1109164.0	1108520.0	1106813.6	483.2	485.6	486.4	485.6	482.4	666.9	7.1	7.6	8.1
160	5R	5	1116408.8	1116863.2	1117040.8	1120000.0	1114535.2	480.0	481.6	484.8	.0	479.2	665.2	7.1	7.2	1.4
162	10R	5	1130712.0	1130997.6	1120000.0	1130556.4	1129676.0	522.4	522.4	.0	523.2	522.4	662.0	11.2	12.6	12.6
163	10R	5	1116319.2	1116628.8	1120000.0	1116181.6	1114316.8	514.4	515.2	.0	516.0	511.2	665.3	11.2	11.5	2.9
164	10R	5	1121224.0	1120000.0	1121865.6	1121097.6	1119246.4	514.4	.0	517.6	516.0	512.8	664.1	11.2	11.6	4.0
165	15R	5	1128324.0	1128631.2	1123959.2	1128180.0	1126312.8	572.0	572.8	573.6	572.0	569.6	662.4	15.8	19.2	21.3
166	15R	5	1147207.2	1147500.0	1147336.8	1147052.0	1145156.8	571.2	572.0	572.0	572.0	571.2	658.0	15.8	19.2	21.2
167	15RT	5	1127006.4	1127328.0	1127653.6	1126384.0	1125063.2	572.0	572.0	572.8	572.0	568.0	662.7	15.8	19.1	20.7
168	10RT	5	1108483.2	1108892.8	1109121.6	1108388.0	1106601.6	532.8	533.6	533.6	531.2	524.8	667.0	11.2	13.8	23.1
169	10R	5	1128744.8	1129172.8	1129390.4	1128667.2	1126874.4	527.2	529.6	531.2	531.2	529.6	662.3	11.2	13.5	21.1
170	10R	5	1121175.2	1121606.4	1121813.6	1121039.6	1119311.2	523.2	523.2	524.0	521.6	522.4	664.0	11.2	12.6	13.1
171	5R	5	1115530.8	1116110.4	1116198.4	1115532.8	1113793.6	496.0	498.4	500.8	498.4	496.8	665.3	7.1	9.4	32.6
172	5R	5	1115326.4	1115862.4	1115947.2	1115283.2	1113525.6	509.6	512.0	514.4	512.0	506.4	665.4	7.1	11.1	56.6
173	5R	5	1112488.0	1113022.4	1113109.6	1040000.0	1110722.4	493.6	496.0	498.4	.0	494.4	666.1	7.1	9.1	28.2
175	5L	5	1102024.8	1102637.6	1101928.0	1040000.0	1100840.8	472.0	475.2	471.2	.0	475.2	668.6	7.1	6.2	-12.2
176	5L	5	1111692.8	1112264.0	1111529.6	1040000.0	1110510.4	477.6	479.2	476.8	.0	481.6	666.3	7.1	6.9	-3.0
							ORIENTATION V									
178	15L	1	1108151.2	1108964.0	1108440.0	1108359.2	1107723.2	531.2	533.6	532.0	532.0	529.6	667.0	15.0	13.8	-8.0
179	10LT	1	1090491.2	1091308.8	1090838.0	1090714.4	1090047.2	489.6	492.0	491.2	488.8	487.2	671.2	10.0	8.4	-16.4
180	10L	1	1113756.0	1114574.4	1114103.2	1120000.0	1113338.4	484.8	487.2	486.4	.0	475.2	665.7	10.0	7.5	-25.9
181	10L	1	1106524.0	1107334.4	1106820.0	1040000.0	1106104.8	492.8	494.4	492.0	.0	482.4	667.4	10.0	8.4	-16.3
186	10R	1	1102036.8	1101785.6	1101815.2	1102540.0	1105307.2	462.4	457.6	460.0	465.6	477.6	668.5	10.0	5.1	-49.6
187	10R	1	1116994.4	1116752.8	1116793.6	1120000.0	1120284.0	518.4	518.4	518.4	.0	530.4	664.9	10.0	12.5	23.9
188	15RT	1	1129231.2	1128983.2	1129038.4	1129751.2	1132520.8	570.4	569.6	569.6	571.2	577.6	662.2	15.0	19.1	27.3
190	15L	1	1112454.4	1113268.0	1112794.4	1120000.0	1112001.6	529.6	532.8	530.4	.0	521.6	666.0	15.0	13.4	-10.7
191	10L	1	1111713.6	1112520.0	1112015.2	1040000.0	1111302.4	484.0	485.6	484.8	.0	475.2	666.2	10.0	7.3	-27.1
193	15LT	5	1117944.8	1120000.0	1118072.8	1118109.6	1117565.6	547.2	.0	545.6	546.4	540.0	664.8	15.8	15.6	-1.6
194	15L	5	1120227.2	1120000.0	1120350.4	1120403.2	1119932.8	547.2	.0	547.2	546.4	540.8	664.3	15.8	15.6	-1.1
199	5L	5	1113746.4	1114360.8	1113548.0	1120000.0	1113927.2	460.0	460.0	457.6	.0	450.4	665.7	7.1	4.0	-43.9

1000 METRES

SHOT NO.	AIM		T(1)	T(2)	T(3)	T(4)	T(5)	TAU(1)	TAU(2)	TAU(3)	TAU(4)	TAU(5)	V(T)	AIMED MISS DISTANCE	MEASURED MISS DISTANCE	XERROR
							ORIENTATION VIII									
201	25LT	0	1140538.4	1140180.0	1140222.4	1139700.8	1137160.8	659.2	657.6	658.4	657.6	653.6	659.7	25.0	30.7	22.6
202	25L	0	1129668.8	1129300.0	1129476.8	1128858.4	1126247.2	644.0	644.0	644.0	643.2	636.8	662.2	25.0	28.6	14.3
203	25L	0	1141480.8	1141117.6	1141306.4	1140673.6	1138069.6	645.6	645.6	645.6	644.0	640.8	659.5	25.0	28.9	15.7
204	25L	0	581779.2	581425.6	581492.8	580944.0	579372.0	646.4	646.4	646.4	645.6	641.6	814.3	25.0	24.1	-3.6
205	25L	0	1116953.6	1116599.2	1116624.8	1116111.2	1113557.6	632.0	634.4	633.6	630.4	622.4	665.1	25.0	26.9	7.6
206	25L	0	1141162.4	1140798.0	1140822.4	1140318.4	1137789.6	637.6	634.4	636.0	635.2	635.2	659.5	25.0	27.8	11.0
207	25L	0	1148826.4	1148477.6	1148494.4	1147986.4	1145448.0	645.6	644.0	644.0	643.2	641.6	657.8	25.0	28.9	15.6
208	15L	0	480000.0	551242.4	551267.2	550753.6	548206.4	.0	636.8	636.8	636.8	634.4	824.8	15.0	23.0	53.4
210	15L	5	1134446.4	1134136.8	1134039.2	1133611.2	1131149.6	551.2	548.8	549.6	548.8	544.0	661.1	15.8	16.0	1.4
211	10L	5	1106690.4	1106402.4	1106227.2	1105866.4	1104232.4	508.0	506.4	505.6	505.6	769.6	667.5	11.2	17.4	55.9
212	5L	5	1108972.0	1108740.8	1108437.6	1108187.2	1106039.2	459.2	453.6	453.6	454.4	446.4	667.0	7.1	3.5	-49.9
213	0L	5	1105224.8	1105604.8	1104787.2	1040000.0	1104380.0	465.6	465.6	462.4	.0	467.2	667.8	5.0	5.1	2.3
214	0L	5	1107206.4	1107548.0	1106740.8	1040000.0	1106238.4	464.0	463.2	460.0	.0	464.0	667.4	5.0	4.8	-4.3
218	15R	5	1130604.0	1120000.0	1130788.8	1130960.8	1131136.8	572.8	.0	572.8	572.8	576.8	661.8	15.8	19.4	22.8
							ORIENTATION IX									
219	15L	5	1124165.6	1124520.0	1124948.0	1124763.2	1125697.6	548.0	548.8	550.4	548.8	544.8	663.3	15.8	16.0	1.2
220	15L	5	1124526.4	1124952.0	1125314.4	1125150.4	1126077.6	553.6	556.0	556.0	555.2	550.4	663.2	15.8	16.8	6.3
221	10L	5	1119724.8	1120244.8	1120492.0	1120386.4	1121365.6	517.6	519.2	520.8	519.2	514.4	664.3	11.2	12.0	7.6
222	10L	5	1117496.0	1118039.2	1118259.2	1118159.2	1119160.0	519.2	521.6	522.4	519.2	512.8	664.8	11.2	12.1	8.6
225	0L	5	1108320.0	1109055.2	1108624.0	1108984.0	1110365.6	503.2	504.8	504.0	504.0	500.0	666.9	5.0	10.1	101.7
226	0LT	5	1093797.6	1099552.8	1099152.0	1099468.8	1100772.8	497.6	500.8	499.2	500.0	497.6	669.2	5.0	9.6	91.5
227	0L	5	1101138.4	1101882.4	1101476.8	1101812.8	1103165.6	488.0	489.6	489.6	490.4	488.0	668.6	5.0	8.3	65.4
228	5R	5	1114203.2	1114761.6	1114112.0	1114748.8	1116408.8	500.0	501.6	499.2	502.4	502.4	665.6	7.1	9.8	38.4
229	5R	5	1102732.8	1103239.2	1102570.4	1103241.6	1104899.2	500.0	502.4	498.4	501.6	499.2	668.3	7.1	9.7	37.6
230	10RT	5	1107851.2	1108958.4	1107511.2	1108266.4	1110012.0	540.8	761.6	538.4	540.0	540.8	667.1	11.2	20.8	85.6
231	10R	5	1116036.0	1116289.6	1115724.8	1116482.4	1118261.6	532.8	422.4	531.2	534.4	536.8	665.2	11.2	11.2	-.2
233	10R	5	1127898.4	1128159.2	1127569.6	1128336.8	1130102.4	536.8	428.8	535.2	536.8	533.6	662.5	11.2	11.5	2.7
234	15R	5	1105424.8	1105713.6	1105037.6	1105812.0	1107564.0	566.4	567.2	564.0	565.6	565.6	667.7	15.8	18.3	15.8
235	15R	5	1142291.2	1142560.8	1141901.6	1142688.0	1144516.8	584.8	585.6	582.4	582.4	576.8	659.2	15.8	20.6	30.3
236	15R	5	1130356.8	1130636.0	1129972.8	1130752.8	1132552.0	573.6	573.6	572.0	573.6	572.8	661.9	15.8	19.3	22.2
237	15L	1	1126037.6	1126216.0	1120000.0	1126561.6	1127476.8	541.6	542.4	.0	542.4	538.4	662.8	15.0	15.1	.3
238	15L	1	1129016.0	1129134.4	1120000.0	1129527.2	1130484.8	537.6	537.6	.0	542.4	544.0	662.1	15.0	15.0	-.5
239	15L	1	1111712.8	1111907.2	1120000.0	1112235.2	1113137.6	537.6	537.6	.0	536.8	530.4	666.1	15.0	14.3	-4.6
240	10L	1	1122419.2	1122577.6	1120000.0	1122933.6	1123860.8	493.6	492.8	.0	494.4	488.8	663.6	10.0	8.6	-14.5
241	10L	1	1108921.6	1109089.6	1040000.0	1109433.6	1110313.6	492.0	492.8	.0	492.8	484.8	666.8	10.0	8.4	-16.2
242	5L	1	1100760.8	1101035.2	1101543.2	1101318.4	1102224.0	412.8	413.6	419.2	415.2	411.2	668.7	5.1	-1.5	-129.6
245	5R	1	1108910.4	1108979.2	1108392.0	1109219.2	1111123.2	465.6	463.2	460.8	465.6	471.2	666.9	5.1	5.1	-.1
246	10R	1	1129156.8	1129192.0	1128621.6	1129450.4	1131348.8	524.8	524.8	523.2	526.4	532.0	662.2	10.0	13.1	30.1
248	15R	1	1105320.0	1105352.8	1104782.4	1105604.8	1107450.4	516.8	517.6	516.0	519.2	517.6	667.8	15.0	12.0	-20.4
250	15R	1	1097977.6	1098018.4	1097440.8	1098266.4	1100133.6	552.0	552.8	551.2	553.6	556.8	669.5	15.0	16.7	10.8

1000 METRES

SHOT NO.	AIM		T(1)	T(2)	T(3)	T(4)	T(5)	TAU(1)	TAU(2)	TAU(3)	TAU(4)	TAU(5)	V(T)	AIMED MISS DISTANCE	MEASURED MISS DISTANCE	%ERROR
							ORIENTATION X									
251	15L	1	1111344.0	1110736.0	1111505.6	1111056.0	1110600.8	551.2	548.0	548.0	548.0	544.8	666.4	15.0	16.0	6.3
252	15LT	1	1105560.8	1104957.6	1105721.6	1105242.4	1104631.2	546.4	545.6	549.6	548.0	549.6	667.7	15.0	16.0	6.1
253	15L	1	1122813.6	1122205.6	1122965.6	1122496.8	1121911.2	561.6	556.0	557.6	558.4	556.8	663.7	15.0	17.3	15.2
254	10L	1	1098846.4	1040000.0	1099024.0	1098536.8	1097993.6	491.2	.0	495.2	492.8	488.8	669.3	10.0	8.7	-13.8
255	10L	1	1118126.4	1120000.0	1118286.4	1117858.4	1117564.0	500.0	.0	498.4	499.2	495.2	664.8	10.0	9.4	-6.6
256	5L	1	1101656.0	1101074.4	1101824.8	1101304.0	1100772.8	429.6	422.4	428.8	427.2	420.8	668.7	5.1	.0	-100.5
258	5L	1	1109268.0	1108678.4	1040000.0	1108937.6	1108545.6	420.8	412.8	.0	417.6	410.4	666.9	5.1	-1.5	-128.7
259	5R	1	1095775.2	1096572.0	1096382.4	1096166.4	1096164.0	448.0	452.0	448.8	450.4	448.8	669.9	5.1	3.1	-38.4
260	5R	1	1107762.4	1108544.8	1108335.6	1108133.6	1108016.0	458.4	463.2	460.8	461.6	459.2	667.1	5.1	4.5	-11.9
261	10R	1	1040000.0	1088324.0	1088135.2	1087948.0	1087948.0	.0	522.4	520.0	520.8	519.2	671.8	10.0	12.4	23.6
262	10R	1	1120000.0	1114047.2	1113884.0	1113664.8	1113564.0	.0	523.2	521.6	522.4	520.8	665.8	10.0	12.5	24.8
263	15R	1	1120000.0	1133467.2	1133305.6	1133146.4	1133272.8	.0	559.2	558.4	558.4	558.4	662.0	15.0	2.5	-83.5
264	15R	1	1120000.0	1118731.2	1118559.2	1118479.2	1118890.4	.0	557.6	552.0	556.0	557.6	664.6	15.0	17.0	13.1
265	15R	1	1040000.0	1109284.8	1109097.6	1108945.6	1109032.8	.0	551.2	548.8	550.4	550.4	666.9	15.0	16.3	8.2
266	15R	1	1120000.0	1131009.6	1130840.0	1130644.0	1130581.6	.0	564.0	561.6	562.4	561.6	661.8	15.0	17.9	19.1
267	10L	5	1113374.4	1112922.4	1113591.2	1112904.0	1111394.4	527.2	526.4	528.0	526.4	524.0	665.9	11.2	13.1	17.4
268	15L	5	1125020.8	1124533.6	1120000.0	1124567.2	1123146.4	572.8	571.2	.0	572.0	566.4	663.3	15.8	19.0	20.0
269	15LT	5	1099948.8	1099425.6	1100126.4	1099492.0	1098152.8	558.4	556.8	558.4	556.8	555.2	669.1	15.8	17.2	8.6
270	15L	5	1122202.4	1121694.4	1120000.0	1121744.8	1120344.0	556.8	554.4	.0	553.6	548.8	664.0	15.8	16.7	5.6
271	15L	5	1126027.2	1125532.0	1120000.0	1125584.8	1124210.4	572.0	570.4	.0	570.4	565.6	663.1	15.8	18.8	19.2
272	10L	5	1110035.2	1109551.2	1110236.8	1109570.4	1108124.0	523.2	521.6	523.2	521.6	515.2	666.7	11.2	12.4	11.1
273	10L	5	1117880.0	1117503.2	1118118.4	1117371.2	1115508.0	540.0	537.6	539.2	538.4	531.2	664.9	11.2	14.6	30.2
274	10L	5	1123174.4	1122800.0	1123404.8	1122652.8	1120739.2	541.6	536.8	534.4	534.4	519.2	663.6	11.2	14.0	25.4
275	10L	5	1127309.6	1126954.4	1127560.0	1126800.0	1124885.6	534.4	532.0	534.4	532.8	526.4	662.7	11.2	13.8	23.8
276	5LT	5	1097724.8	1098160.8	1098208.0	1097500.0	1095360.0	524.0	524.8	524.0	522.4	509.6	669.5	7.1	12.4	76.0
277	5L	5	1123792.8	1124313.6	1124320.8	1123673.6	1121831.2	508.8	511.2	509.6	508.0	499.2	663.4	7.1	10.6	49.6
278	0L	5	1101677.6	1101846.4	1102092.8	1101276.0	1098803.0	480.0	480.0	481.6	478.4	463.2	668.6	5.0	6.6	32.7
279	0L	5	1091596.0	1091772.8	1092006.4	1091194.4	1088747.2	476.0	476.8	476.8	474.4	459.2	671.0	5.0	6.2	23.5
280	0L	5	1105990.4	1106167.2	1106406.4	1105588.0	1103124.8	488.0	487.2	488.8	485.6	472.0	667.6	5.0	7.6	52.3
281	0L	5	1085022.4	1085185.6	1085416.0	1084599.2	1082911.2	478.4	476.0	477.6	474.4	813.6	672.5	5.0	15.5	209.1
282	5L	5	1110750.4	1110520.0	1111036.8	1110226.4	1108018.4	496.0	495.2	497.6	494.4	482.4	666.5	7.1	8.7	23.7
283	5L	5	1114824.8	1114620.8	1115120.0	1114301.6	1112042.4	488.8	486.4	488.0	484.8	470.4	665.6	7.1	7.5	5.8
284	5R	5	1109008.8	1109499.2	1109528.8	1108853.6	1106904.0	498.4	499.2	500.8	498.4	491.2	666.8	7.1	9.3	32.2
285	5RT	5	1093485.6	1094012.0	1094006.4	1093360.0	1091477.6	499.2	501.6	501.6	499.2	492.0	670.5	7.1	9.6	35.2
286	5R	5	1126136.8	1126695.2	1126684.8	1126066.4	1124346.4	512.8	514.4	516.0	513.6	508.0	662.9	7.1	11.3	60.0
287	10R	5	1107340.0	1107873.6	1107876.0	1107236.0	1105412.0	504.8	505.6	506.4	504.8	495.2	667.2	11.2	10.1	-9.6
288	10R	5	1119334.4	1119037.6	1118937.6	1118481.6	1117432.0	540.0	541.6	541.6	540.0	536.0	664.6	11.2	14.9	33.2
289	10R	5	1103849.6	1104541.6	1104424.8	1103956.0	1102778.4	531.2	533.6	532.0	531.2	530.4	668.0	11.2	13.8	23.7
290	10R	5	1127719.2	1128405.6	1128309.6	1127835.2	1126671.2	539.2	541.6	541.6	540.0	536.0	662.5	11.2	14.9	33.0
291	15R	5	1123787.2	1124519.2	1124389.6	1123985.6	1123105.6	571.2	572.8	571.2	569.6	567.2	663.4	15.8	19.0	19.9
292	15R	5	1132469.6	1133196.0	1133077.6	1132662.4	1131741.6	573.6	575.2	573.6	573.6	572.0	661.4	15.8	19.4	22.7
293	15RT	5	1101827.2	1102574.4	1102420.8	1102051.2	1101252.8	561.6	564.0	562.4	561.6	560.8	668.5	15.8	17.8	12.7
294	15R	5	1127461.6	1128211.2	1128071.2	1127704.0	1126966.4	570.4	572.8	571.2	571.2	567.2	662.5	15.8	19.0	20.1
295	15L	5	1124899.2	1125630.4	1125499.2	1125096.0	1124212.8	576.0	578.4	574.4	574.4	571.2	663.1	15.8	19.6	23.7

IX.2 CALCULATED MISS VECTORS

300 mm Measurement Base

Date of Test 29-01-85

SHOT NO.	AIM		ANALYSIS	COORDINATES X	Y	Z	MISS DISTANCE	ERROR DISTANCE	ANTICLOCK-WISE ANGULAR ERROR IN TARGET PLANE IN DEGREES	%MISS DISTANCE ERROR	SMALLEST VARIANCE	AIMED SEQUENCE	OBSERVED SEQUENCE
							ORIENTATION II						
7	10L	0	AIMED:	-8.6603	-5.0000	.0000	10.0000					53412	53412
			4-TRIANGLES:	-5.1526	-6.5782	-7.8990	11.4986	8.7857	21.9238	13.0325	.4016		
			MMD METHOD:	-6.5514	-.6840	-9.4477	11.5172	10.5988	-24.0397	13.1737			
9	10L	0	AIMED:	-8.6603	-5.0000	.0000	10.0000					53412	53412
			4-TRIANGLES:	-2.6613	-10.7196	2.1603	11.2543	8.5655	46.0575	11.1452	.0181		
			MMD METHOD:	-8.3260	-3.0612	6.9270	11.2550	7.2009	-9.8131	11.1509			
10	10L	0	AIMED:	-8.6603	-5.0000	.0000	10.0000					53412	53412
			4-TRIANGLES:	-7.7072	-6.9952	-2.2465	10.6480	3.1521	12.2275	6.0858	27.1167		
			MMD METHOD:	-11.5387	-1.2045	-2.3342	11.8339	5.3047	-24.0405	15.4972			
12	10L	0	AIMED:	-8.6603	-5.0000	.0000	10.0000					53412	53412
			4-TRIANGLES:	-8.0691	-7.6601	1.4626	11.2217	3.0927	13.5103	10.8870	.3236		
			MMD METHOD:	-11.0871	-.9650	1.5564	11.2373	4.9591	-25.0255	11.0108			
13	15L	0	AIMED:	-12.9904	-7.5000	.0000	15.0000					53412	53412
			4-TRIANGLES:	-10.6206	-6.1318	-8.3252	15.1090	9.2396	.0000	.7212	.0757		
			MMD METHOD:	-11.6747	-.6066	-9.5775	15.1127	11.8734	-27.0255	.7459			
15	15L	0	AIMED:	-12.9904	-7.5000	.0000	15.0000					53412	53412
			4-TRIANGLES:	-12.4745	-3.9772	-2.3123	13.3918	4.5371	-12.3162	-12.0088	41.2876		
			MMD METHOD:	-14.6995	-.2522	-1.9811	14.8345	7.7057	-29.0172	-1.1155			
							ORIENTATION I						
18	20L	0	AIMED:	.0000	.0000	20.0000	20.0000					54123	54213
			4-TRIANGLES:	-12.6275	-7.2905	16.1734	21.7758	15.0747	.0000	8.1547	12.5814		
			MMD METHOD:	-12.6630	-.6580	18.0557	22.0434	12.8233	-17.6981	9.3521			
20	15L	0	AIMED:	.0000	.0000	15.0000	15.0000					54123	54213
			4-TRIANGLES:	.0000	-12.0898	7.9649	14.4777	13.9877	52.7386	-3.6079	46.2670		
			MMD METHOD:	.0000	-1.6298	15.9322	16.0153	1.8767	5.0595	6.3393			
21	15L	1	AIMED:	-.5000	.8660	15.0000	15.0333					54123	54213
			4-TRIANGLES:	10.1020	5.8324	7.6571	13.9534	13.8197	3.8141	-7.7389	44.2531		
			MMD METHOD:	10.8475	.5637	11.0259	15.4776	12.0271	27.9293	2.8707			
22	15L	1	AIMED:	-.5000	.8660	15.0000	15.0333					54123	54213
			4-TRIANGLES:	14.1052	8.1437	12.1472	20.3183	16.5655	3.8141	26.0110	2.4607		
			MMD METHOD:	15.7920	.8206	12.8489	20.3753	16.4334	33.0299	26.2130			
34	15L	0	AIMED:	.0000	.0000	15.0000	15.0000					54123	54213
			4-TRIANGLES:	8.0733	-4.6611	10.1548	13.7849	10.5062	38.4854	-8.8144	61.7849		
			MMD METHOD:	6.9949	-.3635	14.2399	15.8693	7.0454	14.9374	5.4777			
35	10L	0	AIMED:	.0000	.0000	10.0000	10.0000					54123	54213
			4-TRIANGLES:	4.6816	-5.0987	7.1389	9.9797	7.4710	43.2237	-.2035	13.1315		
			MMD METHOD:	4.0136	-.6284	9.8096	10.6176	4.0670	14.5773	5.8164			
39	15R	0	AIMED:	.0000	.0000	-15.0000	15.0000					12345	21345
			4-TRIANGLES:	.0000	.0000	-14.1862	14.1862	.8138	.0000	-5.7367	11.3870		
			MMD METHOD:	.0000	.0000	-14.5933	14.5933	.4067	.0000	-2.7966			
40	15L	5	AIMED:	-2.5000	4.3301	15.0000	15.8114					54123	54123
			4-TRIANGLES:	.0000	3.9496	9.7523	13.2364	7.4248	-20.0407	-19.4539	56.5419		
			MMD METHOD:	.0000	.7767	15.2140	15.2333	4.3500	15.9033	-3.7917			
41	10LT	5	AIMED:	-2.5000	4.3301	10.0000	11.1803					54123	45123
			4-TRIANGLES:	2.9851	-1.7235	10.7186	11.2592	8.2006	42.1277	.7002	.3166		
			MMD METHOD:	-	-	-	-	-	-	-			

SHOT NO.	AIM		ANALYSIS	COORDINATES X	Y	Z	MISS DISTANCE	ERROR DISTANCE	ANTICLOCK-WISE ANGULAR ERROR IN TARGET PLANE IN DEGREES	%MISS DISTANCE ERROR	SMALLEST VARIANCE	AIMED SEQUENCE	OBSERVED SEQUENCE
							ORIENTATION I						
42	10L	5	AIMED:	-2.5000	4.3301	10.0000	11.1803					54123	54123
			4-TRIANGLES:	-4.9262	-2.8441	9.6546	11.2057	7.5813	26.5651	.2266	13.2264		
			MMD METHOD:	-3.4708	-.1803	11.2595	11.7837	4.7826	18.5810	5.1204			
43	5L	5	AIMED:	-2.5000	4.3301	5.0000	7.0711					54123	54123
			4-TRIANGLES:	-1.2469	2.6066	4.7680	5.5752	2.1435	13.8593	-26.8312	.2646		
			MMD METHOD:	-1.5017	.2322	5.3907	5.6007	4.2358	34.9854	-26.2525			
44	0L	5	AIMED:	-2.5000	4.3301	.0000	5.0000					14325	15432
			4-TRIANGLES:	-1.2050	-4.9550	2.0170	5.4838	9.5895	28.6702	8.8223	.8469		
			MMD METHOD:	-	-	-	-	-	-	-			
49	15RT	5	AIMED:	-2.5000	4.3301	-15.0000	15.8114					12345	12345
			4-TRIANGLES:	.0000	.0000	-14.5377	14.5377	5.0213	-18.4349	-8.7616	11.8528		
			MMD METHOD:	.0000	.0000	-14.9510	14.9510	5.0002	-18.4349	-5.7544			
							ORIENTATION V						
52	10L	0	AIMED:	-3.5355	6.1237	7.0711	10.0000					51432	51432
			4-TRIANGLES:	-1.9201	6.1676	6.6915	9.3007	1.6601	8.7923	-7.5192	11.7806		
			MMD METHOD:	-3.7708	.5851	9.1503	9.9141	5.9208	-20.0153	-.8662			
58	15R	0	AIMED:	5.3033	-9.1856	-10.6066	15.0000					23145	23145
			4-TRIANGLES:	3.8140	-2.2020	-15.1032	15.7322	8.4384	-9.3481	4.6539	.2347		
			MMD METHOD:	3.7155	-.1931	-15.2924	15.7385	10.2637	-14.2997	4.6922			
60	10L	5	AIMED:	-7.8657	3.6237	7.0711	11.1803					51432	51324
			4-TRIANGLES:	-3.0018	1.7331	9.5819	10.1895	5.7910	15.5434	-9.7240	1.4411		
			MMD METHOD:	-	-	-	-	-	-	-			
							ORIENTATION VIII						
67	15L	0	AIMED:	5.3033	-9.1856	10.6066	15.0000					54231	54231
			4-TRIANGLES:	3.2467	-13.5530	-1.6367	14.0322	13.1606	-25.5598	-6.8971	.2469		
			MMD METHOD:	12.3324	-4.5247	-4.9579	14.0407	17.7027	66.7005	-6.8320			
68	10L	0	AIMED:	3.5355	-6.1237	7.0711	10.0000					54231	54231
			4-TRIANGLES:	5.7564	-5.7440	5.5559	9.8487	2.7152	12.5646	-1.5358	3.7373		
			MMD METHOD:	6.9981	-.7311	7.1573	10.0367	6.4092	35.5040	.3654			
75	15R	0	AIMED:	-5.3033	9.1856	-10.6066	15.0000					13425	13425
			4-TRIANGLES:	-6.4489	10.7689	-7.7565	14.7554	3.4558	.7999	-1.6576	22.0736		
			MMD METHOD:	-8.0353	2.0762	-13.0766	15.4879	8.0068	23.9031	3.1502			
76	15L	5	AIMED:	.9732	-11.6856	10.6066	15.8114					54321	54231
			4-TRIANGLES:	.0000	-11.5839	7.6185	13.8647	3.1442	-6.4597	-14.0406	43.0004		
			MMD METHOD:	.0000	-1.5620	15.2770	15.3567	11.1913	14.6350	-2.9611			
81	5R	5	AIMED:	-6.0979	.5619	-3.5355	7.0711					31425	43125
			4-TRIANGLES:	-5.3487	1.6450	-3.0373	6.3670	1.4081	-7.9483	-11.0577	3.4976		
			MMD METHOD:	-	-	-	-	-	-	-			
82	10R	5	AIMED:	-7.8657	3.6237	-7.0711	11.1803					13425	41325
			4-TRIANGLES:	-7.1748	6.7532	-5.6391	11.3527	3.5102	-11.6619	1.5182	9.2551		
			MMD METHOD:	-	-	-	-	-	-	-			
83	15R	5	AIMED:	-9.6334	6.6856	-10.6066	15.8114					13425	13425
			4-TRIANGLES:	-10.8235	6.2489	-5.3307	13.5972	5.4261	10.2465	-16.3695	60.6914		
			MMD METHOD:	-15.3296	.7966	-3.1080	15.6619	11.1066	39.3783	-.9551			

1000 METRES

SHOT NO.	AIM		ANALYSIS	COORDINATES X	Y	Z	MISS DISTANCE	ERROR DISTANCE	ANTICLOCK-WISE ANGULAR ERROR IN TARGET PLANE IN DEGREES	%MISS DISTANCE ERROR	SMALLEST VARIANCE	AIMED SEQUENCE	OBSERVED SEQUENCE
							ORIENTATION I						
127	OL	5	AIMED:	-2.5000	4.3301	.0000	5.0000					14235	14532
			4-TRIANGLES:	-4.5688	-5.1815	1.0109	6.9817	9.7864	24.6490	28.3841	3.5941		
			MMD METHOD:	-	-	-	-	-	-	-			
							ORIENTATION II						
138	10L	1	AIMED:	-9.1603	-4.1340	.0000	10.0499					53412	54123
			4-TRIANGLES:	6.8944	3.9805	.9172	8.0136	18.0121	-5.7106	-25.4106	11.2648		
			MMD METHOD:	-	-	-	-	-	-	-			
139	10LT	1	AIMED:	-9.1603	-4.1340	.0000	10.0499					53412	35412
			4-TRIANGLES:	8.8774	1.7147	-.5877	9.0606	18.9713	13.3572	-10.9183	8.3952		
			MMD METHOD:	-	-	-	-	-	-	-			
140	10L	1	AIMED:	-9.1603	-4.1340	.0000	10.0499					53412	54123
			4-TRIANGLES:	8.2568	1.1806	1.3944	8.4566	18.2632	16.1520	-18.8408	.8643		
			MMD METHOD:	-	-	-	-	-	-	-			
146	15R	1	AIMED:	12.4904	8.3660	.0000	15.0333					54123	54123
			4-TRIANGLES:	10.8632	6.2719	-8.8698	15.3629	9.2577	-3.8141	2.1452	82.1939		
			MMD METHOD:	13.8066	.7174	-11.2730	17.8387	13.6863	-30.8396	15.7263			
147	15RT	1	AIMED:	12.4904	8.3660	.0000	15.0333					54123	54123
			4-TRIANGLES:	12.3003	7.1016	10.8625	17.8808	10.9375	-3.8141	15.9249	11.8747		
			MMD METHOD:	-	-	-	-	-	-	-			
151	10LT	5	AIMED:	-11.1603	-.6699	.0000	11.1803					53412	53412
			4-TRIANGLES:	-10.5990	1.5434	-7.0362	12.8152	7.3974	-11.7199	12.7573	11.8317		
			MMD METHOD:	-11.3128	.0023	-6.9368	13.2702	6.9710	-3.4468	15.7488			
162	10R	5	AIMED:	6.1603	9.3301	.0000	11.1803					54123	35412
			4-TRIANGLES:	10.2355	5.9095	1.1113	11.8711	5.4354	-26.5651	5.8188	19.6307		
			MMD METHOD:	-	-	-	-	-	-	-			
165	15R	5	AIMED:	10.4904	11.8301	.0000	15.8114					54123	54123
			4-TRIANGLES:	5.9171	14.4552	10.2214	18.6666	11.5014	19.3038	15.2956	22.2815		
			MMD METHOD:	12.1450	1.8363	14.8198	19.2532	17.9233	-39.6068	17.8764			
166	15R	5	AIMED:	10.4904	11.8301	.0000	15.8114					54123	54123
			4-TRIANGLES:	.0000	13.9465	-4.9308	14.7925	11.7830	41.5651	-6.8881	150.2444		
			MMD METHOD:	.0000	4.7327	-18.5917	19.1847	22.4951	41.5651	17.5831			
167	15RT	5	AIMED:	10.4904	11.8301	.0000	15.8114					54123	54123
			4-TRIANGLES:	12.0375	6.9498	4.9143	14.7428	7.0965	-18.4349	-7.2480	150.1467		
			MMD METHOD:	17.7524	.9224	7.2474	19.1970	14.9746	-45.4604	17.6360			
							ORIENTATION V						
188	15RT	1	AIMED:	4.4373	-9.6856	-10.6066	15.0333					23145	23145
			4-TRIANGLES:	.0000	-10.8545	-14.3079	18.3601	6.2215	13.7774	18.1199	21.4702		
			MMD METHOD:	.0000	-.9595	-18.9105	18.9348	12.9370	-1.8457	20.6051			
194	15L	5	AIMED:	-9.6334	6.6856	10.6066	15.8114					51432	51342
			4-TRIANGLES:	-9.0981	5.2470	11.7354	15.7431	1.9032	-1.1784	-.4339	4.8004		
			MMD METHOD:	-	-	-	-	-	-	-			

1000 METRES

SHOT NO.	AIM		ANALYSIS	COORDINATES X	Y	Z	MISS DISTANCE	ERROR DISTANCE	ANTICLOCK-WISE ANGULAR ERROR IN TARGET PLANE IN DEGREES	%MISS DISTANCE ERROR	SMALLEST VARIANCE	AIMED SEQUENCE	OBSERVED SEQUENCE
							ORIENTATION VIII						
201	25LT	0	AIMED:	8.8388	-15.3093	17.6777	25.0000					54231	54231
			4-TRIANGLES:	15.2490	-19.8331	16.3501	29.8867	7.9572	6.4498	16.3506	53.6912		
			MMD METHOD:	19.3534	-3.0239	23.7306	30.7707	17.2663	30.9042	18.7540			
202	25L	0	AIMED:	8.8388	-15.3093	17.6777	25.0000					54231	54231
			4-TRIANGLES:	.0000	.0000	22.0795	22.0795	18.2175	.0000	-13.2272	340.3004		
			MMD METHOD:	.0000	.0000	28.7451	28.7451	20.8564	.0000	13.0287			
203	25L	0	AIMED:	8.8388	-15.3093	17.6777	25.0000					54231	54231
			4-TRIANGLES:	.0000	.0000	28.3119	28.3119	20.6298	.0000	11.6979	42.0119		
			MMD METHOD:	.0000	.0000	29.0339	29.0339	21.0111	.0000	13.8938			
204	25L	0	AIMED:	8.8388	-15.3093	17.6777	25.0000					54231	54231
			4-TRIANGLES:	.0000	10.9287	12.8535	16.8715	28.1039	66.3207	-48.1788	300.5063		
			MMD METHOD:	.0000	.0000	24.1907	24.1907	18.9393	.0000	-3.3456			
208	15L	0	AIMED:	5.3033	-9.1656	10.6066	15.0000					54231	15423
			4-TRIANGLES:	.0000	-22.0883	6.2929	22.9672	14.6018	-31.5658	34.6896	6.8682		
			MMD METHOD:	-	-	-	-	-	-	-			
218	15R	5	AIMED:	-9.6334	6.6856	-10.6066	15.8114					13425	21345
			4-TRIANGLES:	14.0053	-8.0860	-8.7319	18.3787	27.9375	-46.8081	13.9689	31.2716		
			MMD METHOD:	-	-	-	-	-	-	-			
							ORIENTATION IX						
225	0L	5	AIMED:	-2.5000	4.3301	.0000	5.0000					13425	13425
			4-TRIANGLES:	-2.8074	8.2720	2.4266	9.0662	4.6391	11.2539	44.8502	21.6339		
			MMD METHOD:	-10.0699	1.5590	.0422	10.1900	8.0613	-51.1995	50.9322			
236	15R	5	AIMED:	-15.4904	-3.1699	.0000	15.8114					31245	31245
			4-TRIANGLES:	-15.3616	-8.8690	-6.2713	18.8140	8.4751	-18.4349	15.9596	20.3822		
			MMD METHOD:	-17.8822	-.9292	-7.3004	19.3373	8.0023	8.5906	18.2338			
							ORIENTATION X						
267	10L	5	AIMED:	5.0000	-8.6603	5.0000	11.1803					52413	54213
			4-TRIANGLES:	10.5791	-1.4827	7.0026	12.7731	9.3088	-20.2447	12.4697	11.2773		
			MMD METHOD:	11.2665	.0023	6.8901	13.2063	10.8573	-24.1762	15.3410			
269	15LT	5	AIMED:	7.5000	-12.9904	5.0000	15.8114					52413	52413
			4-TRIANGLES:	12.1799	-7.0321	9.9449	17.2250	9.0474	-20.7966	8.2069	.1183		
			MMD METHOD:	13.3346	-.6929	10.8876	17.2288	14.8302	-37.3425	8.2269			
272	10L	5	AIMED:	5.0000	-8.6603	5.0000	11.1803					52413	52413
			4-TRIANGLES:	8.9138	-5.1464	7.2781	12.6060	5.7319	-12.6665	11.3094	.0179		
			MMD METHOD:	9.7576	-.5070	7.9670	12.6072	9.8951	-29.7124	11.3175			
287	10R	5	AIMED:	-5.0000	8.6603	5.0000	11.1803					51423	54123
			4-TRIANGLES:	3.1351	7.7786	5.5003	10.0294	8.1980	20.2140	-11.4760	7.1397		
			MMD METHOD:	6.5587	1.0156	7.9789	10.3784	14.1746	80.1749	-7.7268			
288	10R	5	AIMED:	-5.0000	8.6603	5.0000	11.1803					51423	51432
			4-TRIANGLES:	.0000	12.2659	8.6733	15.0226	7.1759	12.6665	25.5764	.0013		
			MMD METHOD:	.0000	1.8968	14.9028	15.0230	12.9927	57.1448	25.5785			
292	15R	5	AIMED:	-7.5000	12.9904	5.0000	15.8114					51423	51432
			4-TRIANGLES:	-15.4739	8.9338	6.3172	18.9516	9.0429	3.7727	16.5594	18.6993		
			MMD METHOD:	-17.9859	.9346	7.3427	19.4495	16.1489	18.4012	18.7054			

IX.3 MEASURED TIMES

T1 - T5 Times of Flight

TAU 1 - TAU 5 N-Wave Periods

1000 mm Measurement Base

Date of Test 18-06-85

500 METRES

SHOT NO.	AIM		T(1)	T(2)	T(3)	T(4)	T(5)	TAU(1)	TAU(2)	TAU(3)	TAU(4)	TAU(5)	V(T)	AIMED MISS DISTANCE	MEASURED MISS DISTANCE	%ERROR
							ORIENTATION XV									
1	14L	0	521448.8	520781.6	522144.0	519234.4	517884.8	544.8	541.6	556.0	548.0	548.8	834.8	14.8	14.9	.5
2	15L	0	521913.6	521274.4	480000.0	519645.6	518273.6	558.4	556.8	.0	541.6	534.4	835.1	15.2	14.9	-1.9
3	14L	0	524939.2	524252.0	525607.2	522744.0	521425.6	548.8	557.6	556.8	549.6	548.8	833.6	15.0	15.3	2.3
4	15L	0	522475.2	521805.6	523088.8	520240.0	518879.2	583.2	567.2	566.4	572.8	552.0	834.5	15.1	16.7	11.2
5	14L	0	496780.8	522085.6	523439.2	520590.4	519241.6	.0	532.8	552.8	552.8	548.8	834.7	14.9	14.8	-.8
6	15L	0	522741.6	522049.6	523255.2	520452.8	519088.0	567.2	555.2	564.0	559.2	554.4	834.4	15.2	16.0	5.2
7	14L	0	516289.6	515648.0	516844.0	514003.2	512630.4	548.8	556.8	535.2	531.2	523.2	836.7	15.0	14.1	-5.8
8	14L	0	515658.0	480000.0	516295.2	513404.8	512022.4	565.6	.0	566.4	560.0	552.8	837.1	14.5	16.1	10.7
9	14L	0	526402.4	525696.8	526981.6	524144.8	522799.2	557.6	560.8	556.0	552.0	546.4	833.2	14.9	15.5	4.4
10	15L	0	480000.0	519952.8	521260.8	518413.6	517060.0	.0	544.8	549.6	542.4	540.0	835.4	15.1	14.6	-3.4
11	10L	0	512064.8	511292.0	512616.8	509765.6	508377.6	508.0	496.0	508.8	499.2	486.4	838.1	10.1	10.6	5.5
12	9L	0	507073.6	506339.2	507564.0	504728.8	503355.2	509.6	508.8	498.4	490.4	484.8	839.9	9.9	10.5	6.7
13	10L	0	512757.6	512062.4	513342.4	510509.6	509182.4	500.8	508.0	504.0	493.6	492.0	837.9	10.2	10.6	4.7
14	9L	0	506320.8	504842.4	506134.4	503287.2	501913.6	712.0	514.4	506.4	496.8	487.2	840.3	9.7	14.5	49.1
15	9L	0	510234.4	509588.8	510832.8	480000.0	506581.6	504.0	514.4	509.6	.0	489.6	838.9	9.1	11.0	21.1
							ORIENTATION XVI									
18	14L	0	526105.6	526632.0	525637.6	523839.2	522464.8	559.4	567.2	547.2	558.4	553.6	833.2	14.6	15.7	8.1
19	14L	0	519588.8	520120.0	519161.6	517317.6	515926.4	573.6	567.2	560.8	561.6	553.6	835.5	14.9	16.3	9.3
20	14L	0	522143.8	522701.6	521645.6	519912.8	518552.0	548.8	574.4	540.8	564.8	565.6	834.6	14.8	15.9	7.3
21	14L	0	526211.2	526728.0	525788.8	523945.6	522577.6	562.4	560.0	560.0	555.2	551.2	833.2	14.8	15.8	6.9
22	14L	0	524373.6	524855.2	523917.6	522065.6	520697.2	560.8	556.8	564.0	550.4	546.4	833.8	14.7	15.6	6.5
23	9L	0	511381.6	511860.0	510849.6	509063.2	507692.8	510.4	518.4	505.6	505.6	501.6	838.4	9.9	11.4	14.8
24	9L	0	480000.0	515170.4	514248.8	512379.2	511003.2	.0	522.4	507.2	511.2	508.0	837.5	9.8	11.7	19.2
25	9L	0	480000.0	513639.2	512615.2	510827.2	509464.8	.0	504.0	498.4	495.2	488.8	838.1	9.7	10.4	7.0
26	9L	0	480000.0	516683.2	515712.8	513892.0	512513.6	.0	516.0	517.6	508.8	505.6	837.0	9.9	11.7	18.5
27	9L	0	509883.0	510389.6	509326.4	507581.6	506232.0	504.8	510.4	503.2	497.6	495.2	838.9	9.5	10.9	13.7
							ORIENTATION XVII									
29	14L	0	520576.8	519226.4	521974.4	519720.0	519206.4	569.6	566.4	567.2	532.8	523.2	835.0	14.6	15.3	4.8
30	14L	0	480000.0	523364.8	526161.6	524076.0	523562.4	.0	543.2	552.8	552.8	537.6	833.7	14.9	14.8	-.5
31	15L	0	525102.4	523796.8	526576.0	524364.8	523807.2	553.6	561.6	570.4	559.2	548.8	833.4	15.2	15.9	4.3
32	15L	0	521692.0	520319.2	523088.0	520850.8	520318.4	554.4	554.4	570.4	548.0	534.4	834.6	15.1	15.3	1.3
33	15L	0	520966.4	519502.4	522303.2	520140.8	519645.6	512.0	507.2	517.6	496.0	493.6	834.9	15.1	11.1	-26.4
34	9L	0	512644.8	511250.4	513984.8	511849.6	511368.8	506.4	502.4	508.0	497.6	490.4	837.8	9.8	10.7	9.9
35	9L	0	510357.6	509852.0	511620.0	509478.4	508933.6	504.8	504.0	515.2	507.2	504.0	838.6	9.7	11.3	16.4
36	9L	0	517992.8	516535.2	519315.2	517158.4	516612.0	504.0	500.8	512.8	496.8	484.8	835.9	9.6	10.6	10.7
37	9L	0	512661.6	511147.2	513918.4	511769.6	511235.2	516.0	506.4	519.2	504.0	495.2	837.8	9.5	11.4	20.2

500 METRES

SHOT NO.	AIM		T(1)	T(2)	T(3)	T(4)	T(5)	TAU(1)	TAU(2)	TAU(3)	TAU(4)	TAU(5)	V(T)	AIMED MISS DISTANCE	MEASURED MISS DISTANCE	%ERROR
							ORIENTATION XVIII									
38	14L	0	505646.4	531939.2	529371.2	529567.2	528983.2	.0	565.6	568.0	552.0	553.6	831.7	14.9	16.0	7.2
39	9L	0	517001.6	518282.4	515652.0	515977.6	515413.6	504.8	513.6	502.4	509.6	511.2	836.3	9.9	11.4	15.2
40	4L	0	499664.8	500917.6	498261.6	498634.4	498124.0	435.2	443.2	426.4	441.6	452.0	842.4	4.6	5.4	15.8
41	14L.	0	525651.2	526994.4	524364.8	524684.0	524094.4	558.4	562.4	553.6	563.2	570.4	833.3	14.6	16.2	10.5
42	9L	0	514809.6	516156.0	514251.2	513802.4	513147.2	512.8	531.2	747.2	520.8	503.2	837.0	9.1	16.2	77.9
43	4L	0	503872.0	505124.8	502500.8	502814.4	502248.0	433.6	439.2	425.6	432.8	436.0	840.9	4.3	4.8	11.7
44	14L	0	526452.8	527736.0	525148.8	525372.0	524794.4	557.6	558.4	553.6	553.6	553.6	833.0	14.6	15.6	7.0
45	9L	0	516040.0	517425.6	514754.4	515154.4	514548.0	503.2	526.4	504.8	528.8	518.4	836.6	9.7	12.1	24.7
47	14L	0	521359.2	522752.8	520157.6	520388.8	519808.0	567.2	572.8	563.2	558.4	552.0	834.8	14.9	16.2	9.0
48	9L	0	509663.2	511040.8	508427.2	508693.6	508126.4	507.2	512.8	501.6	504.8	500.8	838.8	9.6	11.1	16.2
49	4L	0	496618.4	497920.0	495288.8	495614.4	495069.6	442.4	449.6	432.0	440.0	438.4	843.4	4.6	5.4	18.3
51	9LT	0	507022.4	508364.0	505732.8	506052.8	505506.4	508.0	518.4	504.8	518.4	512.8	839.8	9.7	11.8	20.7
52	4L	0	507122.4	508434.4	505816.0	506093.6	505511.2	435.2	444.0	424.0	435.2	430.4	839.7	4.3	4.8	12.1
53	14L	0	528782.4	530103.2	527513.6	527749.6	527175.2	556.8	559.2	555.2	549.6	550.4	832.2	14.9	15.5	4.3
54	9L	0	511529.6	512794.4	510170.4	510513.6	509967.2	500.0	506.4	494.4	508.0	509.6	838.2	9.4	11.0	16.8
55	4LT	0	496390.4	497746.4	495132.0	495422.4	494884.8	432.8	441.6	426.4	433.6	432.8	843.5	4.4	4.8	10.2
56	14L	0	525159.2	526518.4	523904.0	524173.6	523578.4	564.8	573.6	564.8	568.0	562.4	833.5	14.7	16.6	12.9
57	9L	0	514128.8	515447.2	512798.4	513148.8	512576.0	505.6	514.4	499.2	512.8	513.6	837.3	9.4	11.5	22.2
58	4L	0	494890.4	496151.2	493525.6	493844.0	493294.4	438.4	442.4	428.0	434.4	432.8	844.0	4.3	5.0	16.0
59	14L	0	524948.0	526277.6	523660.8	523947.2	523371.2	560.0	568.0	559.2	564.0	562.4	833.5	14.9	16.2	9.0
60	9L	0	507678.4	508929.6	506284.0	506643.2	506080.8	506.4	516.0	499.2	510.4	506.4	839.5	9.4	11.3	20.1

1000 METRES

SHOT NO.	AIM		T(1)	T(2)	T(3)	T(4)	T(5)	TAU(1)	TAU(2)	TAU(3)	TAU(4)	TAU(5)	V(T)	AIMED MISS DISTANCE	MEASURED MISS DISTANCE	%ERROR
							ORIENTATION XVIII									
62	14L	0	1182397.6	1183736.8	1181353.6	1181087.2	1180232.8	580.0	583.2	576.0	578.4	580.8	650.2	14.5	20.3	40.3
63	9L	0	1192796.0	1194115.2	1191724.8	1191440.0	1190589.6	536.0	541.6	530.4	534.4	534.4	647.9	9.3	14.2	52.5
64	15L	0	1185785.6	1187016.0	1184611.2	1184407.2	1183560.8	587.2	591.2	583.2	588.0	588.0	649.5	15.2	21.4	40.6
65	10L	0	1170191.2	1171413.6	1168994.4	1168818.4	1167994.4	539.2	544.0	534.4	536.8	535.2	653.0	10.2	14.6	43.0
67	15L	0	1186321.6	1187532.0	1185138.4	1184923.2	1134087.2	585.6	589.6	579.2	586.4	585.6	649.4	15.1	21.1	39.6
68	9L	0	1168504.0	1169636.8	1167235.2	1167048.0	1166213.6	537.6	542.4	531.2	531.2	535.2	653.3	9.8	14.3	46.0
69	14L	0	1194712.0	1195916.0	1193540.8	1193298.4	1192429.6	584.8	588.8	580.8	584.0	583.2	647.5	14.7	21.0	43.2
70	15L	0	1168881.6	1170195.2	1167796.0	1167575.2	1153756.0	581.6	587.2	578.4	584.0	584.8	653.2	15.2	20.8	36.7
71	10L	0	1172769.6	1173925.6	1171536.0	1171323.2	1170479.2	541.6	546.4	534.4	540.8	540.8	652.4	10.2	15.0	46.5
73	15L	0	1174248.0	1175485.6	1173082.4	1172876.8	1172043.2	584.8	589.6	580.0	585.6	584.8	652.0	15.2	21.0	38.4
74	9L	0	1166428.8	1167668.0	1165269.6	1165057.6	1164227.2	546.4	549.6	538.4	543.2	544.0	653.8	9.3	15.5	66.8
							ORIENTATION XV									
76	15L	0	1161675.2	1161036.0	1162425.6	1159500.8	1158185.6	580.8	579.2	579.2	572.0	567.2	654.9	15.4	19.7	28.0
77	15L	0	1177656.8	1177062.4	1178487.2	1175546.4	1174239.2	581.6	581.6	581.6	574.4	571.2	651.3	15.2	20.1	32.2
78	9L	0	1148552.8	1147809.6	1149193.6	1146297.6	1144971.2	524.0	524.0	522.4	513.6	507.2	657.9	9.5	12.0	26.3
79	15L	0	1182887.2	1182168.8	1183583.2	1180692.8	1179373.6	581.6	584.8	585.6	571.2	565.6	650.2	15.2	20.1	31.7
80	10L	0	1161073.6	1160315.2	1161725.6	1158840.8	1157520.0	530.4	531.2	530.4	520.8	516.0	655.1	10.0	12.9	28.8
81	14L	0	1149133.6	1148417.6	1149796.8	1146914.4	1145584.0	575.2	576.0	575.2	568.0	561.6	657.8	14.6	19.1	30.5
82	9L	0	1150236.8	1149476.8	1150883.2	1147991.2	1146663.0	528.0	526.4	528.8	519.2	512.0	657.5	9.7	12.6	29.5
83	14L	0	1176419.2	1176712.8	1176026.4	1173985.6	1172539.2	570.4	572.8	570.4	564.8	561.6	651.6	14.5	18.7	29.4
84	14L	0	1120000.0	1167803.2	1167090.4	1165083.2	1163645.4	.0	574.4	565.6	567.2	564.0	653.8	14.7	18.7	27.0

IX.4 CALCULATED MISS VECTORS

1000 mm Measurement Base

Date of Test 18-06-85

500 METRES

SHOT NO.	AIM		ANALYSIS	COORDINATES X	Y	Z	MISS DISTANCE	ERROR DISTANCE	ANTICLOCK-WISE ANGULAR ERROR IN TARGET PLANE IN DEGREES	%MISS DISTANCE ERROR	SMALLEST VARIANCE	AIMED SEQUENCE	OBSERVED SEQUENCE
							ORIENTATION XV						
1	14L	0	AIMED:	.0000	.0000	14.8030	14.8400					45213	54213
			4-TRIANGLES:	9.6560	4.5016	-4.6339	11.6179	22.1652	-44.1703	-27.7339	83.6382		
			MMD METHOD:	14.1331	4.6536	-.5013	14.8879	21.3452	-83.8521	.3217			
2	15L	0	AIMED:	.0000	.0000	15.1250	15.2002					45213	35421
			4-TRIANGLES:	10.4211	5.3270	9.4143	15.0202	13.0226	-29.5029	-1.1984	19.1751		
			MMD METHOD:	-	-	-	-	-	-	-			
3	14L	0	AIMED:	.0000	.0000	14.7500	14.9767					45213	54213
			4-TRIANGLES:	-.2399	9.6470	6.5292	11.6513	12.6769	-55.9093	-28.5409	98.0755		
			MMD METHOD:	-1.1082	13.1179	7.9799	15.3944	14.8035	-58.6870	2.7133			
4	15L	0	AIMED:	.0000	.0000	15.1250	15.0502					45213	54213
			4-TRIANGLES:	-.2737	-13.3130	-4.9738	14.2144	24.1096	69.5141	-5.8800	87.4664		
			MMD METHOD:	-.6913	-17.0315	-.4120	17.1005	23.1010	88.6183	11.9897			
6	15L	0	AIMED:	.0000	.0000	14.8630	15.2037					45213	54213
			4-TRIANGLES:	8.7960	-6.2434	6.0606	12.3726	13.9223	45.8511	-22.8825	103.5098		
			MMD METHOD:	10.8672	-10.9898	4.5714	16.1174	18.5685	67.4143	5.6687			
7	14L	0	AIMED:	.0000	.0000	14.6750	14.9780					45213	54213
			4-TRIANGLES:	-10.2532	-2.7679	8.7957	13.7896	12.1390	17.4679	-8.6179	16.2936		
			MMD METHOD:	-10.8826	-1.4386	9.4511	14.4853	12.1569	8.6551	-3.4016			
8	14L	0	AIMED:	.0000	.0000	14.4950	14.5250					45213	25413
			4-TRIANGLES:	-12.4774	7.6106	8.4498	16.8821	15.8161	-42.0087	13.9620	.0414		
			MMD METHOD:	-	-	-	-	-	-	-			
9	14L	0	AIMED:	.0000	.0000	14.4200	14.8768					45213	54213
			4-TRIANGLES:	-7.5703	-3.2823	7.2566	10.9882	10.9269	24.3384	-35.3887	122.6673		
			MMD METHOD:	-8.5084	1.6659	13.0900	15.7009	8.7715	-7.2570	5.2489			
10	15L	0	AIMED:	.0000	.0000	14.7500	15.0908					45213	15423
			4-TRIANGLES:	1.9730	-13.0548	7.6140	15.2412	15.0081	59.7479	.9869	1.5342		
			MMD METHOD:	-	-	-	-	-	-	-			
11	10L	0	AIMED:	.0000	.0000	9.8500	10.0775					42135	54213
			4-TRIANGLES:	6.6375	-3.6287	4.5111	8.8076	9.2589	38.8129	-14.4181	38.4237		
			MMD METHOD:	8.9242	-4.4769	4.4219	10.9196	11.3643	45.3543	7.7114			
12	9L	0	AIMED:	.0000	.0000	9.5500	9.8546					42135	54213
			4-TRIANGLES:	-5.6420	-3.4724	6.8103	9.5011	7.1691	27.0160	-3.7203	23.4391		
			MMD METHOD:	-5.1514	-3.4523	8.8701	10.8228	6.2384	21.2664	8.9463			
13	10L	0	AIMED:	.0000	.0000	9.8500	10.1544					42135	54213
			4-TRIANGLES:	-.8455	5.8016	5.9408	8.3467	7.0466	-44.3207	-21.6582	43.6392		
			MMD METHOD:	-3.0234	4.4590	9.3549	10.7953	5.4101	-25.4850	5.9361			
15	9L	0	AIMED:	.0000	.0000	9.1200	9.1200					42135	45213
			4-TRIANGLES:	-4.1314	3.7570	8.0190	9.7718	5.6917	-25.1034	6.6702	18.2564		
			MMD METHOD:	-	-	-	-	-	-	-			

SHOT NO.	AIM		ANALYSIS	COORDINATES X	Y	Z	MISS DISTANCE	ERROR DISTANCE	ANTICLOCK-WISE ANGULAR ERROR IN TARGET PLANE IN DEGREES	%MISS DISTANCE ERROR	SMALLEST VARIANCE	AIMED SEQUENCE	OBSERVED SEQUENCE
							ORIENTATION XVI						
18	14L	0	AIMED:	-10.2960	.0750	10.2960	14.5609					54312	54312
			4-TRIANGLES:	-11.7172	2.7111	-4.6980	12.9118	15.2901	-28.3495	-12.7727	80.1658		
			MMD METHOD:	-15.7837	-.8395	-.5936	15.8172	12.2284	4.7640	7.9422			
19	14L	0	AIMED:	-10.5340	.1500	10.5340	14.8981					54312	54312
			4-TRIANGLES:	-8.1284	-7.0997	7.1720	12.9582	8.3456	33.8509	-14.9704	101.1730		
			MMD METHOD:	-7.1492	-12.6699	7.7796	16.4973	13.5422	50.7765	9.6936			
20	14L	0	AIMED:	-10.4800	.0750	10.4800	14.8211					54312	54312
			4-TRIANGLES:	-14.1330	4.5467	-4.9667	15.6551	16.4906	-34.7592	5.3271	.0015		
			MMD METHOD:	-14.2385	4.5884	-5.0221	15.7800	16.5775	-34.8583	6.0766			
21	14L	0	AIMED:	-10.4600	.1500	10.4600	14.7934					54312	54312
			4-TRIANGLES:	-6.3334	-4.4676	7.2154	10.5893	6.9913	25.5817	-39.7019	139.1410		
			MMD METHOD:	.0000	-6.0641	14.7516	15.9494	12.9013	30.7527	7.2475			
22	14L	0	AIMED:	-10.3700	.0000	10.3700	14.6654					54312	54312
			4-TRIANGLES:	8.0738	-3.5092	8.6038	12.3096	18.8576	83.9043	-19.1376	95.5695		
			MMD METHOD:	8.0871	-.4727	13.5912	15.8223	18.7421	6.9250	7.3121			
23	9L	0	AIMED:	-7.0160	-.1500	7.0160	9.9233					54312	54312
			4-TRIANGLES:	-7.0963	-2.0127	5.0572	8.9433	2.7043	12.3149	-10.9572	50.0516		
			MMD METHOD:	-9.9855	1.5716	5.5592	11.5362	3.7288	-9.0033	13.9815			
26	9L	0	AIMED:	-6.9900	.0370	6.9900	9.8854					54312	15432
			4-TRIANGLES:	.5592	-9.7776	7.5317	12.3548	12.3940	63.4551	19.9871	3.1729		
			MMD METHOD:	-	-	-	-	-	-	-			
27	9L	0	AIMED:	-6.7500	-.1500	6.7500	9.5471					54312	54312
			4-TRIANGLES:	-5.6427	-1.9013	5.5682	8.1523	2.3853	12.5868	-17.1100	51.4766		
			MMD METHOD:	-6.2783	2.0491	8.8008	11.0032	3.0438	-11.7787	13.2332			
							ORIENTATION XVII						
31	15L	0	AIMED:	10.7700	.4500	10.7700	15.2377					52413	25413
			4-TRIANGLES:	2.8325	11.2010	5.7402	12.9009	14.2789	-59.8862	-18.1132	90.1860		
			MMD METHOD:	8.4488	13.3455	3.1924	16.1145	15.1361	-56.6411	5.4409			
32	15L	0	AIMED:	10.6900	-.1500	10.6900	15.1187					52413	25413
			4-TRIANGLES:	10.1440	5.8566	6.6347	13.4618	7.2680	-26.8410	-12.3084	54.9277		
			MMD METHOD:	10.8805	6.2819	9.4447	15.7178	6.5541	-24.1780	3.8118			
33	15L	0	AIMED:	10.6900	-.1500	10.6900	15.1187					52413	25413
			4-TRIANGLES:	6.0367	-1.9221	7.5217	9.8342	5.9018	10.7681	-53.7357	29.7607		
			MMD METHOD:	5.5238	.3076	9.9649	11.3977	5.2368	-2.1773	-32.6472			
34	9L	0	AIMED:	6.9100	-.0750	6.9100	9.7725					52413	25413
			4-TRIANGLES:	5.3312	-2.6909	5.4480	8.0835	3.3872	19.0056	-20.8943	51.7794		
			MMD METHOD:	5.5092	-1.3343	9.3897	10.9680	3.1140	6.7783	10.8999			
35	9L	0	AIMED:	6.8500	-.1500	6.8500	9.6885					52413	25413
			4-TRIANGLES:	6.7050	3.6713	1.9724	7.8947	6.1980	-31.7810	-22.7217	56.0601		
			MMD METHOD:	10.1110	5.0369	.9813	11.3387	8.4841	-33.5948	14.5536			
36	9L	0	AIMED:	6.8000	-.1500	6.8000	9.6178					52413	25413
			4-TRIANGLES:	6.5116	-1.5369	5.5833	8.7142	1.8673	9.2939	-10.3701	41.4963		
			MMD METHOD:	8.0040	2.2419	7.1705	10.9775	2.7034	-12.6953	12.3860			
37	9L	0	AIMED:	6.6900	-.3000	6.6900	9.4658					52413	25413
			4-TRIANGLES:	6.9842	-3.1407	6.0671	9.7700	2.9230	16.9782	3.1132	37.3854		
			MMD METHOD:	8.3813	-2.3324	7.7721	11.6658	2.8569	9.7249	18.8582			

500 METRES

SHOT NO.	AIM		ANALYSIS	COORDINATES X	Y	Z	MISS DISTANCE	ERROR DISTANCE	ANTICLOCK-WISE ANGULAR ERROR IN TARGET PLANE IN DEGREES	%MISS DISTANCE ERROR	SMALLEST VARIANCE	AIMED SEQUENCE	OBSERVED SEQUENCE
							ORIENTATION XVIII						
38	14L	0	AIMED:	-14.9370	.3000	.0000	14.9400					53412	15342
			4-TRIANGLES:	.9455	13.6181	5.9178	14.8784	21.5556	-87.1791	-.4143	28.0514		
			MMD METHOD:	-	-	-	-	-	-	-			
39	9L	0	AIMED:	-9.8870	-.3000	.0000	9.8916					53412	53412
			4-TRIANGLES:	-6.7010	3.2638	-4.1811	8.5462	6.3509	-27.7070	-15.7421	52.1007		
			MMD METHOD:	-10.3641	3.5072	-2.9261	11.3259	4.8254	-20.4341	12.6644			
40	4L	0	AIMED:	-4.6300	-.1870	.0000	4.6338					53412	53412
			4-TRIANGLES:	-3.2930	.9105	-2.1325	4.0275	2.7459	-17.7693	-15.0545	6.5211		
			MMD METHOD:	-4.5908	.0709	-2.2286	5.1036	2.2438	-3.1976	9.2060			
41	14L.	0	AIMED:	-14.6200	-.0700	.0000	14.6202					53412	53412
			4-TRIANGLES:	-8.8270	3.3981	-6.9065	11.7116	9.6585	-21.3293	-24.8346	114.0630		
			MMD METHOD:	-12.9926	-.5898	-9.2335	15.9504	9.3902	2.3247	8.3395			
43	4L	0	AIMED:	-4.3000	-.0700	.0000	4.3006					53412	53412
			4-TRIANGLES:	-2.8606	.8129	.6638	3.0471	1.8144	-16.7962	-41.1382	7.3041		
			MMD METHOD:	-4.7281	-.3140	.1236	4.7401	.5080	2.8674	9.2725			
44	14L	0	AIMED:	-14.5800	-.2800	.0000	14.5827					53412	53412
			4-TRIANGLES:	-7.6181	-4.1304	6.1254	10.6121	10.0406	27.3656	-37.4159	128.5882		
			MMD METHOD:	-11.9680	-4.5803	8.9483	15.6296	10.2658	19.8420	6.6982			
45	9L	0	AIMED:	-9.7000	-.3000	.0000	9.7046					53412	53412
			4-TRIANGLES:	-7.7466	4.9765	-7.4329	11.8332	9.3223	-34.4885	17.9879	2.4980		
			MMD METHOD:	-7.7917	5.1016	-7.7215	12.0914	9.6165	-35.0196	19.7394			
47	14L	0	AIMED:	-14.9000	.0000	.0000	14.9000					53412	53412
			4-TRIANGLES:	-9.1439	-3.1726	8.6147	12.9572	10.8356	19.1352	-14.9940	100.2466		
			MMD METHOD:	-10.7052	1.1069	12.4686	16.4709	13.2018	-5.9031	9.5376			
48	9L	0	AIMED:	-9.5800	.3000	.0000	9.5847					53412	53412
			4-TRIANGLES:	-6.6617	-2.4697	4.1145	8.2102	5.7547	22.1350	-16.7412	55.6451		
			MMD METHOD:	-10.8452	.1370	2.9164	11.2313	3.1832	1.0700	14.6610			
49	4L	0	AIMED:	-4.6000	.0000	.0000	4.6000					53412	53412
			4-TRIANGLES:	-3.7003	.8773	.9256	3.9139	1.5607	-13.3379	-17.5289	8.6263		
			MMD METHOD:	-5.4429	-.3577	.6619	5.4947	1.1298	3.7600	16.2824			
51	9LT	0	AIMED:	-9.7400	.0000	.0000	9.7400					53412	53412
			4-TRIANGLES:	-7.2357	3.3236	-5.6060	9.7380	6.9818	-24.6713	-.0203	39.8949		
			MMD METHOD:	-9.2165	2.9153	-6.6746	11.7471	7.3023	-17.5528	17.0856			
52	4L	0	AIMED:	-4.3000	.0300	.0000	4.3001					53412	53412
			4-TRIANGLES:	-3.4556	.7719	.5458	3.5826	1.2495	-12.1915	-20.0270	5.4818		
			MMD METHOD:	-4.9075	-.0860	-.0608	4.9086	.6214	1.4040	12.3964			
53	14L	0	AIMED:	-14.8700	-.1400	.0000	14.8707					53412	53412
			4-TRIANGLES:	-7.2392	-3.3632	7.6615	11.0642	11.2835	24.3790	-34.4036	117.3474		
			MMD METHOD:	-6.3500	.7532	14.2142	15.5863	16.5961	-7.3037	4.5915			

500 METRES

SHOT NO.	AIM		ANALYSIS	COORDINATES X	Y	Z	MISS DISTANCE	ERROR DISTANCE	ANTICLOCK-WISE ANGULAR ERROR IN TARGET PLANE IN DEGREES	XMISS DISTANCE ERROR	SMALLEST VARIANCE	AIMED SEQUENCE	OBSERVED SEQUENCE
							ORIENTATION XVIII						
54	9L	0	AIMED:	-9.4000	-.3000	.0000	9.4048					53412	53412
			4-TRIANGLES:	-6.4398	2.3544	-5.1996	8.6053	6.5455	-21.9101	-9.2911	40.3861		
			MMD METHOD:	-8.4496	.4456	-6.7892	10.8483	6.8958	-4.8467	13.3067			
55	4LT	0	AIMED:	-4.3800	.0800	.0000	4.3807					53412	53412
			4-TRIANGLES:	-3.0500	1.0772	.6710	3.3035	1.7927	-18.4067	-32.6099	6.6406		
			MMD METHOD:	-4.7987	.6214	.1345	4.8406	.6975	-6.3326	9.5002			
56	14L	0	AIMED:	-14.7100	.0000	.0000	14.7100					53412	53412
			4-TRIANGLES:	-9.2790	5.3572	-5.4046	12.0004	9.3491	-30.0000	-22.5790	131.7490		
			MMD METHOD:	-14.4549	8.3455	-.4410	16.6969	8.3611	-30.0000	11.8997			
57	9L	0	AIMED:	-9.3800	-.0500	.0000	9.3801					53412	53412
			4-TRIANGLES:	-7.3866	2.6140	-4.9945	9.2919	6.0013	-19.7936	-.9491	39.5340		
			MMD METHOD:	-10.0590	1.0861	-3.1777	11.3654	5.3442	-6.4679	17.4673			
58	4L	0	AIMED:	-4.3000	-.0200	.0000	4.3000					53412	53412
			4-TRIANGLES:	-3.1030	-1.3364	1.6211	3.7473	2.4071	23.0350	-14.7491	8.1258		
			MMD METHOD:	-4.8329	-1.0990	.9016	5.0376	1.5037	12.5445	14.6408			
59	14L	0	AIMED:	-14.9000	.2800	.0000	14.9026					53412	53412
			4-TRIANGLES:	-9.0311	4.9267	-5.7549	11.7878	9.4421	-27.5368	-26.4240	122.0325		
			MMD METHOD:	-14.4080	6.8390	-3.1150	16.2501	7.2778	-24.3157	8.2922			
60	9L	0	AIMED:	-9.4200	-.4500	.0000	9.4307					53412	53412
			4-TRIANGLES:	-7.7441	2.6306	-4.1139	9.1551	5.4058	-21.4968	-3.0107	42.0001		
			MMD METHOD:	-11.0367	1.1142	-2.4505	11.3602	3.3265	-8.4999	16.9845			

1000 METRES

SHOT NO.	AIM		ANALYSIS	COORDINATES X	Y	Z	MISS DISTANCE	ERROR DISTANCE	ANTICLOCK-WISE ANGULAR ERROR IN TARGET PLANE IN DEGREES	%MISS DISTANCE ERROR	SMALLEST VARIANCE	AIMED SEQUENCE	OBSERVED SEQUENCE
							ORIENTATION XVIII						
62	14L	0	AIMED:	-14.4800	.6150	.0000	14.4931					54312	54312
			4-TRIANGLES:	-12.1445	-4.7822	7.3510	14.9799	9.4139	23.9252	3.2498	184.4646		
			MMD METHOD:	-19.7453	-1.1290	4.5611	20.2967	7.1811	5.7044	28.5939			
63	9L	0	AIMED:	-9.2900	.5720	.0000	9.3076					54312	54312
			4-TRIANGLES:	-9.9648	-2.8638	4.9626	11.4946	6.0735	19.5576	19.0265	67.4137		
			MMD METHOD:	-13.9966	.2203	2.5856	14.2351	5.3816	2.6218	34.6154			
64	15L	0	AIMED:	-15.2400	-.0750	.0000	15.2402					54312	54312
			4-TRIANGLES:	-13.2795	4.7145	-7.2970	15.8688	8.9459	-19.8277	3.9614	203.5169		
			MMD METHOD:	-21.2660	.1589	-2.4989	21.4129	6.5278	-.7102	28.8270			
65	10L	0	AIMED:	-10.2000	.0000	.0000	10.2000					54312	54312
			4-TRIANGLES:	-9.6121	-3.0657	5.6686	11.5726	6.4713	17.6898	11.8607	78.4891		
			MMD METHOD:	-14.0129	.1802	4.3702	14.6797	5.8025	-.7366	30.5162			
67	15L	0	AIMED:	-15.1300	.0000	.0000	15.1300					54312	54312
			4-TRIANGLES:	-14.3461	3.5435	-7.5040	16.5734	8.3355	-13.8745	8.7090	167.6482		
			MMD METHOD:	-20.6161	-2.5536	-3.7684	21.1127	7.1287	7.0609	28.3369			
68	9L	0	AIMED:	-9.7600	-.4110	.0000	9.7686					54312	54312
			4-TRIANGLES:	-9.7071	-3.0283	7.0150	12.3535	7.4876	14.9150	20.9238	48.0839		
			MMD METHOD:	-12.0268	-.8114	7.6518	14.2776	7.9905	1.4485	31.5808			
69	14L	0	AIMED:	-14.6760	-.0770	.0000	14.6762					54312	54312
			4-TRIANGLES:	-13.0835	-4.6362	7.1712	15.6237	8.6457	19.2115	6.0645	195.9745		
			MMD METHOD:	-20.8814	.1593	2.6633	21.0512	6.7570	-.7376	30.2933			
70	15L	0	AIMED:	-15.2000	.5250	.0000	15.2091					54312	54312
			4-TRIANGLES:	-13.1922	5.3205	-7.5081	16.0846	9.1324	-19.9864	5.4433	167.8418		
			MMD METHOD:	-19.9985	3.3042	-4.3435	20.7297	7.0438	-7.4035	26.6316			
71	10L	0	AIMED:	-10.2250	-.0370	.0000	10.2251					54312	54312
			4-TRIANGLES:	-10.7270	-3.6256	4.2814	12.1055	5.6090	18.4675	15.5340	74.6301		
			MMD METHOD:	-14.9064	-1.4934	.1701	14.9820	4.9057	5.5136	31.7510			
73	15L	0	AIMED:	-15.2000	.0800	.0000	15.2002					54312	54312
			4-TRIANGLES:	-13.8715	4.5146	-6.9903	16.1761	8.3842	-17.7263	6.0328	178.1290		
			MMD METHOD:	-20.9506	.1897	-2.0097	21.0476	6.0926	-.2172	27.7817			
74	9L	0	AIMED:	-9.2500	-.6000	.0000	9.2694					54312	54312
			4-TRIANGLES:	-10.7115	-4.3953	5.3365	12.7488	6.7095	18.5988	27.2916	73.7869		
			MMD METHOD:	-14.8262	-3.4952	2.7534	15.4794	6.8598	9.5537	40.1177			
							ORIENTATION XV						

1000 METRES

SHOT NO.	AIM		ANALYSIS	COORDINATES X	Y	Z	MISS DISTANCE	ERROR DISTANCE	ANTICLOCK-WISE ANGULAR ERROR IN TARGET PLANE IN DEGREES	%MISS DISTANCE ERROR	SMALLEST VARIANCE	AIMED SEQUENCE	OBSERVED SEQUENCE
						ORIENTATION XV							
76	15L	0	AIMED:	.0000	.0000	15.6880	15.4272					54213	54213
			4-TRIANGLES:	-7.5015	-5.4156	11.6887	14.9073	10.0795	24.8591	-3.4881	175.3878		
			MMD METHOD:	.0000	-3.9385	19.6368	20.0279	5.5772	11.3412	22.9713			
77	15L	0	AIMED:	.0000	.0000	15.6830	15.2078					54213	54213
			4-TRIANGLES:	-7.7392	-4.4683	11.5832	14.6298	9.8342	21.0943	-3.9509	196.1992		
			MMD METHOD:	.0000	.0000	20.3408	20.3408	4.6528	.0000	25.2347			
78	9L	0	AIMED:	.0000	.0000	9.0800	9.4624					42135	54213
			4-TRIANGLES:	-4.9112	-2.8355	7.9424	9.7592	5.7840	19.6469	3.0411	53.3289		
			MMD METHOD:	-1.6963	-.9794	12.1764	12.3330	3.6640	4.5985	23.2754			
79	15L	0	AIMED:	.0000	.0000	14.7870	15.2436					45213	54213
			4-TRIANGLES:	.5435	9.8101	15.2480	18.1393	9.8360	-32.7561	15.9635	87.1730		
			MMD METHOD:	1.0592	5.4398	19.7395	20.5027	7.4324	-15.4071	25.6505			
80	10L	0	AIMED:	.0000	.0000	9.5670	10.0480					42135	54213
			4-TRIANGLES:	-.3170	5.6159	8.5922	10.2696	5.7087	-33.1689	2.1576	67.2499		
			MMD METHOD:	-.9229	.5328	13.2362	13.2790	3.8208	-2.3053	24.3316			
81	14L	0	AIMED:	.0000	.0000	14.1050	14.6394					45213	54213
			4-TRIANGLES:	-7.7999	-3.9865	11.1401	14.1715	9.2478	19.6897	-3.3015	173.1686		
			MMD METHOD:	-1.7365	1.0026	19.3253	19.4290	5.5922	-2.9698	24.6519			
82	9L	0	AIMED:	.0000	.0000	9.1750	9.7142					42135	54213
			4-TRIANGLES:	5.6056	-2.8796	7.8181	10.0418	6.4464	20.2200	3.2624	63.3769		
			MMD METHOD:	3.0141	-.5706	12.5783	12.9470	4.5818	2.5972	24.9694			
83	14L	0	AIMED:	.0000	.0000	13.7750	14.4658					45213	54312
			4-TRIANGLES:	-8.5585	-3.4008	10.2729	13.7965	9.8528	18.3168	-4.8506	164.8425		
			MMD METHOD:	-5.5900	3.2274	17.7996	18.9338	7.6067	-10.2772	23.5982			
84	14L	0	AIMED:	.0000	.0000	14.1650	14.6994					45213	15432
			4-TRIANGLES:	-6.8264	-16.1075	8.3416	19.3813	18.4381	62.6217	24.1568	.0131		
			MMD METHOD:	-	-	-	-	-	-	-			